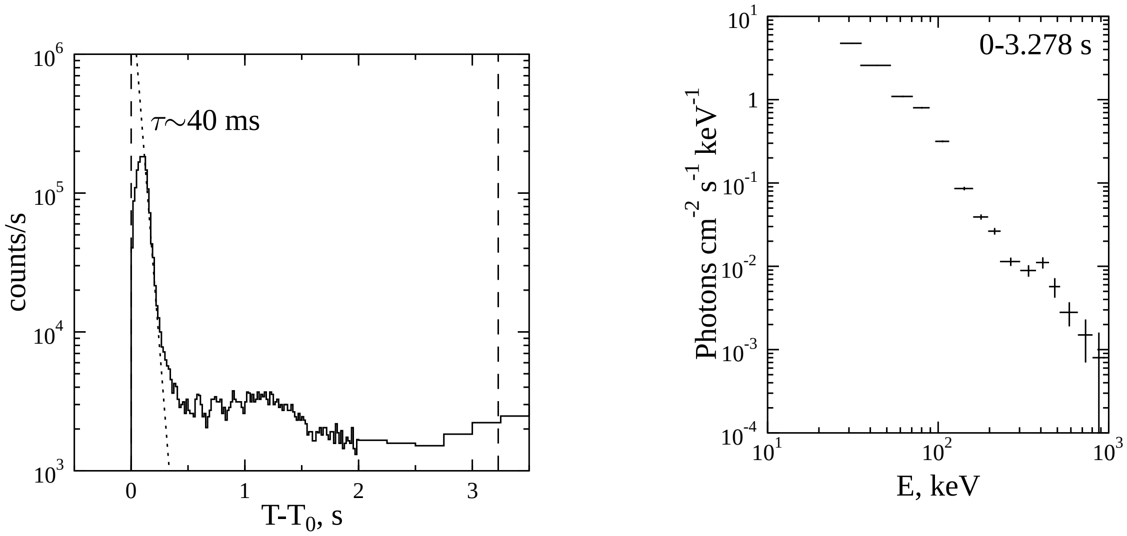

Fig. 2.1.— Burst 790305. The time history and energy spectrum of the initial pulse in the March 5 event. The huge pulse decays exponentially with a time constant $\tau \sim 40$ ms. Strong and fast spectral variability apparently exists in the pulse. Only one energy spectrum averaged over a 3.3 s-time interval is available.

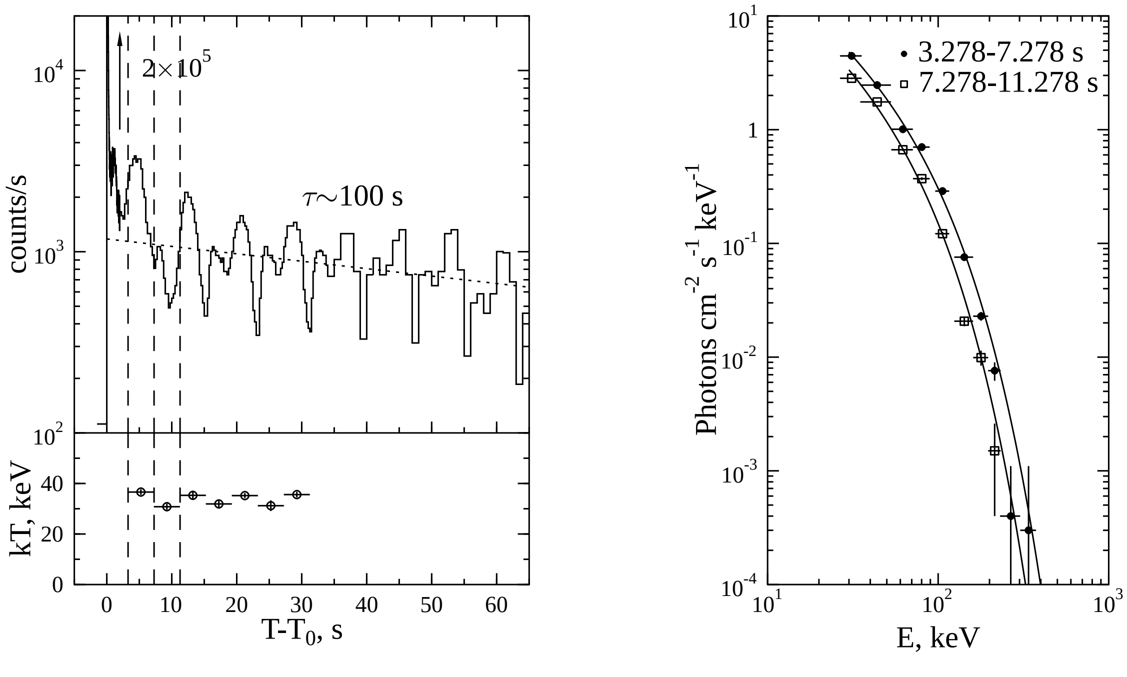

Fig. 2.2.— Burst 790305. The pulsating (8s) exponentially decaying ($\tau \sim 100$ s) tail of the outburst. Average values of kT differ slightly for pulses and interpulses. As an example, two energy spectra are shown.

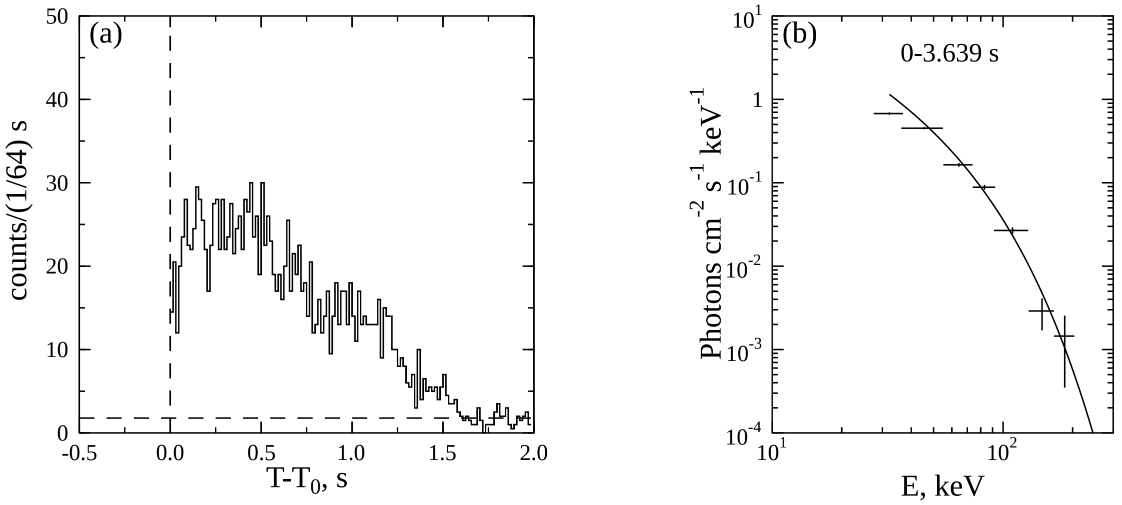

Fig. 2.3.— Burst 790306.

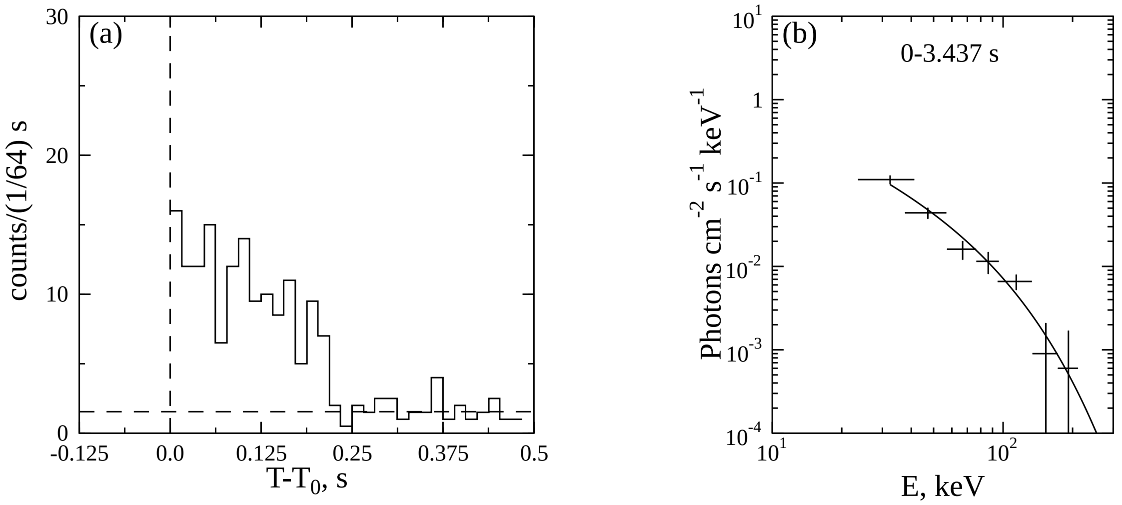

Fig. 2.4.— Burst 790404.

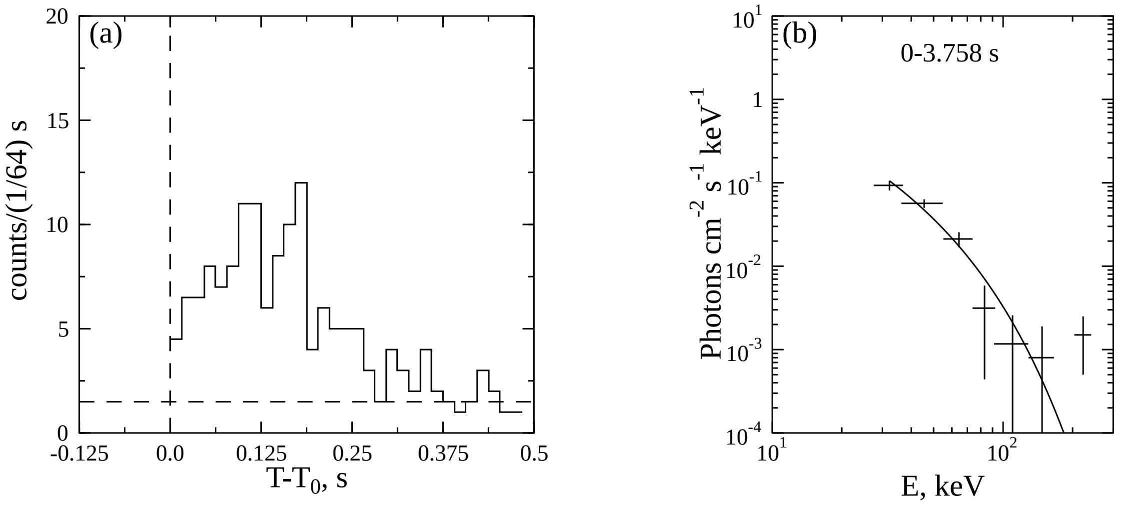

Fig. 2.5.— Burst 790424.

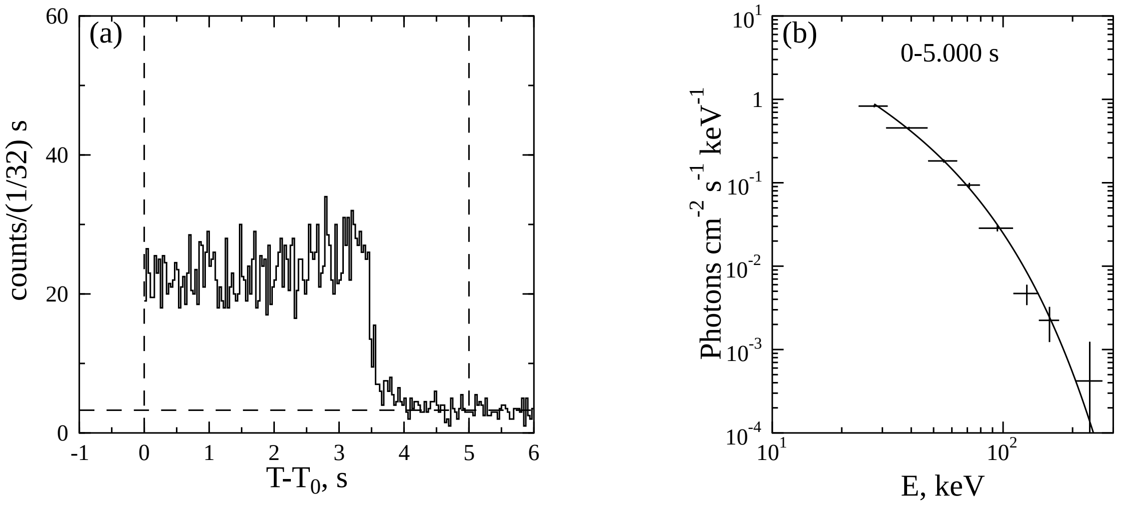

Fig. 2.6.— Burst 811201.

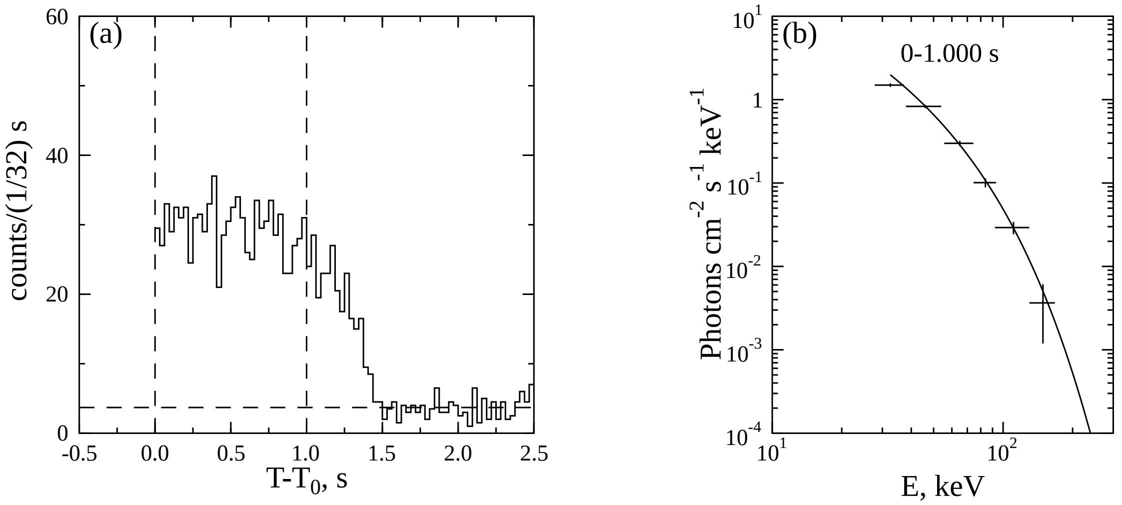

Fig. 2.7.— Burst 820102.

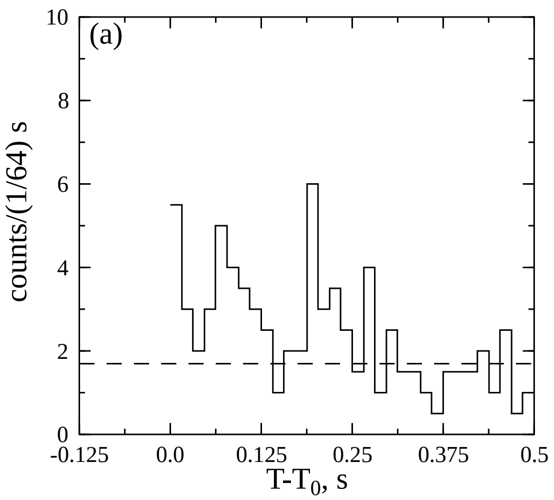

Fig. 2.8.— Burst 820215.

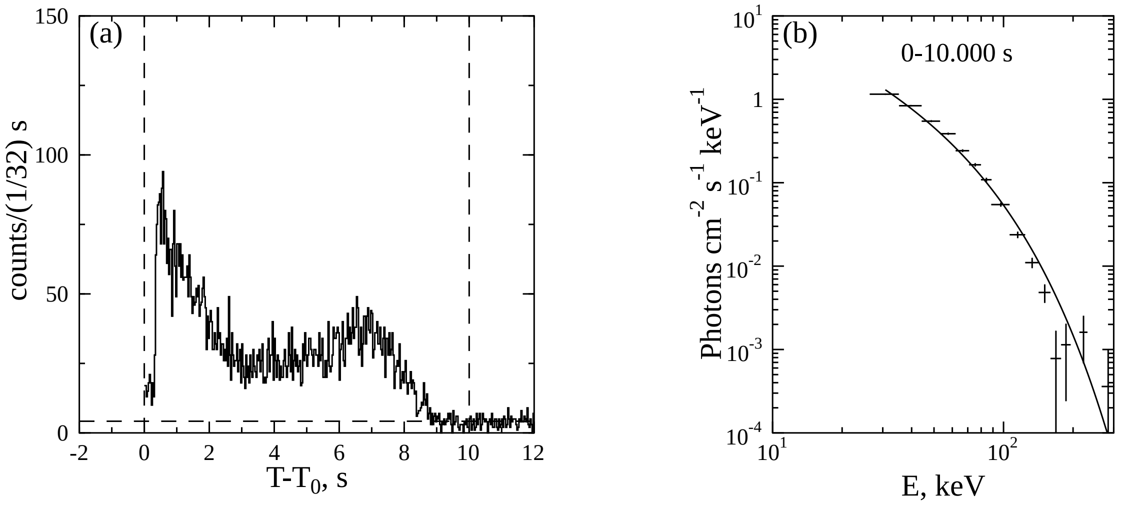

Fig. 2.9.— Burst 820227.

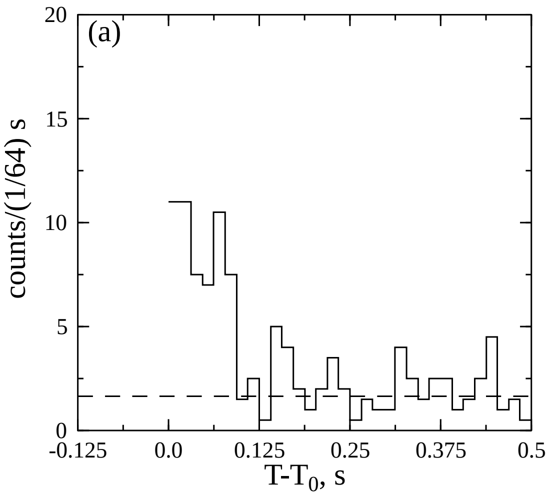

Fig. 2.10.— Burst 820423a.

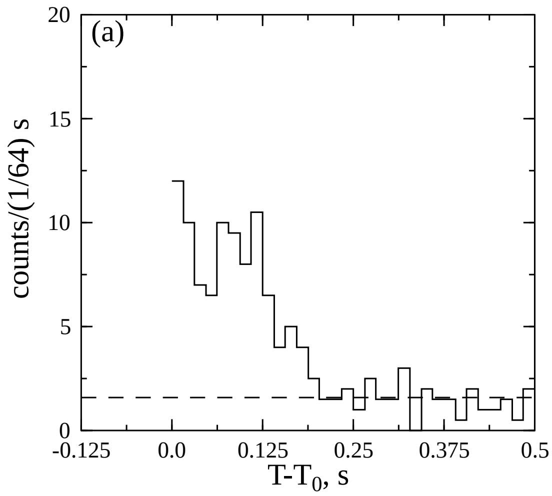

Fig. 2.11.— Burst 820423b.

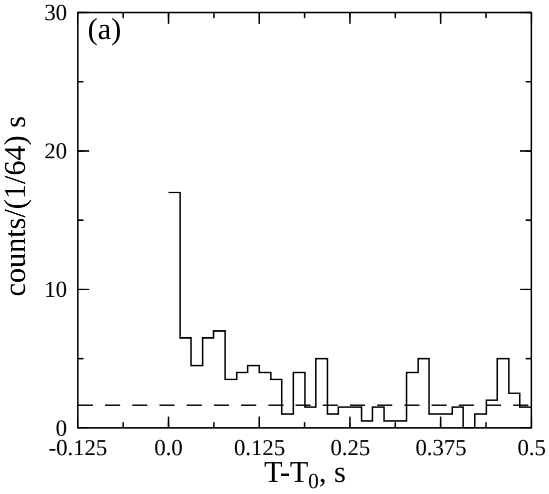

Fig. 2.12.— Burst 820510.

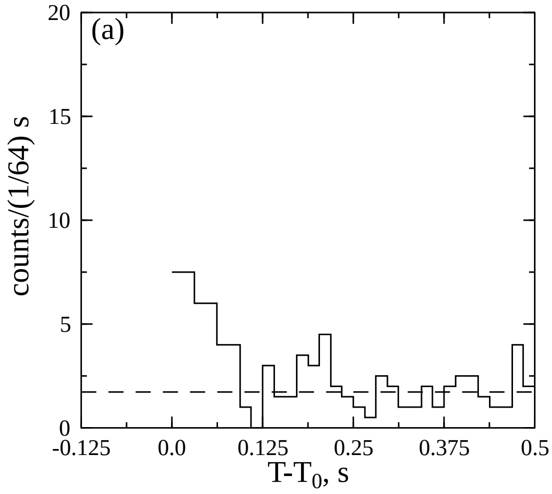

Fig. 2.13.— Burst 820530.

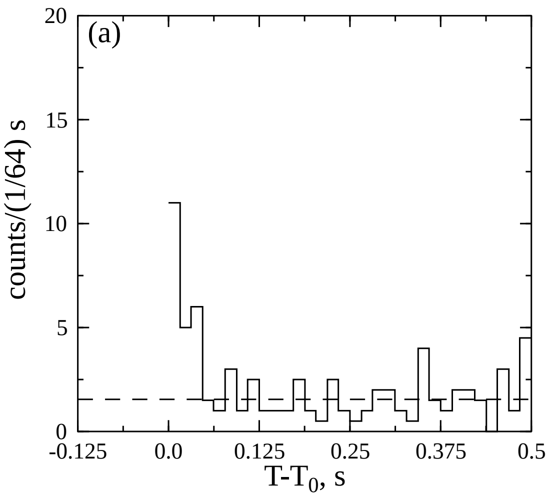

Fig. 2.14.— Burst 820708.

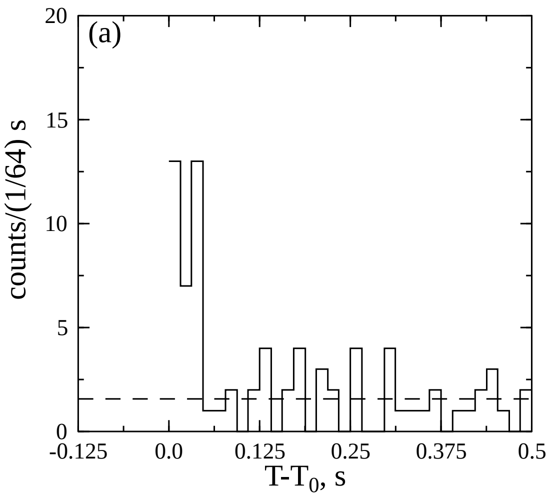

Fig. 2.15.— Burst 820921.

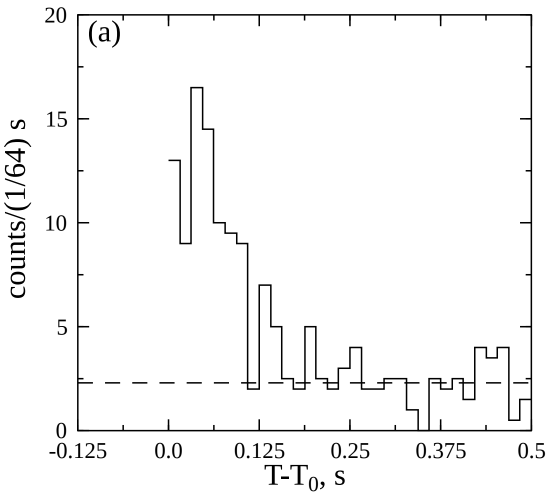

Fig. 2.16.— Burst 821231.

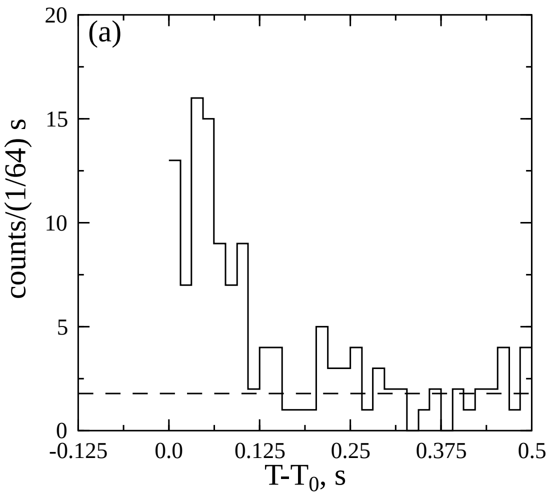

Fig. 2.17.— Burst 830321.

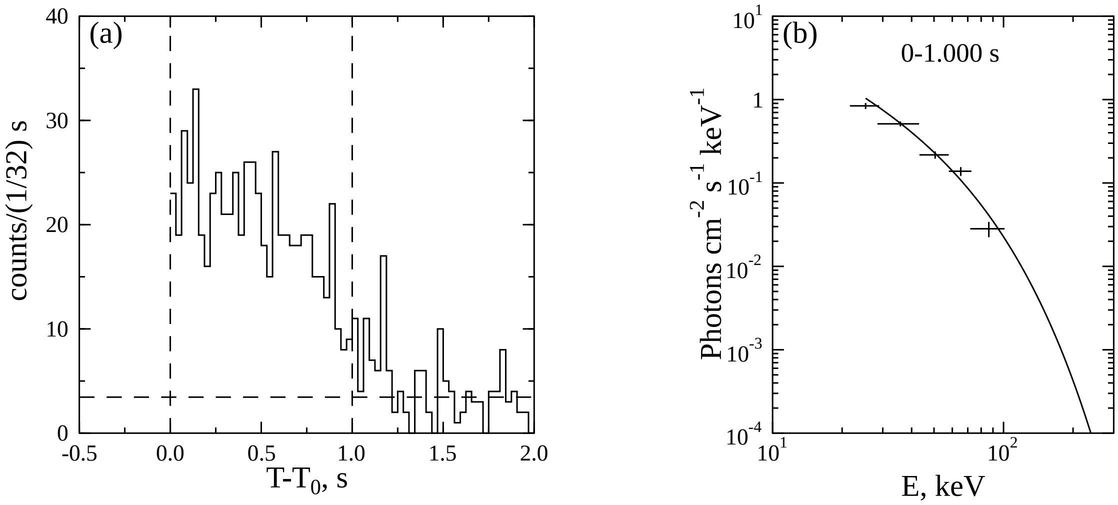

Fig. 2.18.— Burst 830405.

Figures 2.1–2.18 display the time histories (a) and energy spectra (b) of repeating bursts. Being obtained by two spacecraft, time history data are presented as average count rates. Energy spectra from one spacecraft are shown. For weaker events, energy spectra are omitted because of their low accuracy. In these cases, only rough estimates of kT are available.

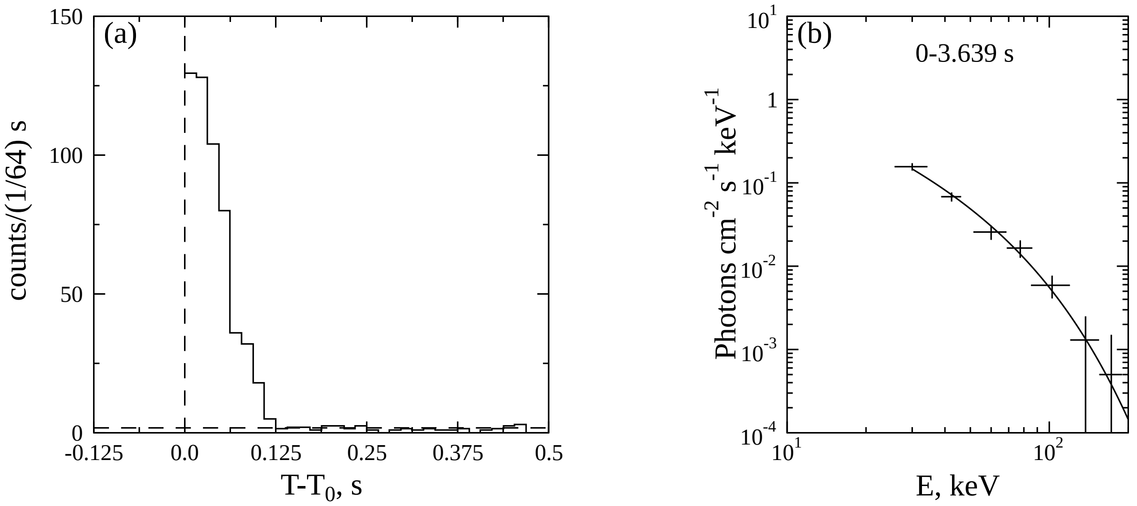

Fig. 3.1.— Burst 790324.

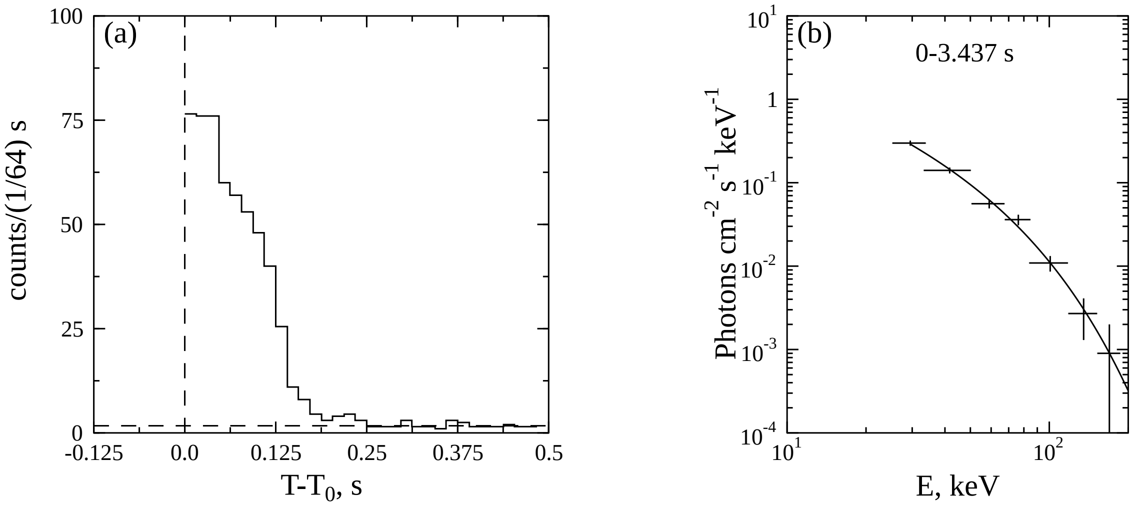

Fig. 3.2.— Burst 790325.

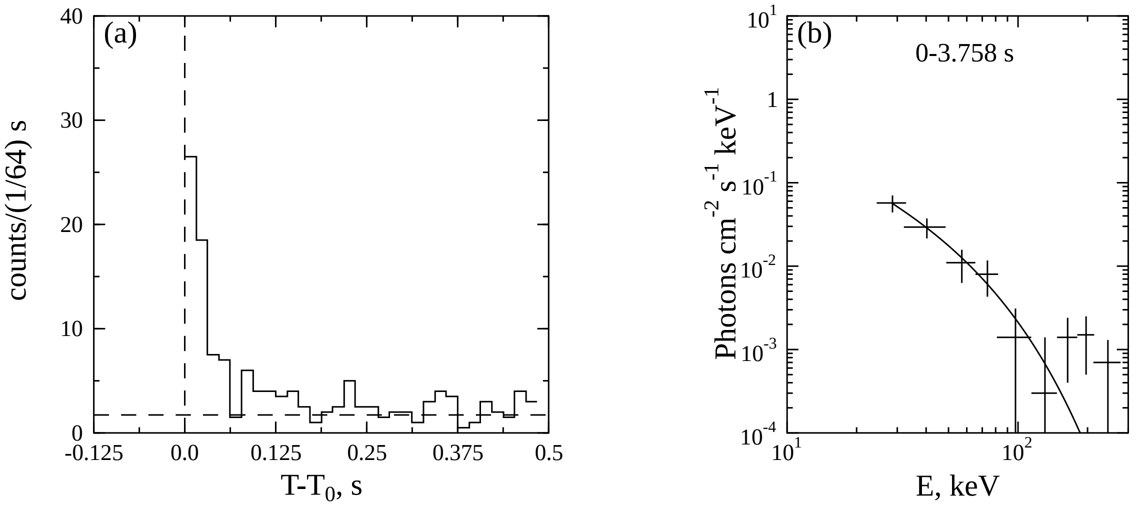

Fig. 3.3.— Burst 790327.

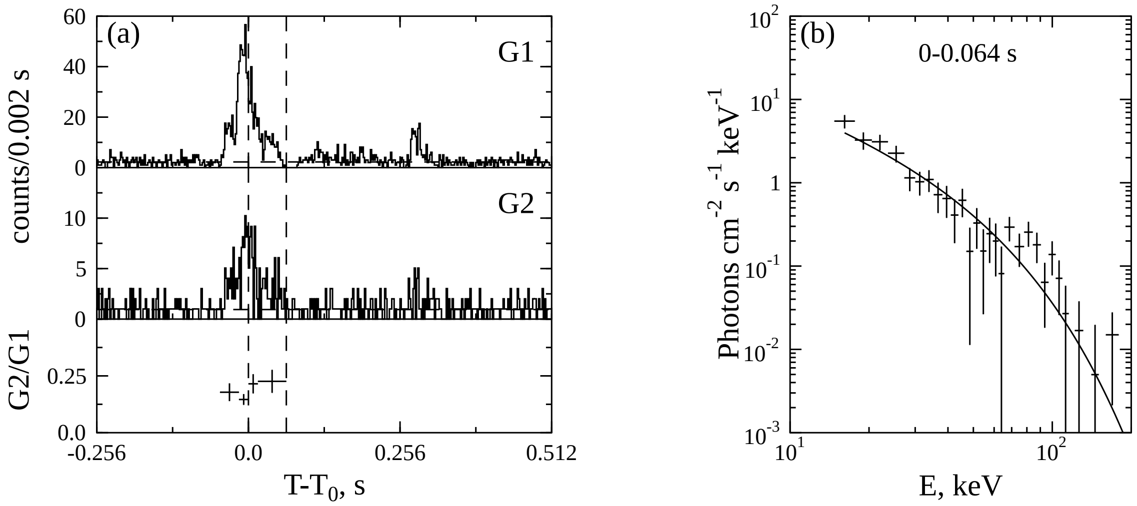

Fig. 3.4.— Burst 980526.

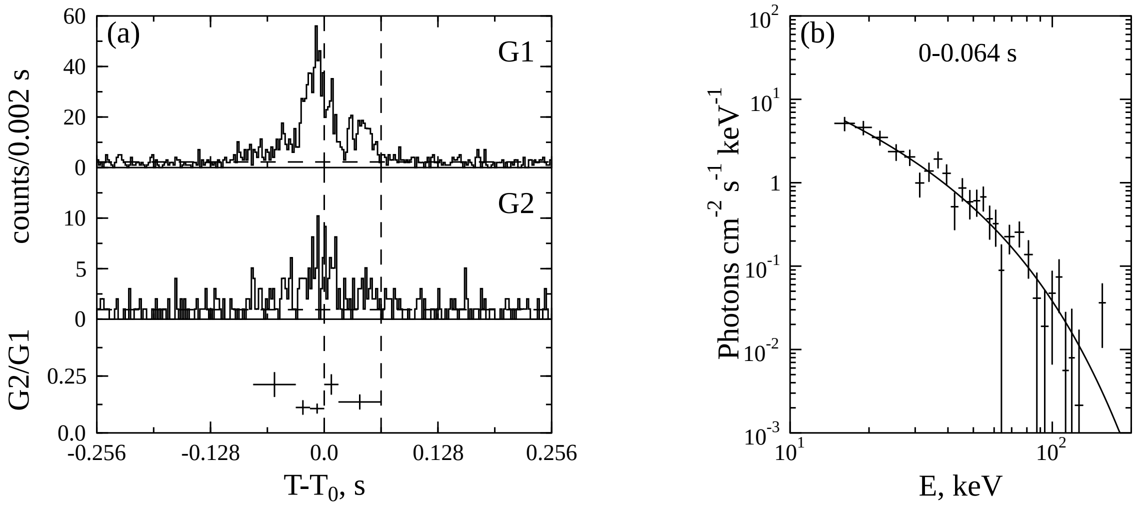

Fig. 3.5.— Burst 980527.

Figures 3.1-3.5. — Three single bursts seen from Venera missions in March 1979. Two bursts recorded on the Wind spacecraft at the beginning of SGR 1900+14 reactivation in May 1998.

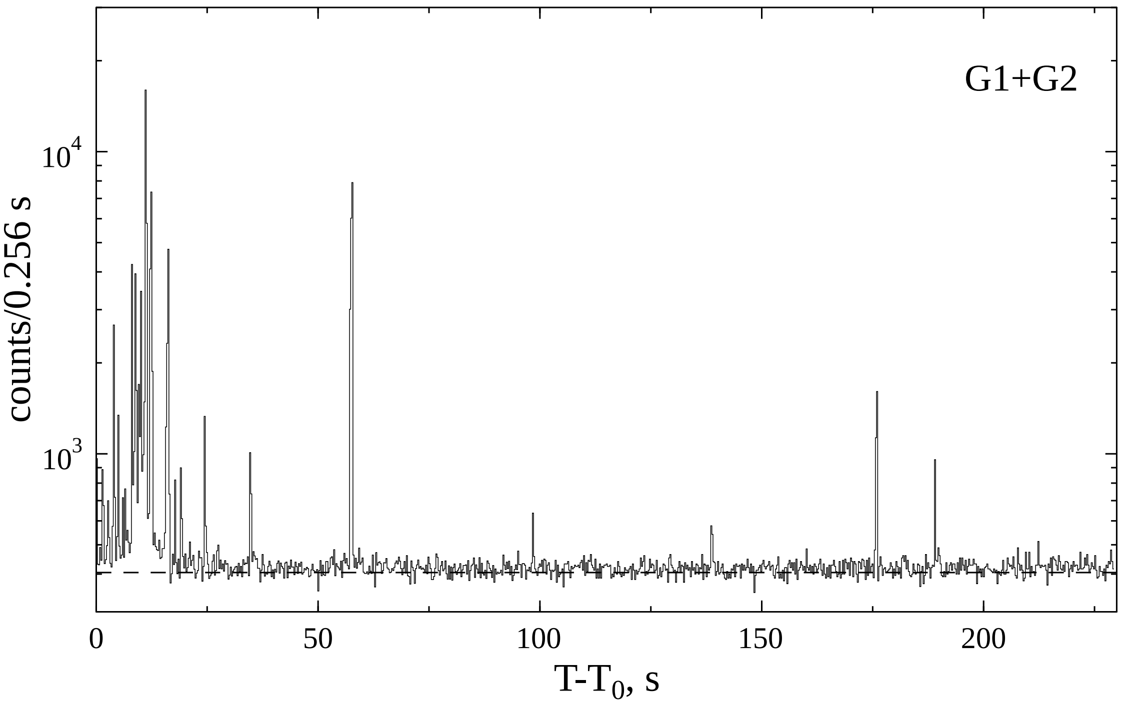

Fig. 3.6.— General pattern of the event 980530a. The first series of numerous soft bursts.

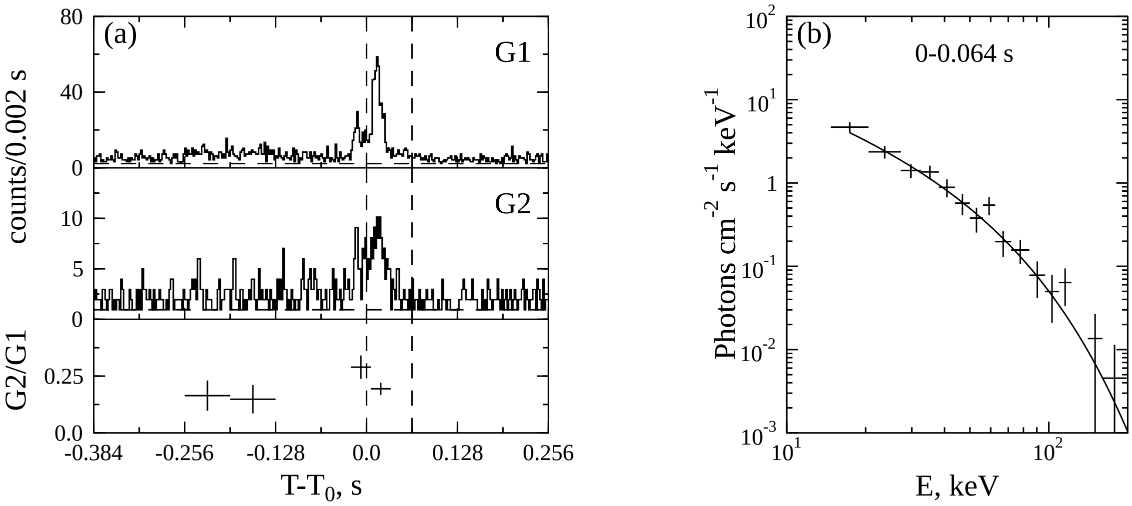

Fig. 3.7.— Starting burst in the event 980530a. (a) – time structure. (b) – energy spectrum.

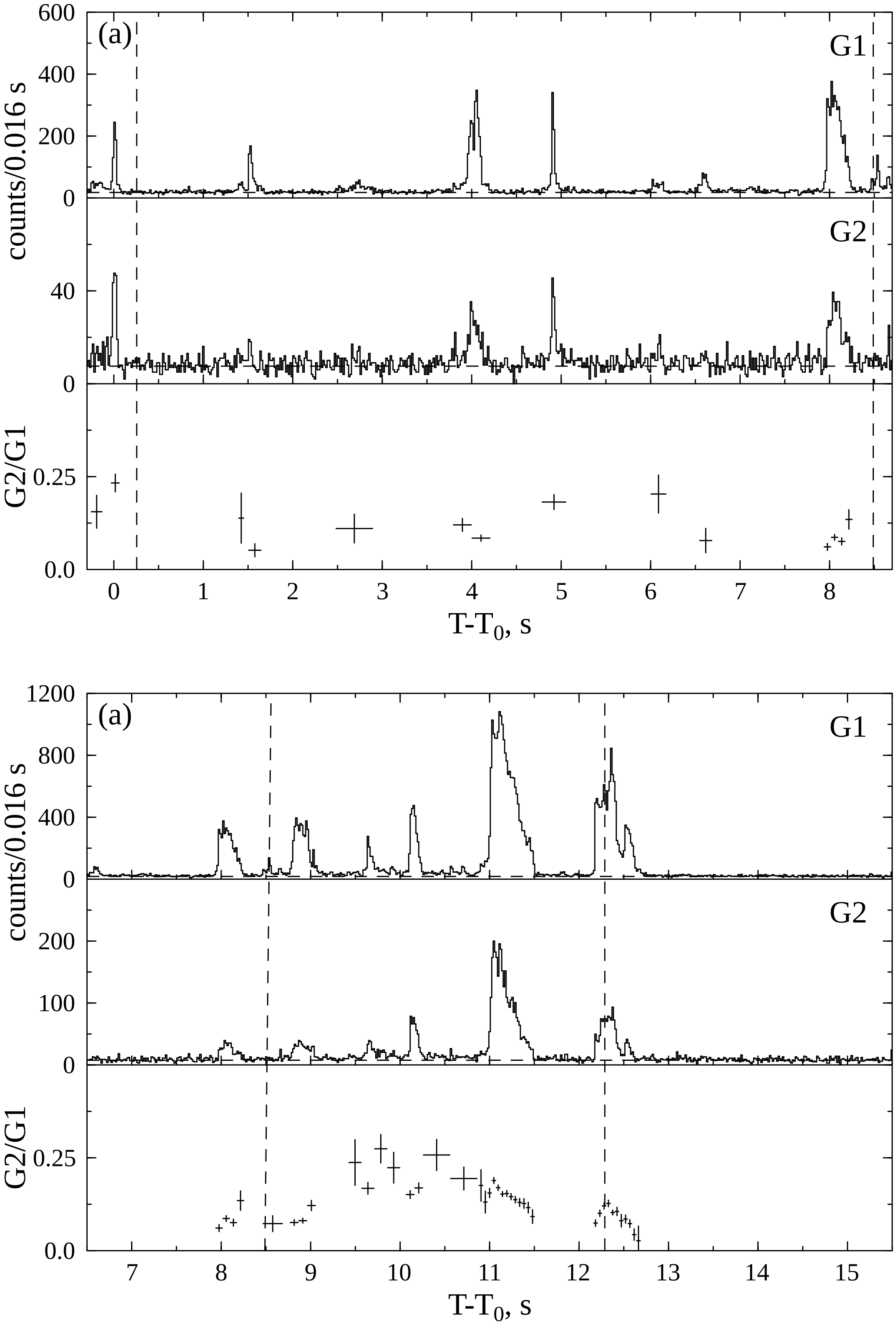

Fig. 3.8.— Crowded part of the event 980530a. Time structures.

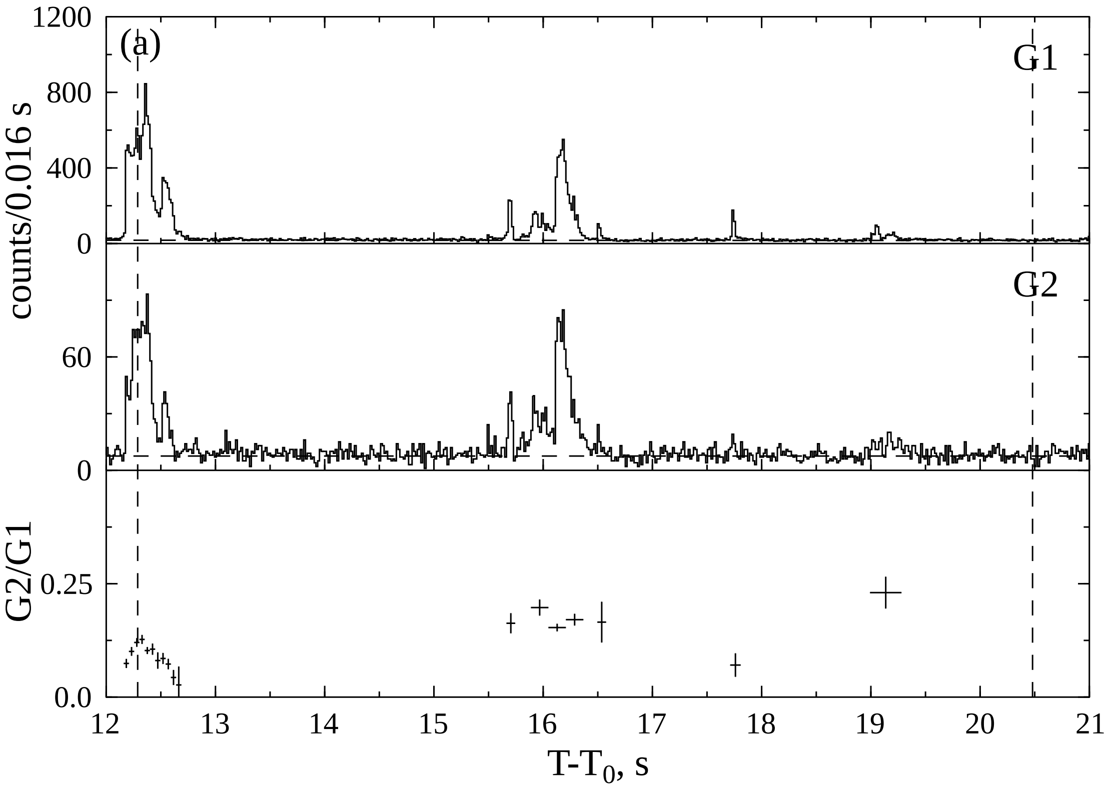

Fig. 3.9.— Crowded part of the event 980530a. Time structures (continued).

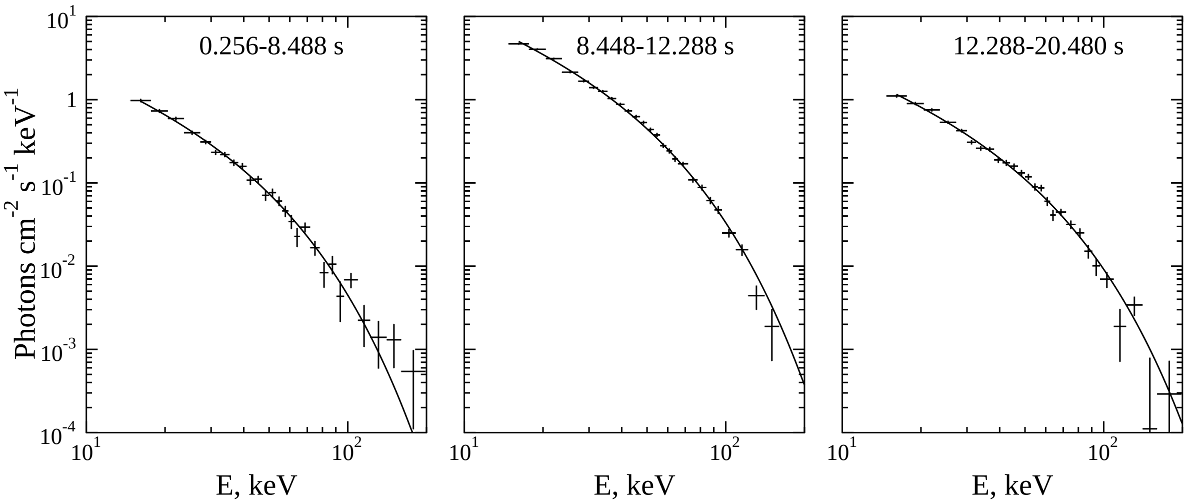

Fig. 3.10.— Energy spectra of the event 980530a accumulated in time intervals which include several separate bursts.

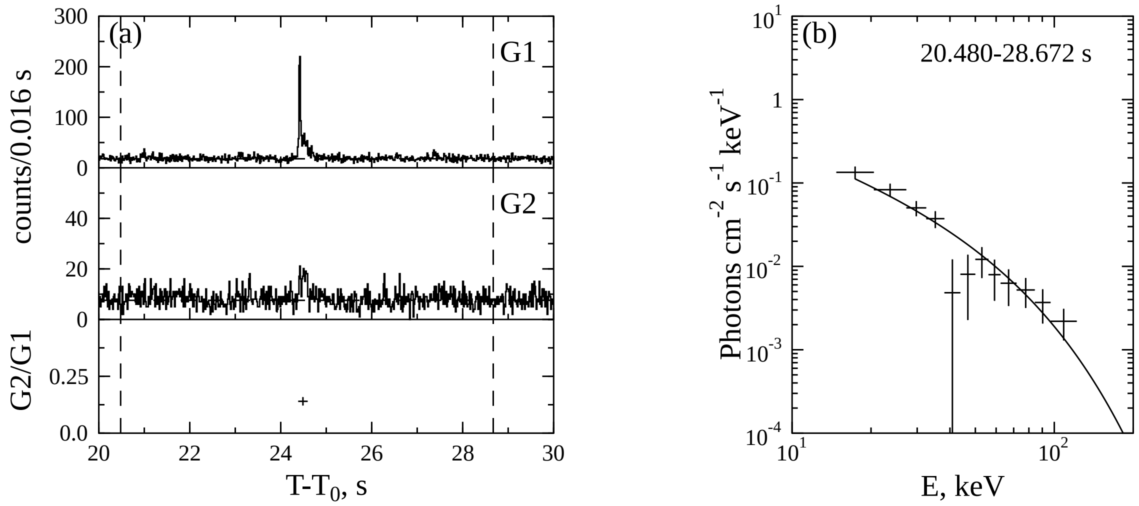

Fig. 3.11.— Event 980530a (continued).

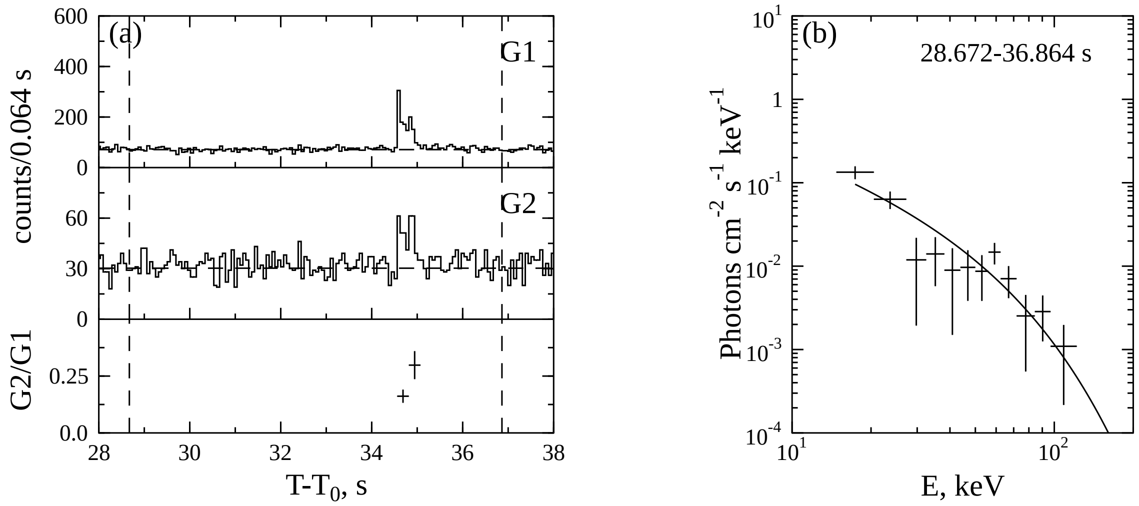

Fig. 3.12.— Event 980530a (continued).

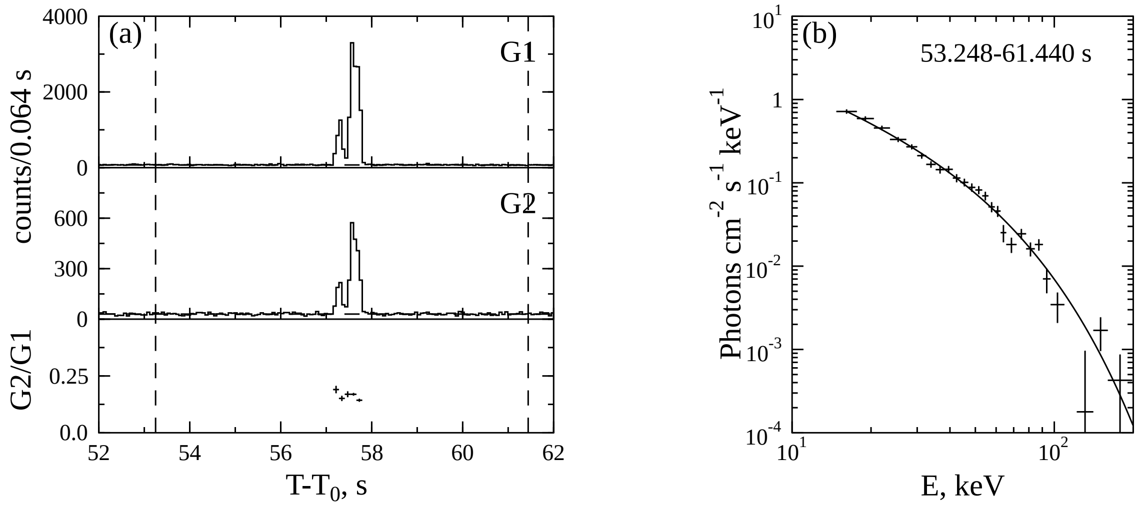

Fig. 3.13.— Event 980530a (continued).

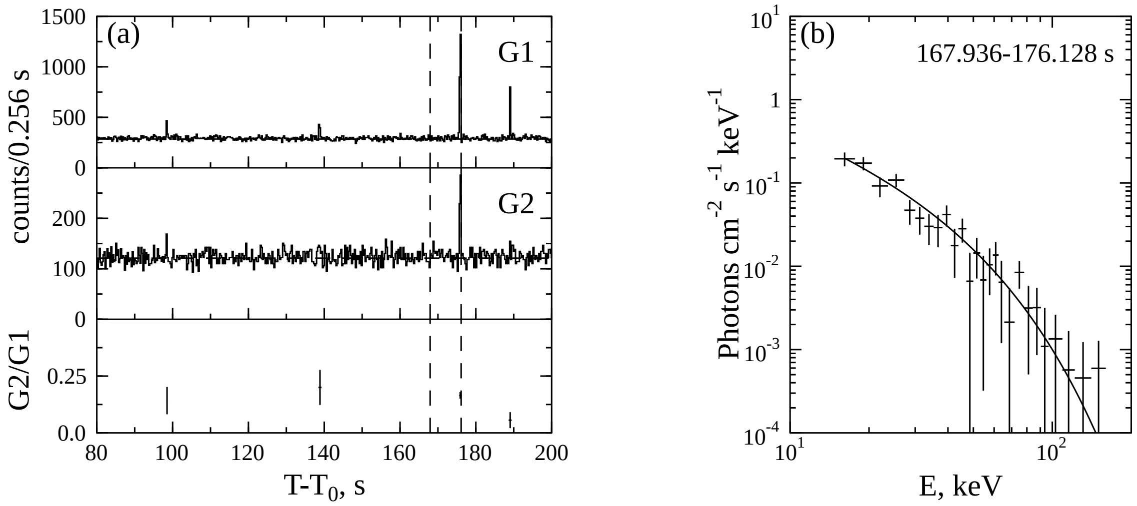

Fig. 3.14.— Burst 980530a (continued).

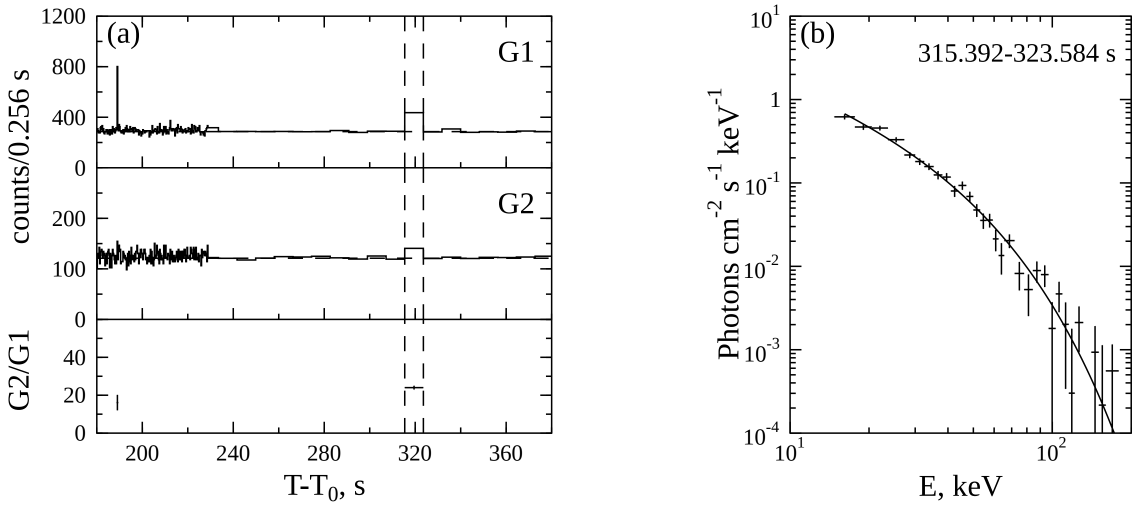

Fig. 3.15.— Event 980530a (continued). See comments to Fig. 3.42.

Figures 3.11-3.15 display serial bursts in event 980530a when their occurence rate had declined. (a) – time histories. (b) – energy spectra.

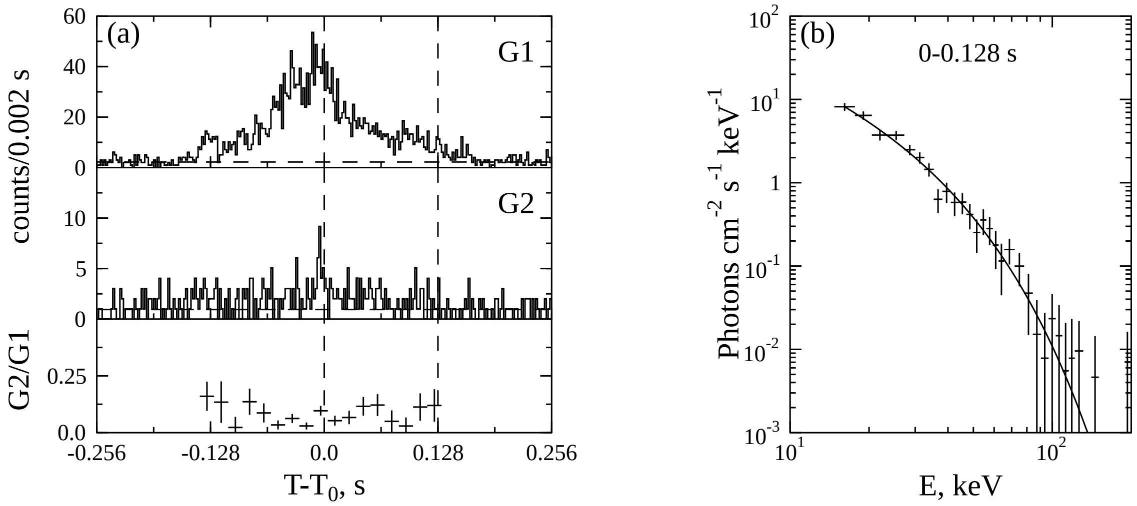

Fig. 3.16.— Burst 980530b.

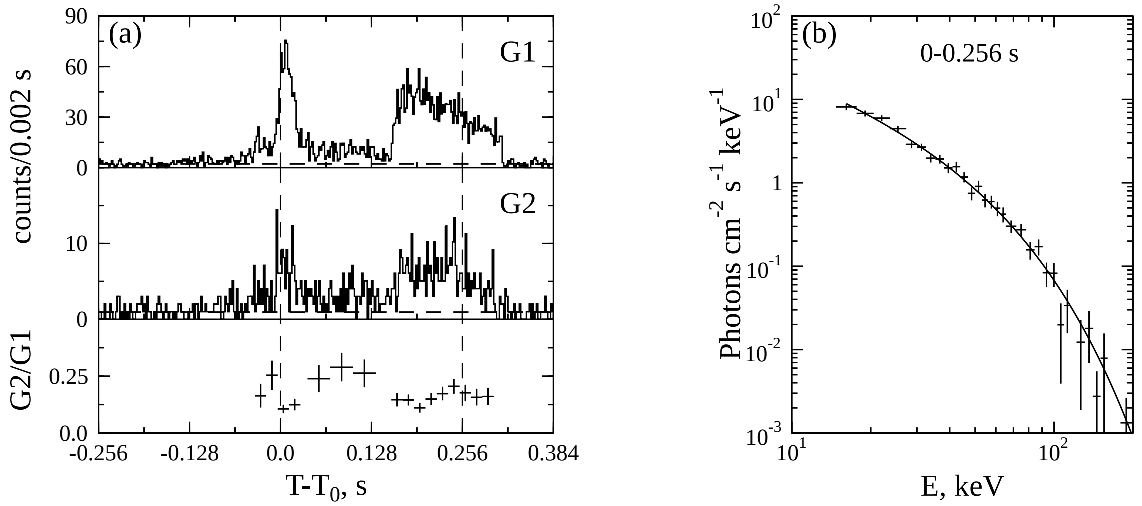

Fig. 3.17.— Burst 980530c.

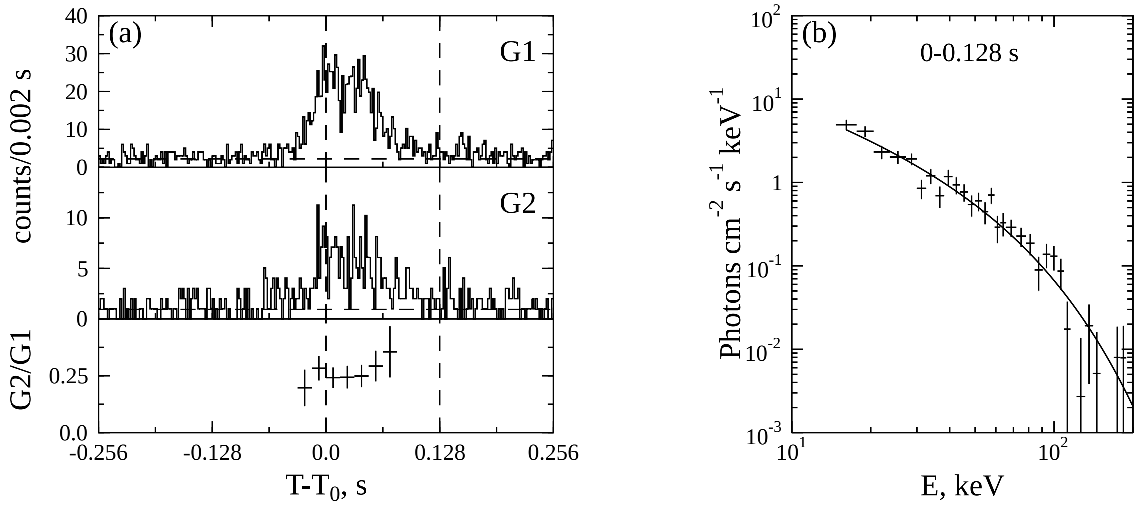

Fig. 3.18.— Burst 980530d.

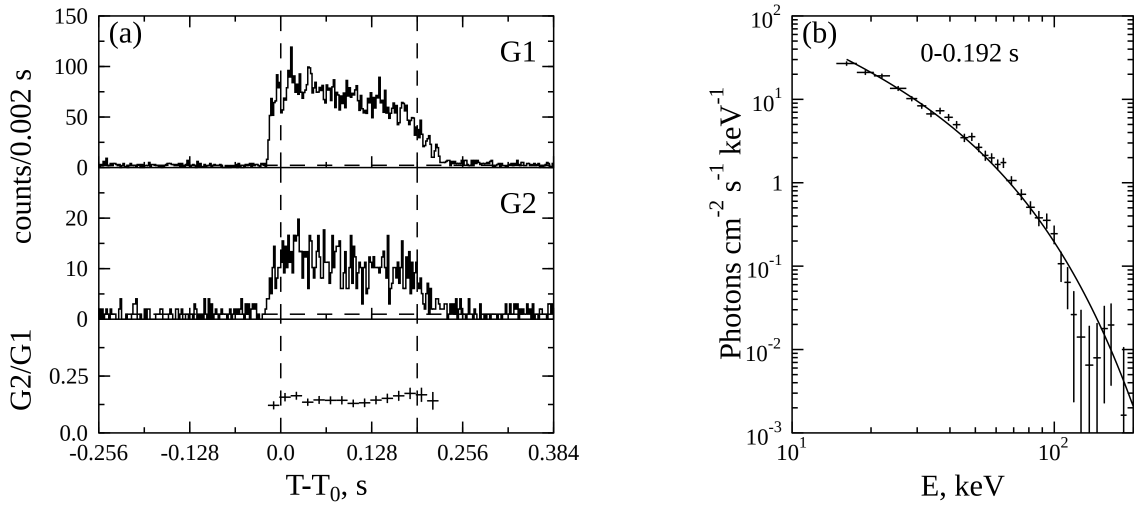

Fig. 3.19.— Burst 980607a.

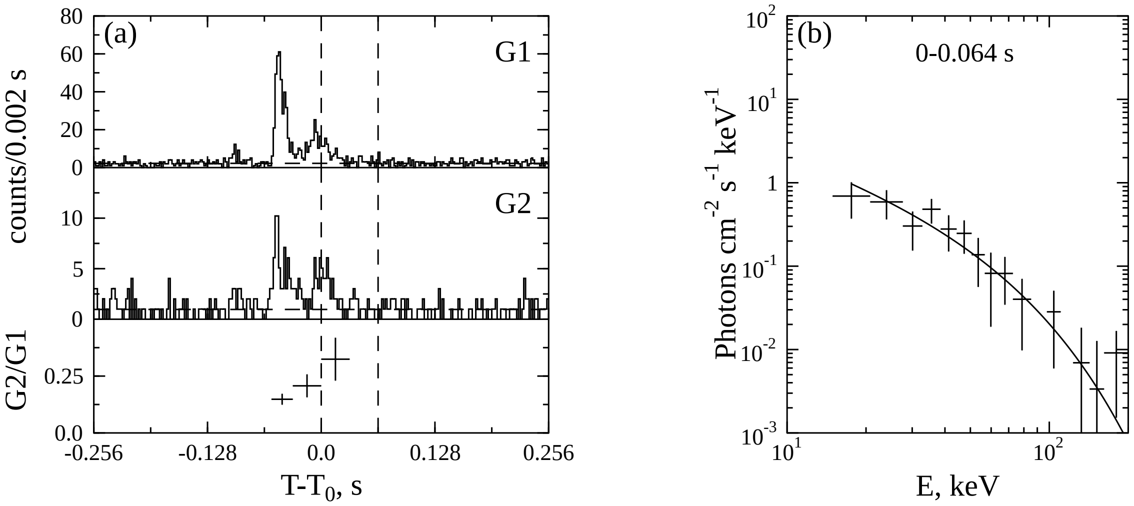

Fig. 3.20.— Burst 980607b.

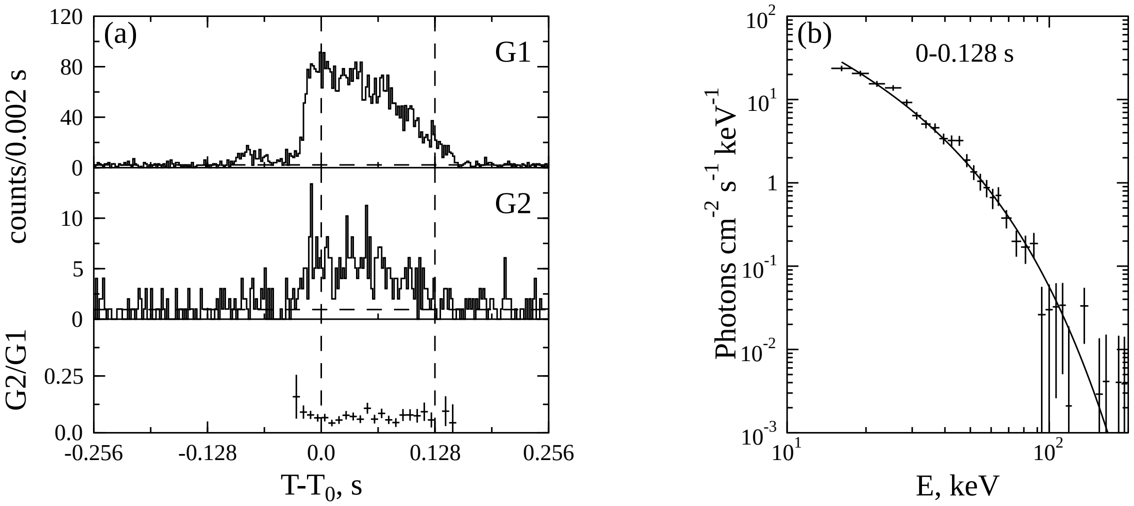

Fig. 3.21.— Burst 980616a.

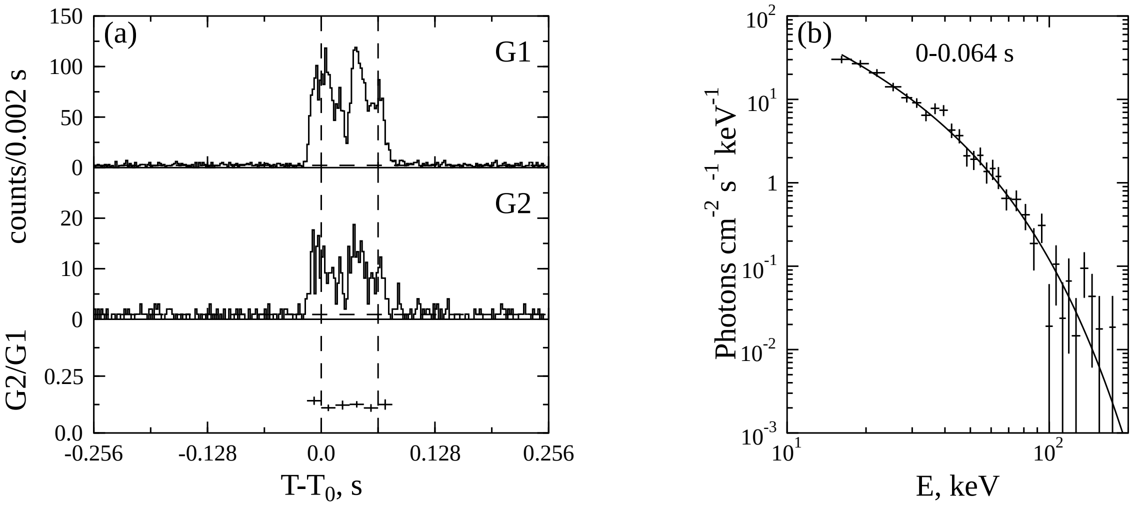

Fig. 3.22.— Burst 980616b.

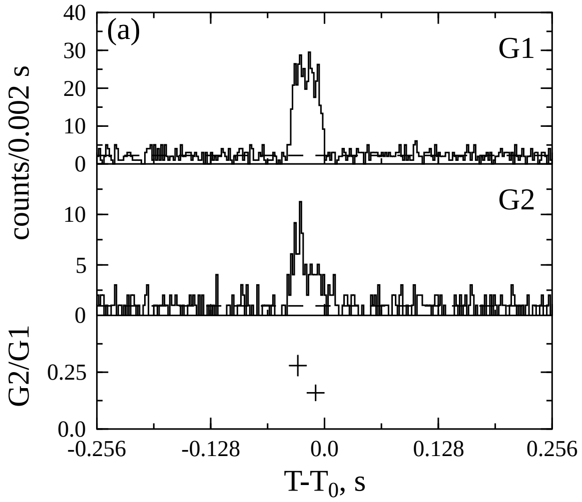

Fig. 3.23.— Burst 980719a.

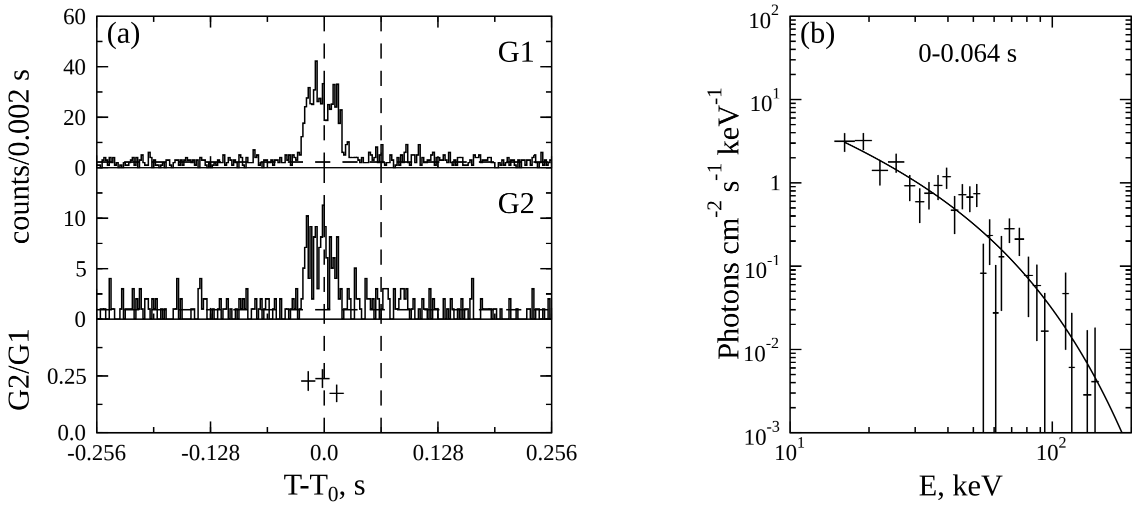

Fig. 3.24.— Burst 980719b.

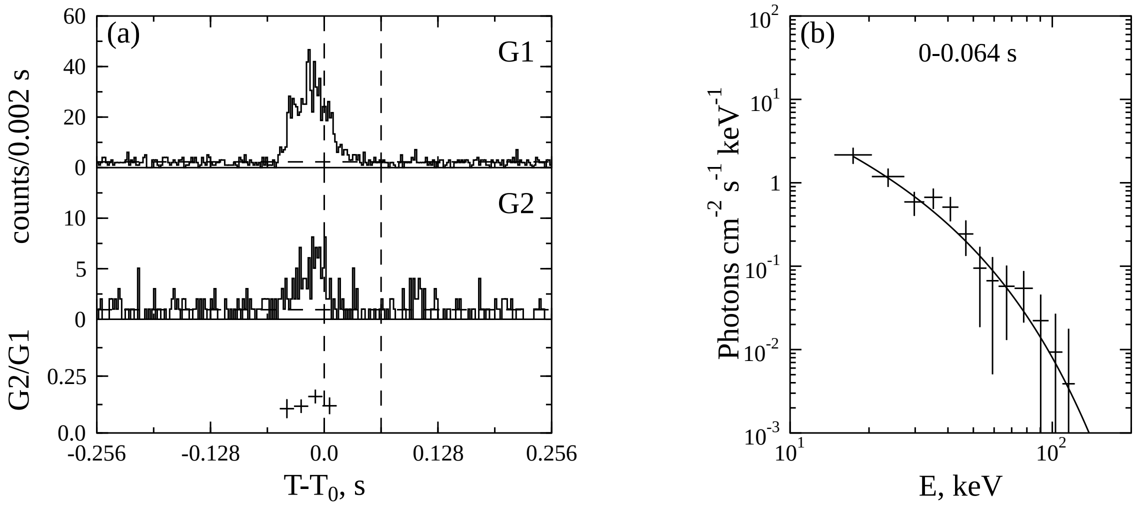

Fig. 3.25.— Burst 980721.

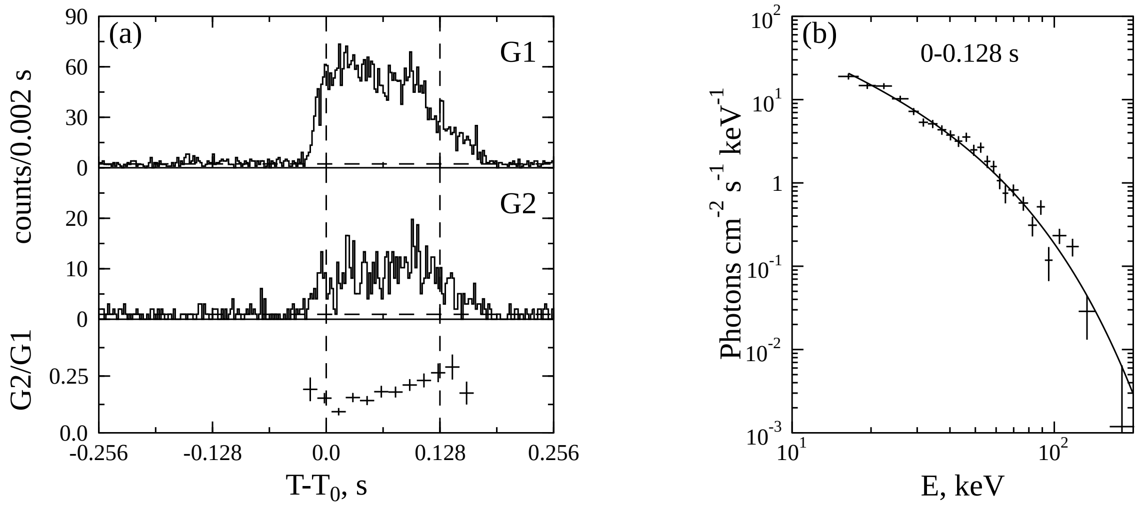

Fig. 3.26.— Burst 980821.

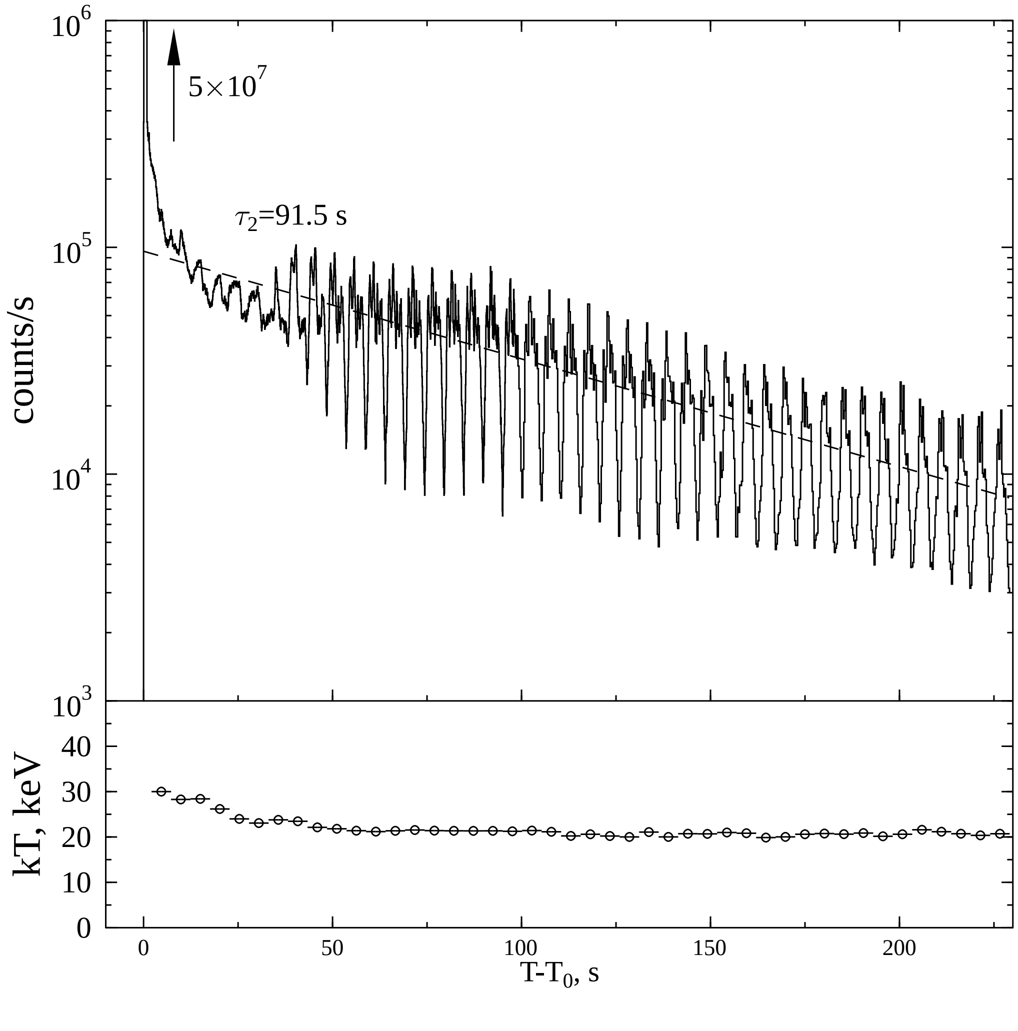

Fig. 3.27.— The giant outburst on 1998 August 27. General view.

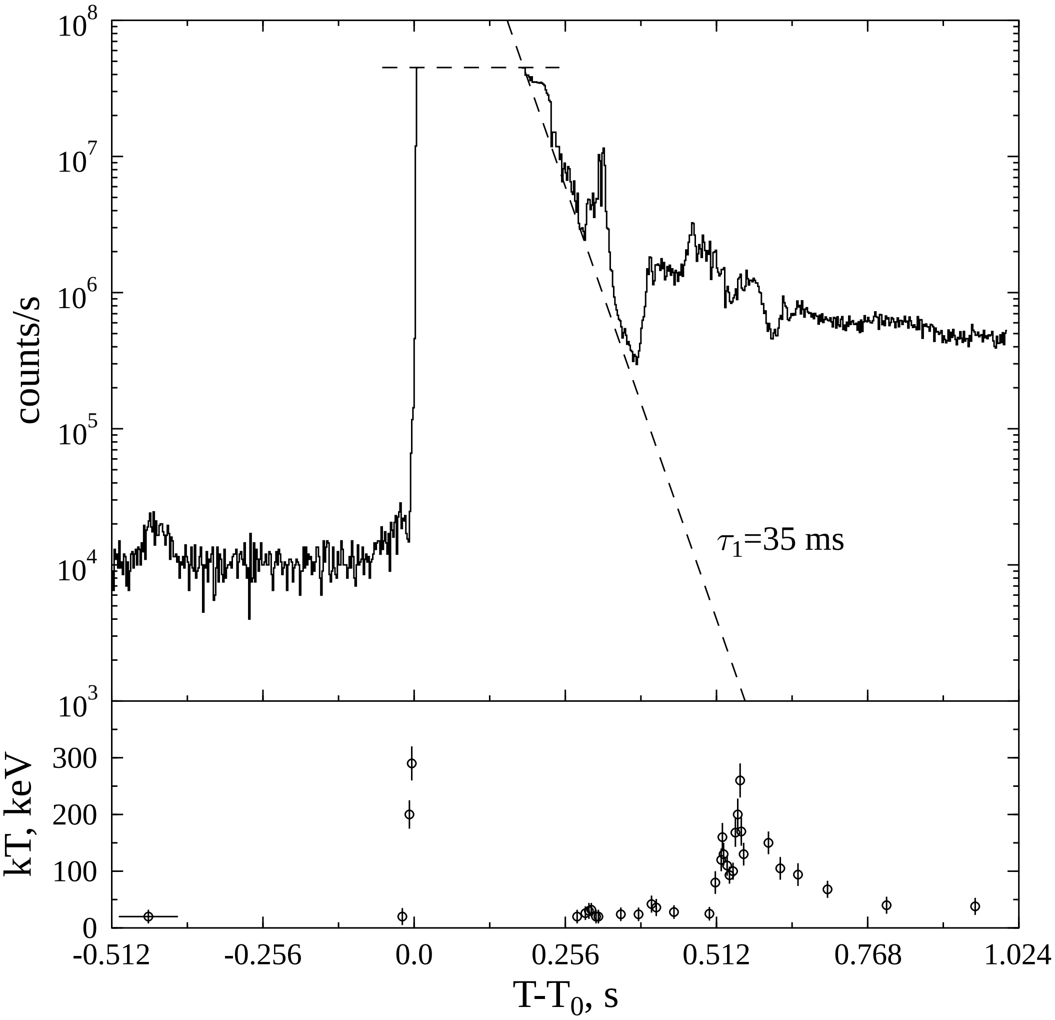

Fig. 3.28.— Initial pulse of the outburst 980827.

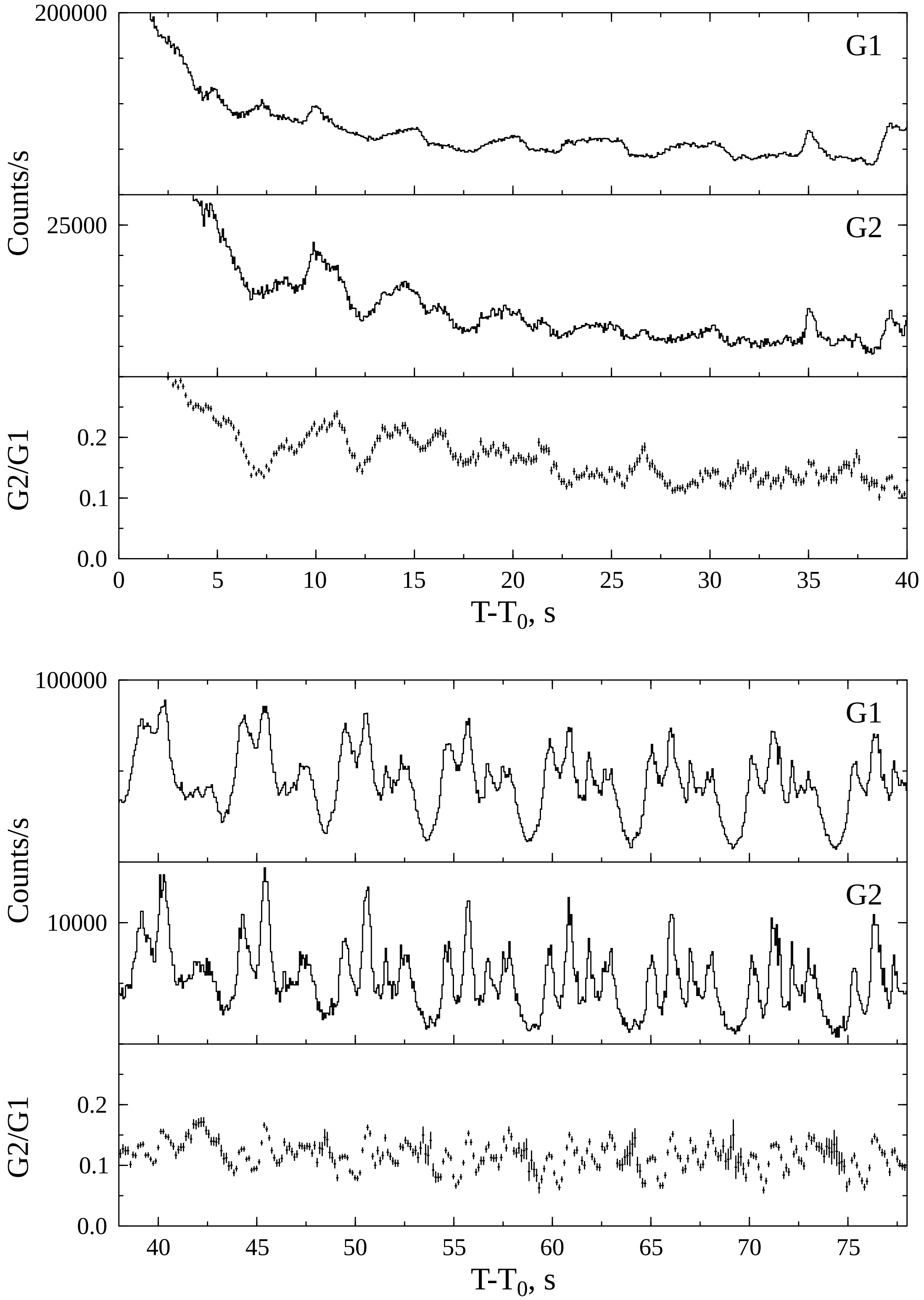

Fig. 3.29.— Pulsating tail of the 980827 outburst.

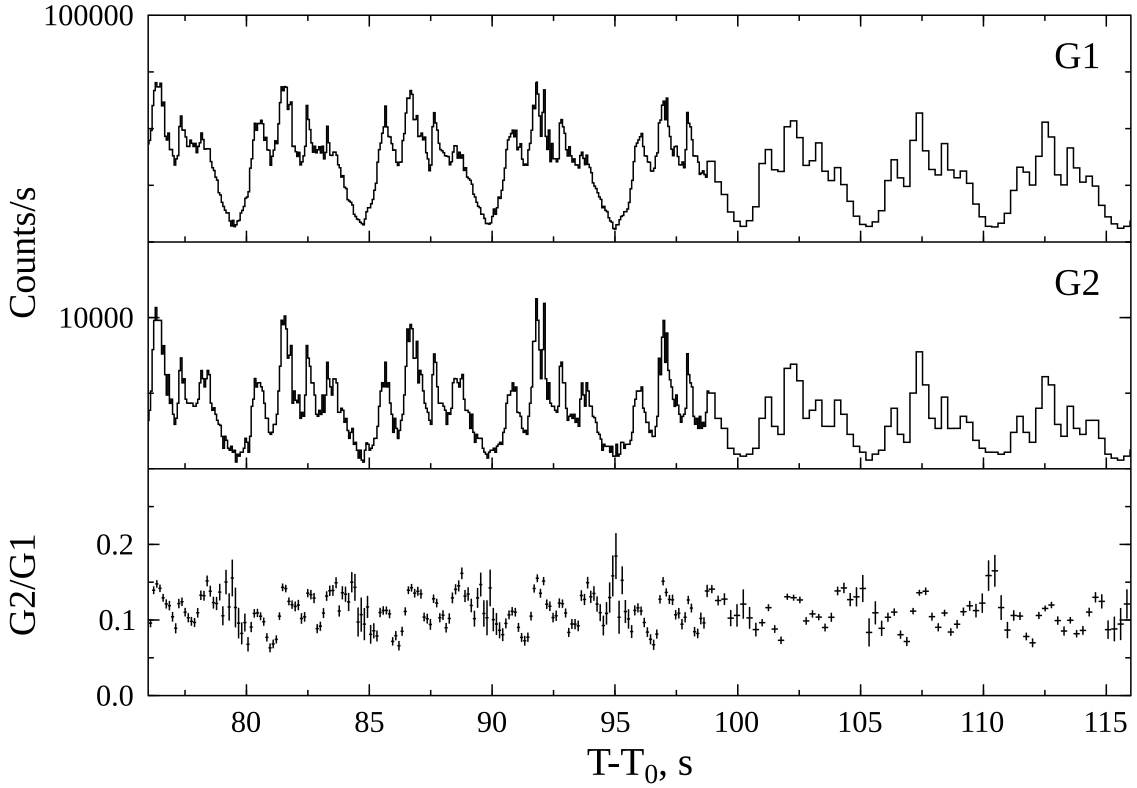

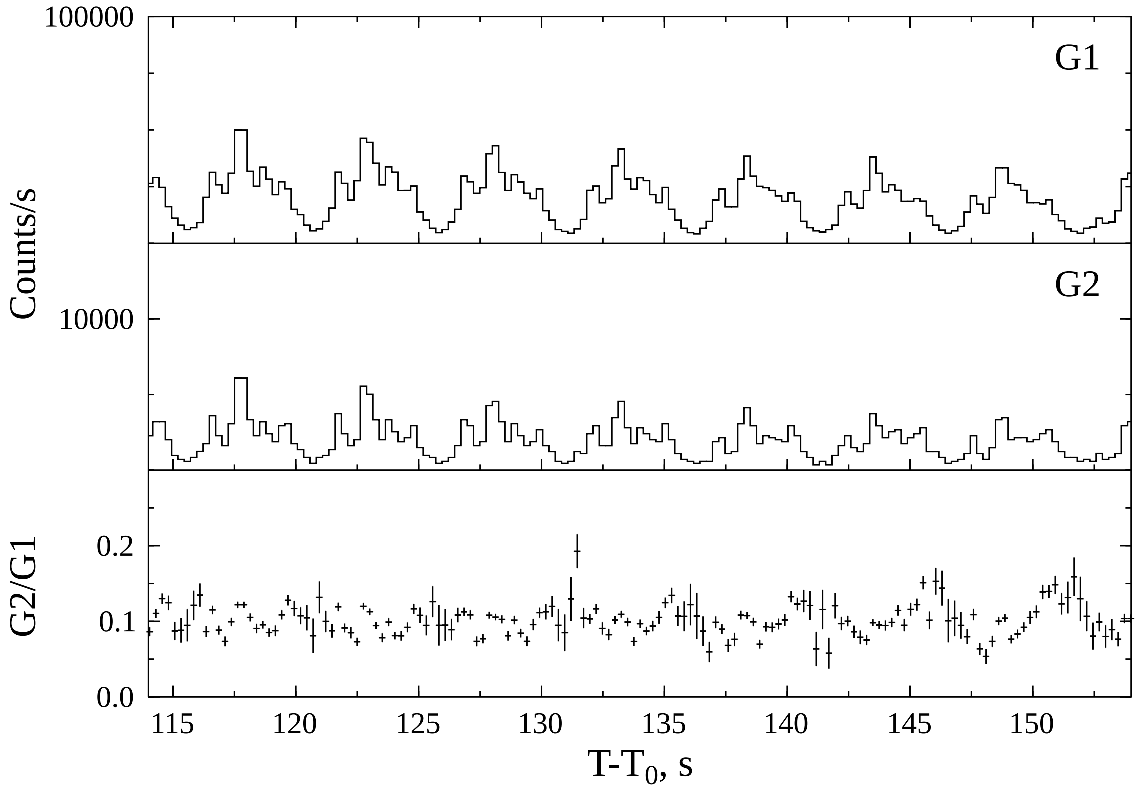

Fig. 3.30.— Pulsating tail of the 980827 outburst (continued).

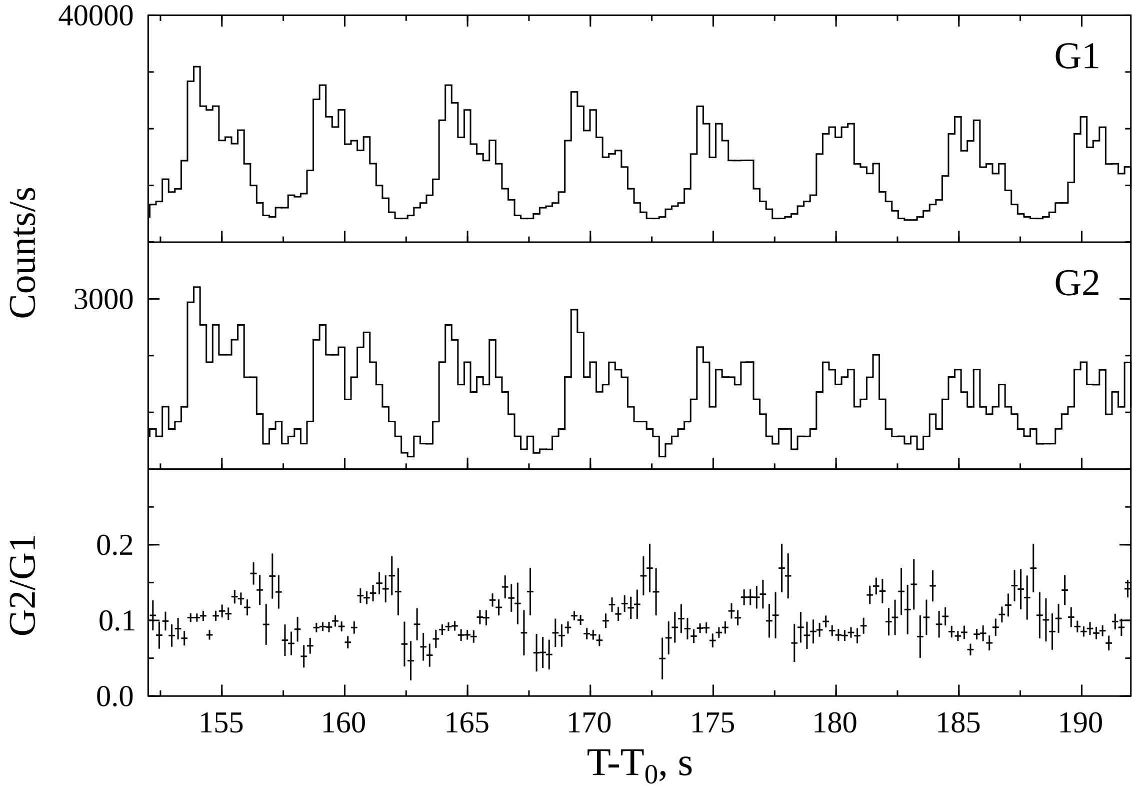

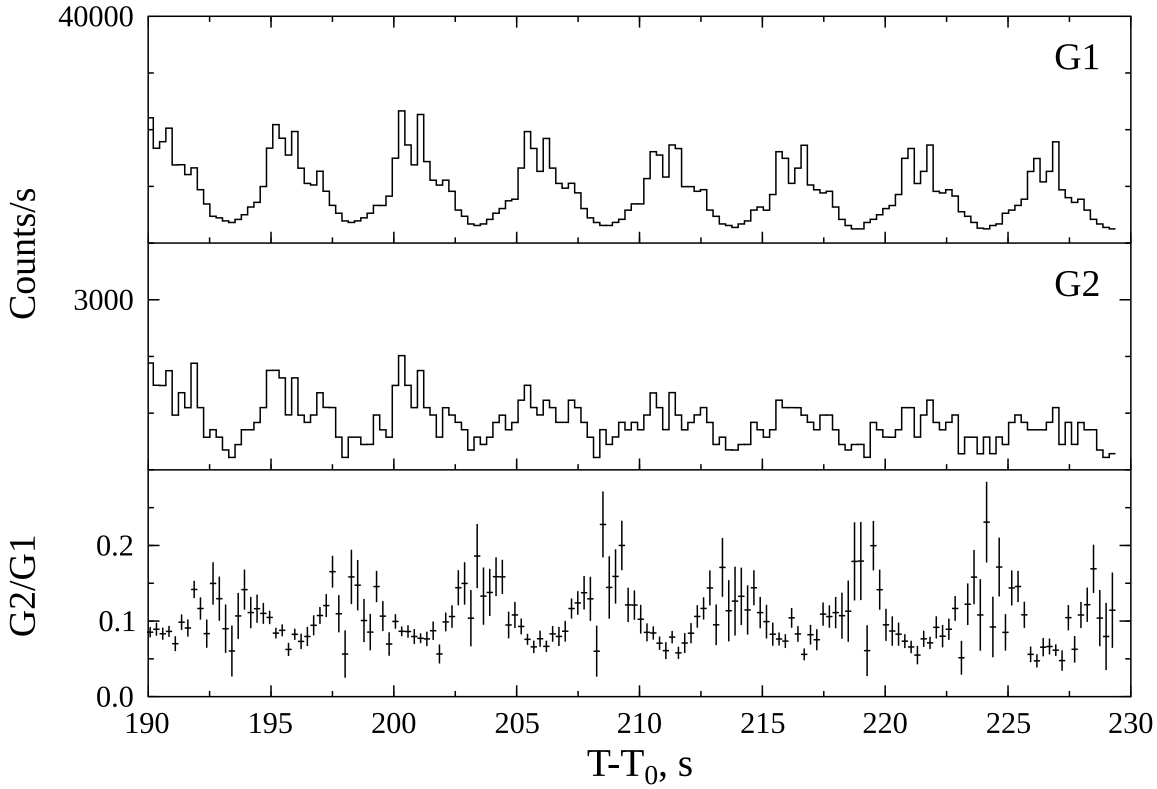

Fig. 3.31.— Pulsating tail of the 980827 outburst (continued).

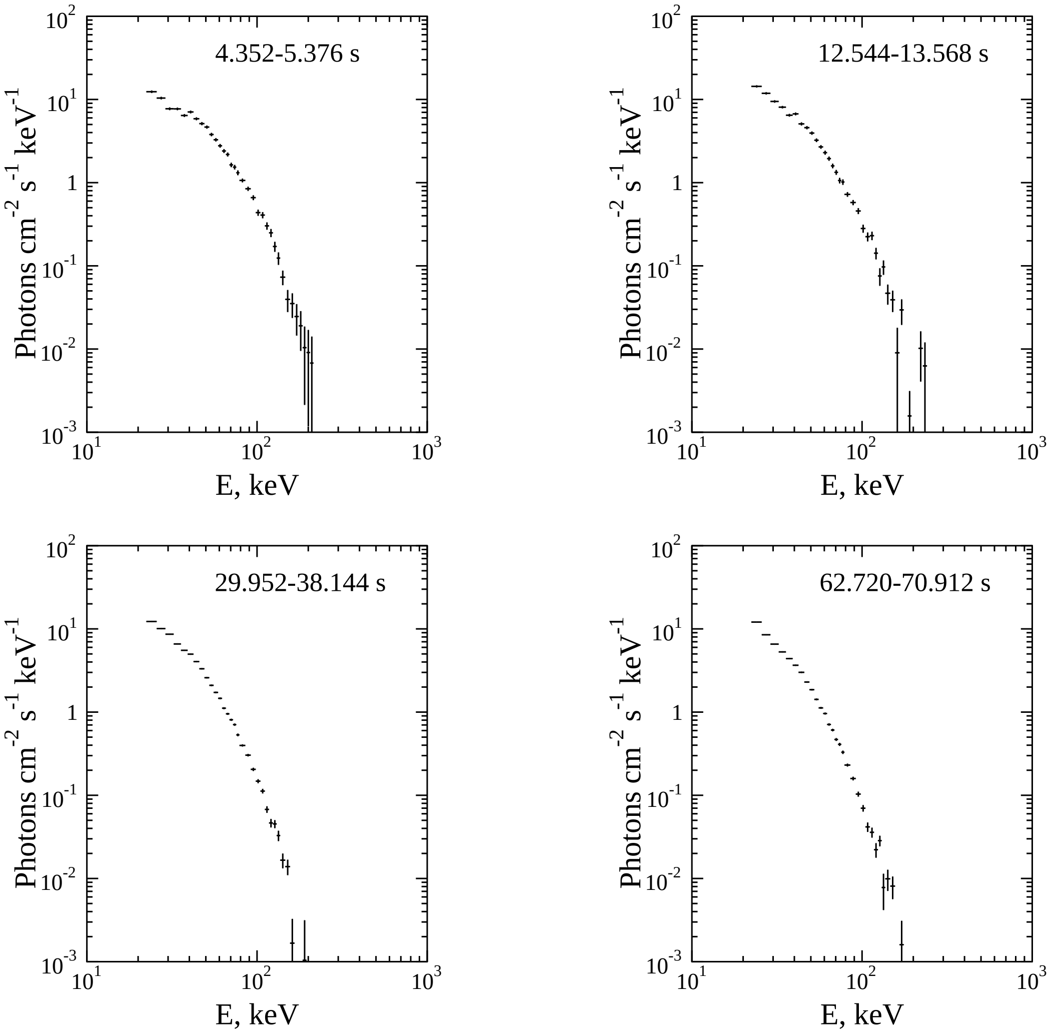

Fig. 3.32.— Some energy spectra of the 980827 outburst (For more details see Mazets et al. 1999).

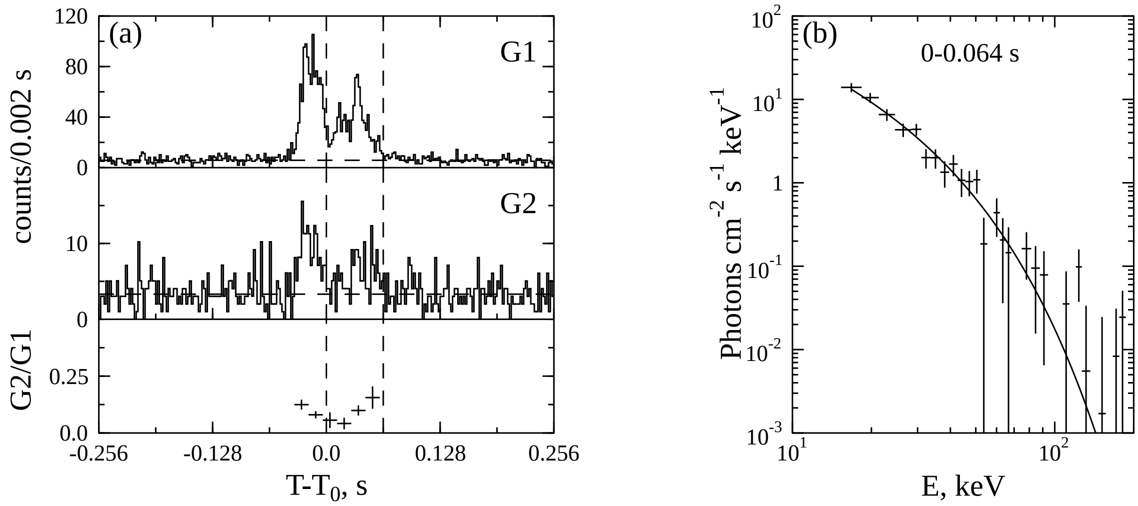

Fig. 3.33.— Burst 980828.

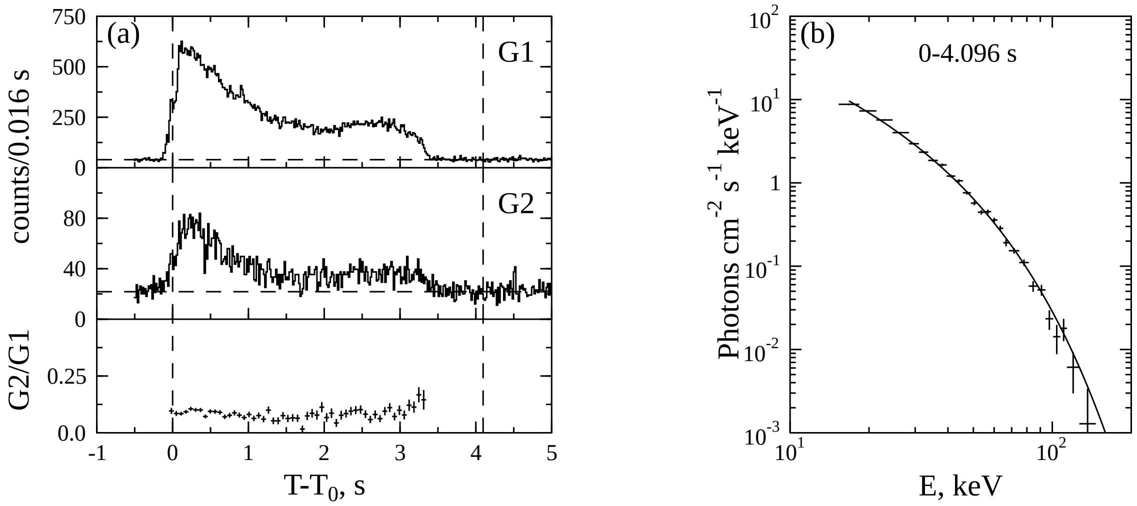

Fig. 3.34.— Long burst 980829a.

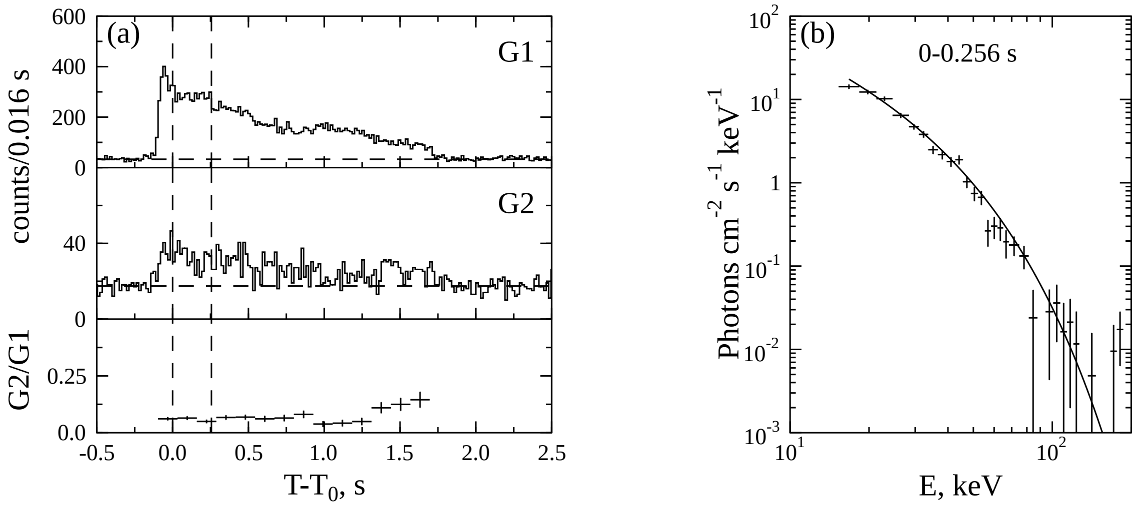

Fig. 3.35.— Long burst 980829b.

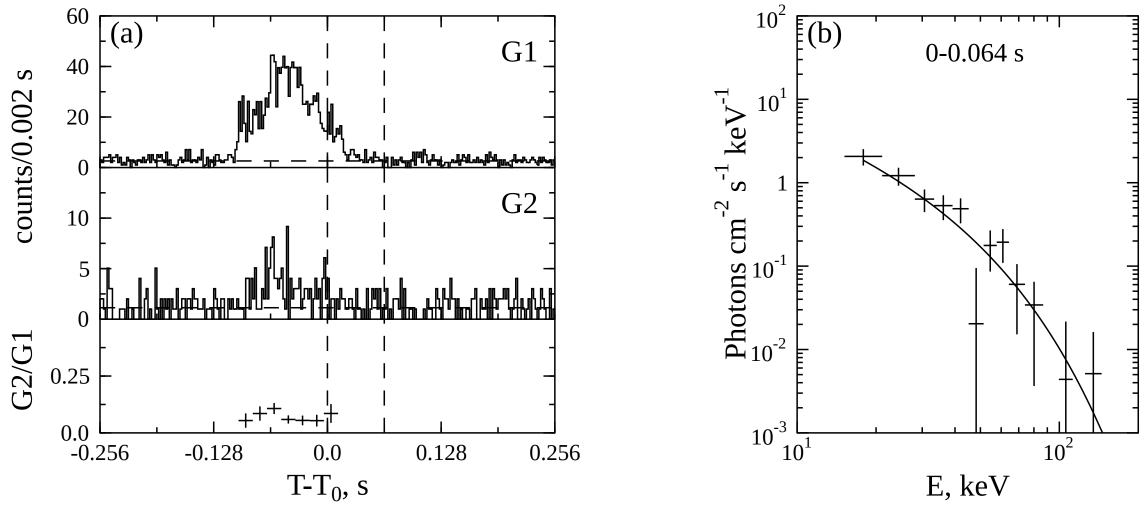

Fig. 3.36.— Burst 980831a.

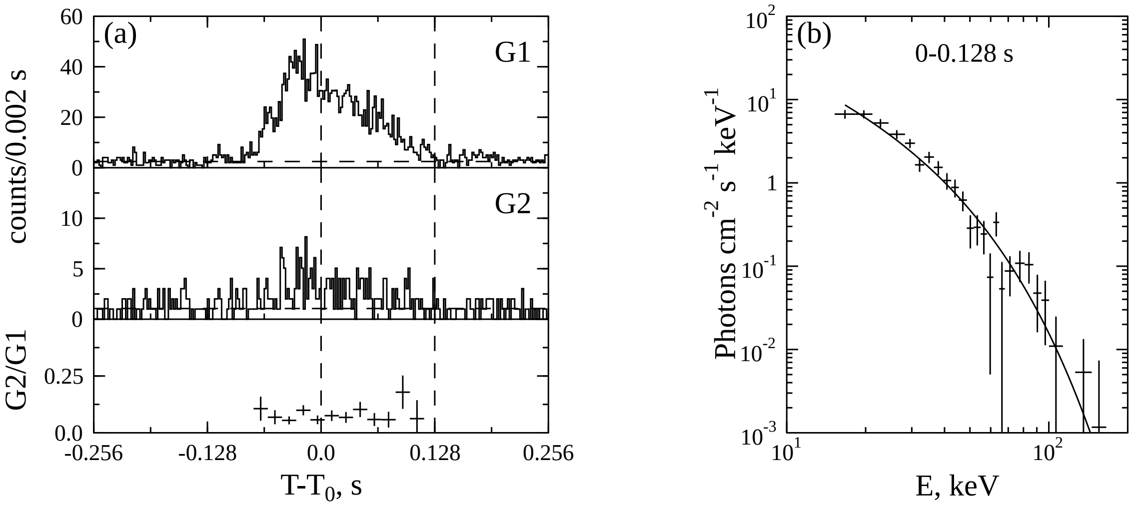

Fig. 3.37.— Burst 980831b.

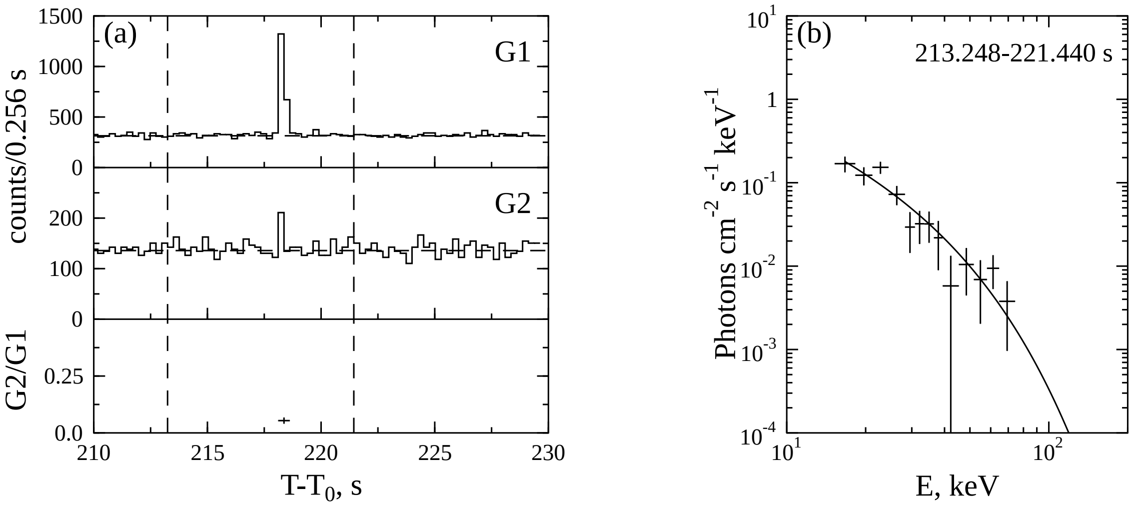

Fig. 3.38.— Burst 980831b (continued).

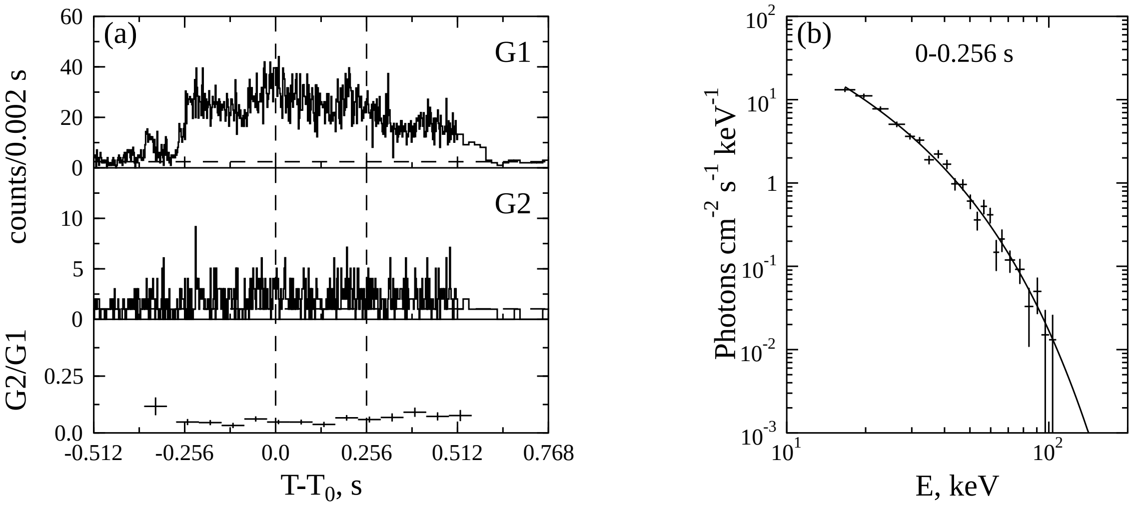

Fig. 3.39.— Burst 980831c.

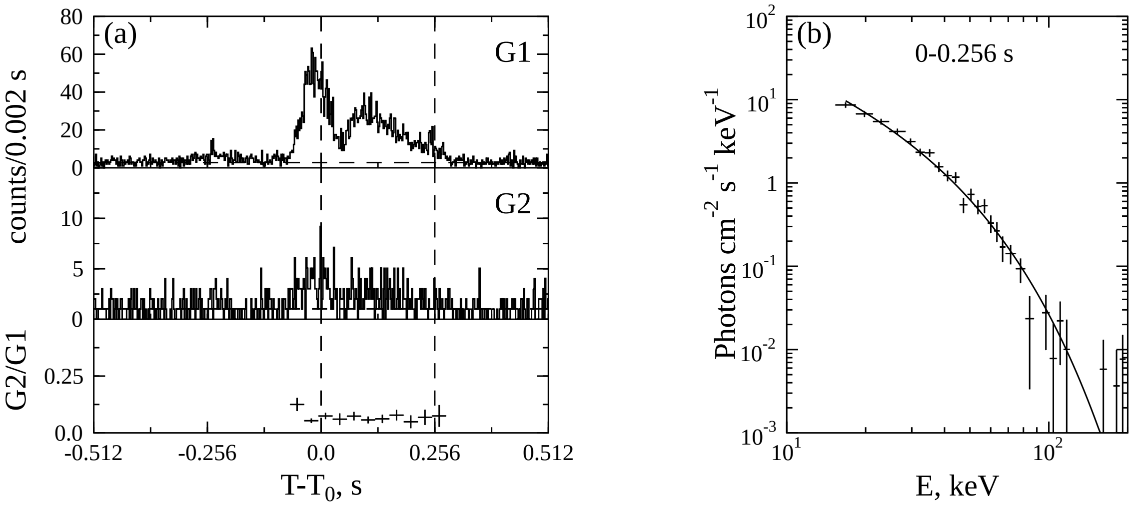

Fig. 3.40.— Burst 980901a.

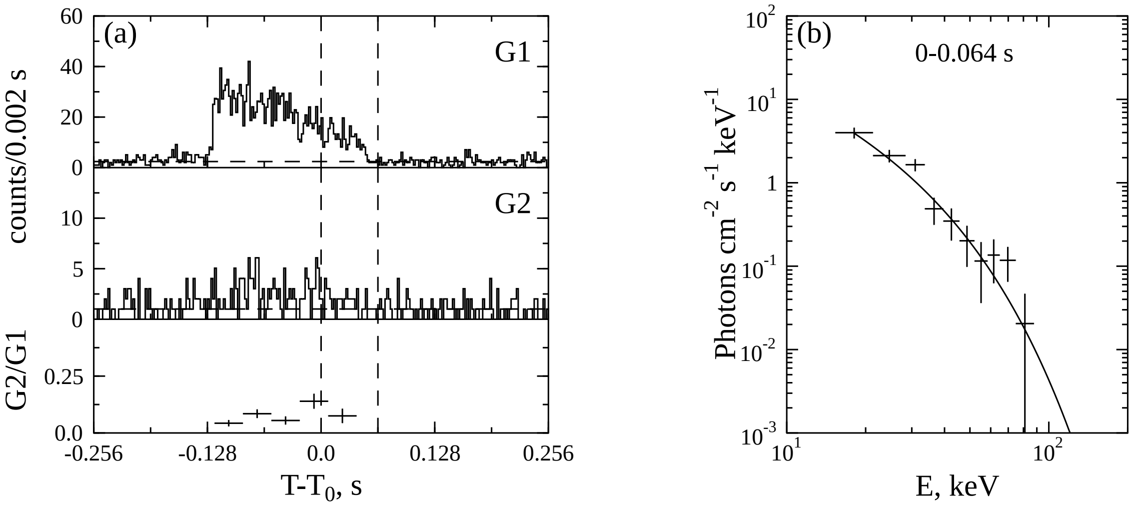

Fig. 3.41.— Event 980901c comprised a series of bursts. First burst caused a trigger.

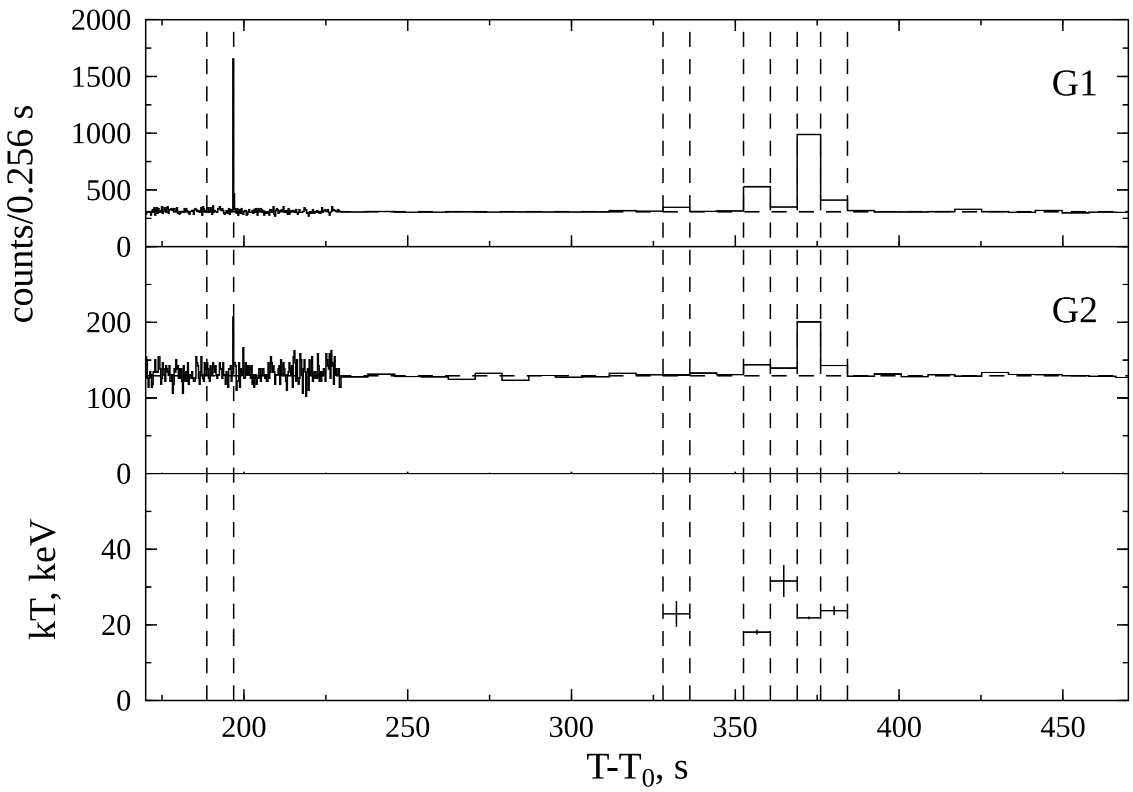

Fig. 3.42.— Final phase of the event 980901c. Unresolved cluster of bursts. Recording of the high-resolution history finished at T-T$_0$=230 s, but spectral measurements with accumulation times of 8.192 s continued. This allowed the extraction of time history records with coarse time resolution but fine spectral resolution. Corresponding average values of kT are also displayed. Features at T-T$_0$ $\simeq$350-380 s obviously consisted of many unresolved bursts. The accumulated fluence of the $\sim$ 30 s long cluster (see the Table) was up to 2×10^{-5} erg cm^{-2}. Note for comparison that the accumulated fluence for the most crowded 20 s long interval of burst series on 1998 May 30 is 4×10^{-5} erg cm^{-2}.

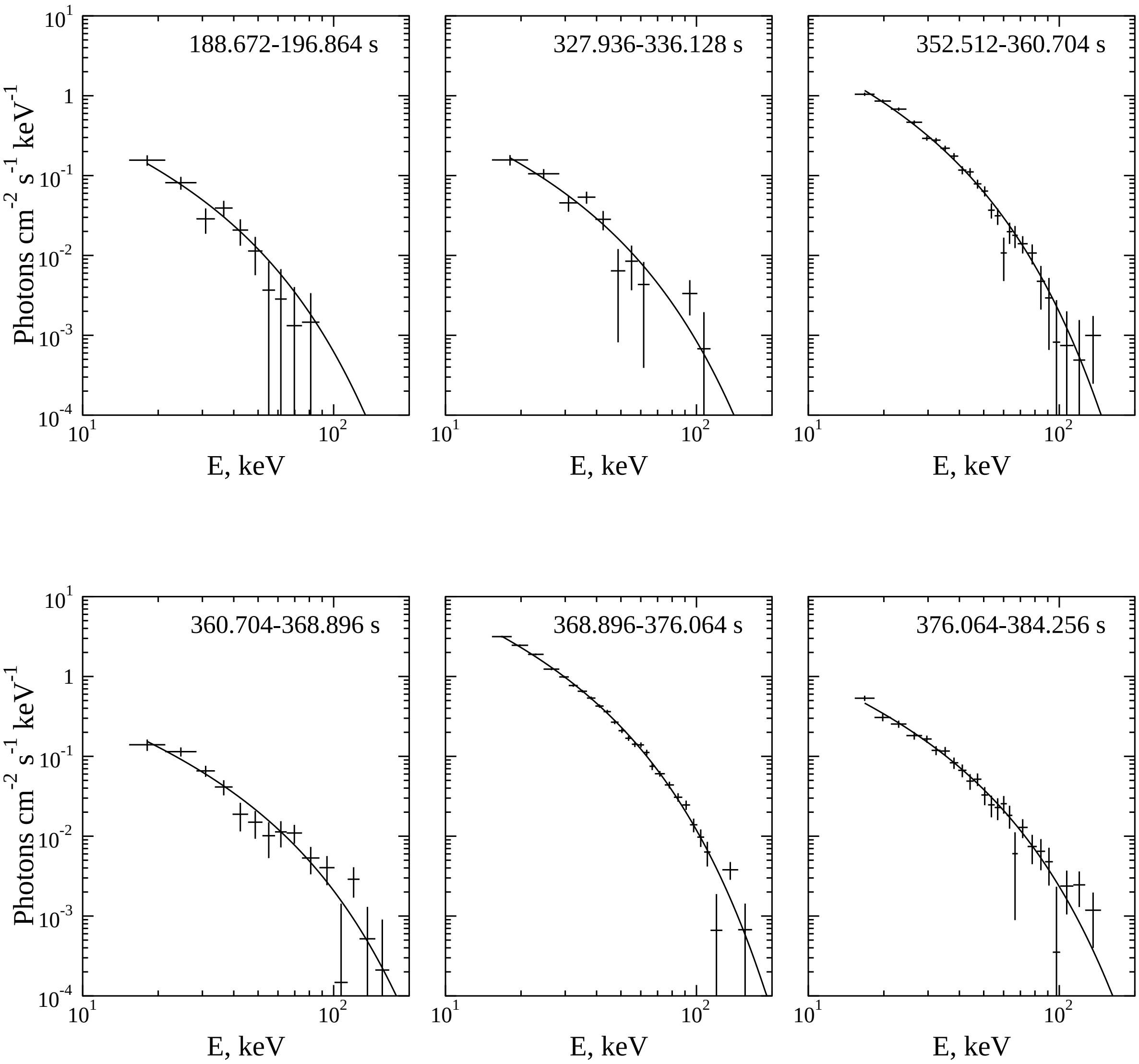

Fig. 3.43.— Energy spectra of the final phase of event 980901c.

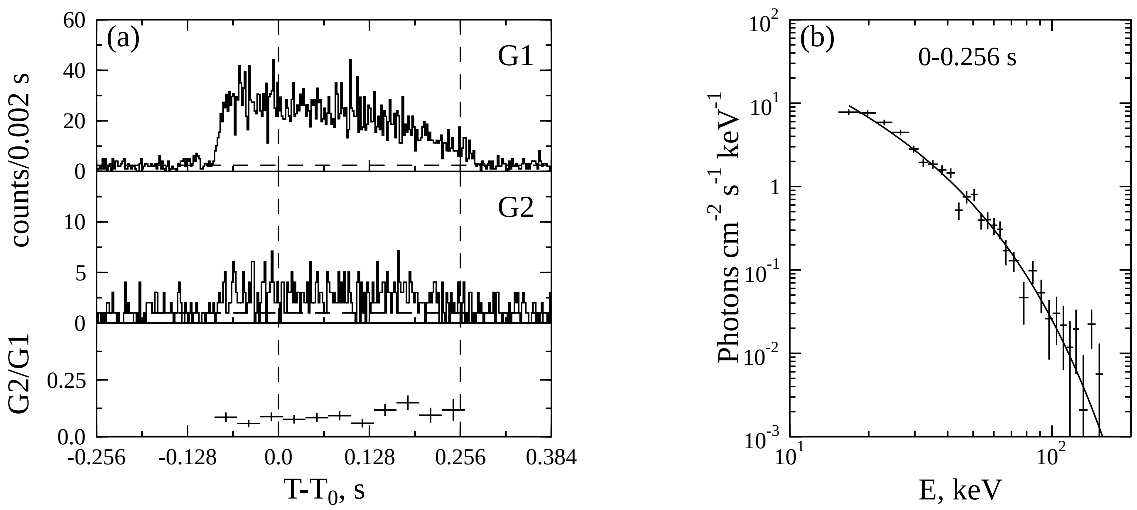

Fig. 3.44.— Burst 980902a.

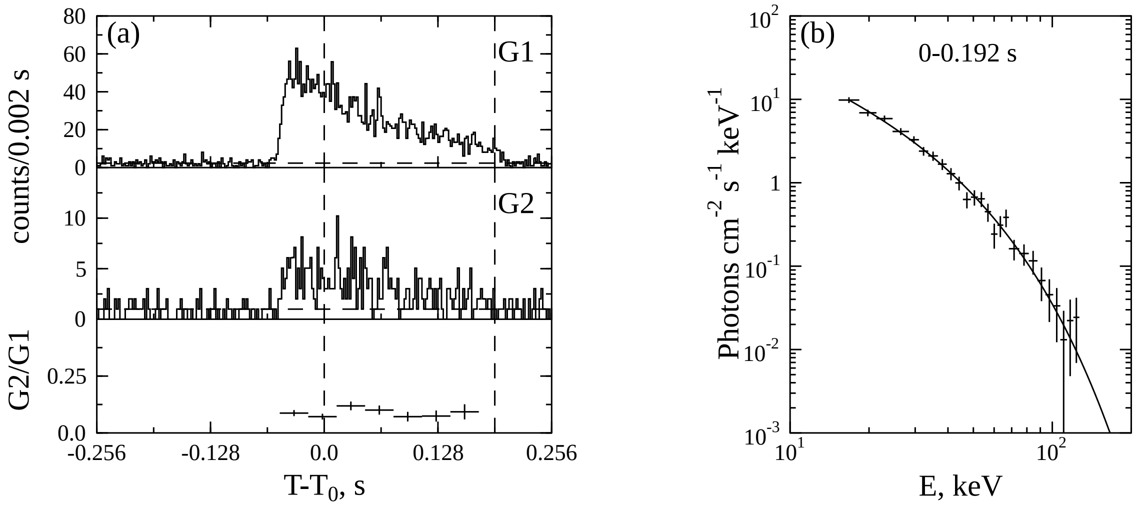

Fig. 3.45.— Burst 980902b.

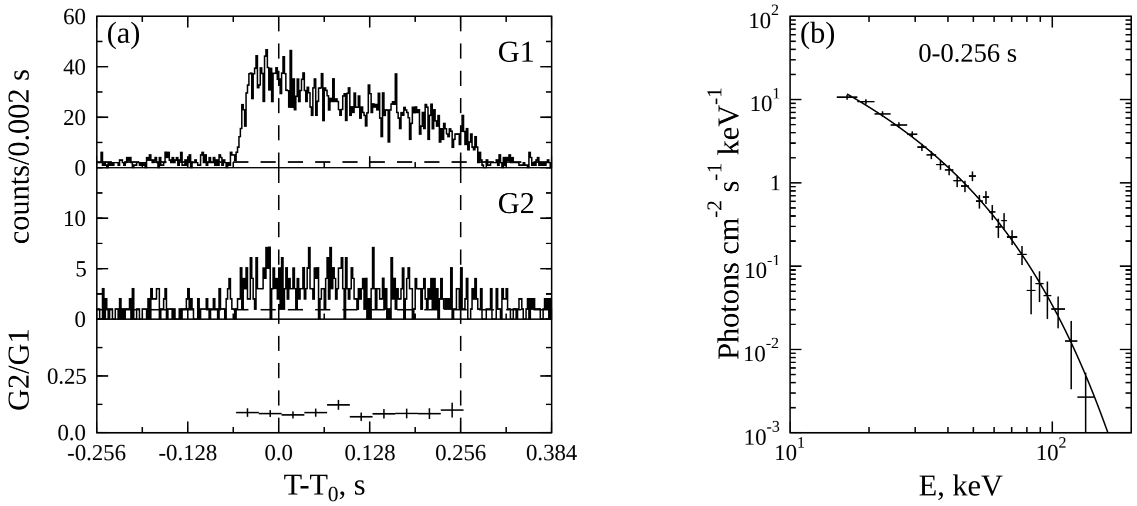

Fig. 3.46.— Burst 980911.

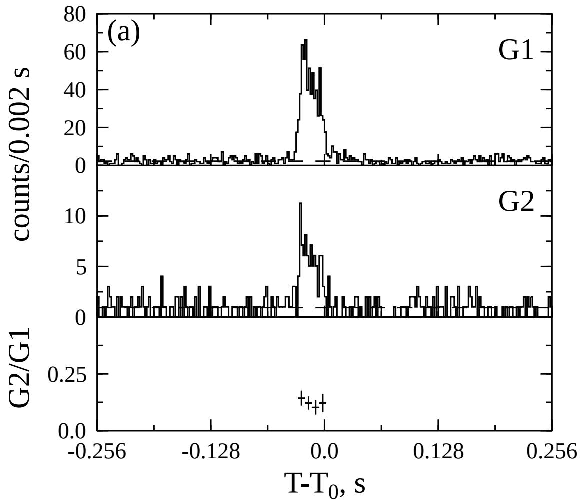

Fig. 3.47.— Burst 980912.

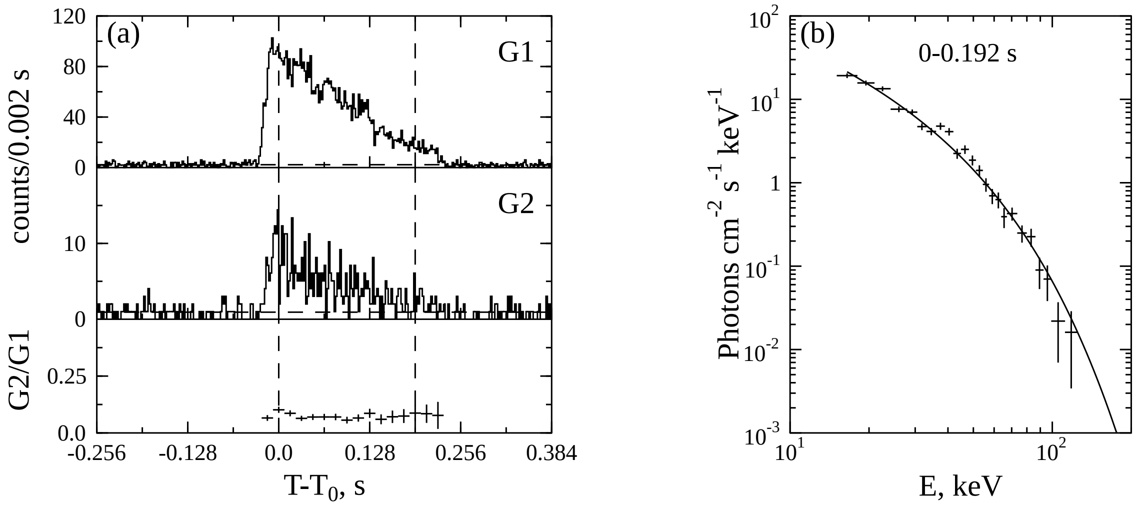

Fig. 3.48.— Burst 980915a.

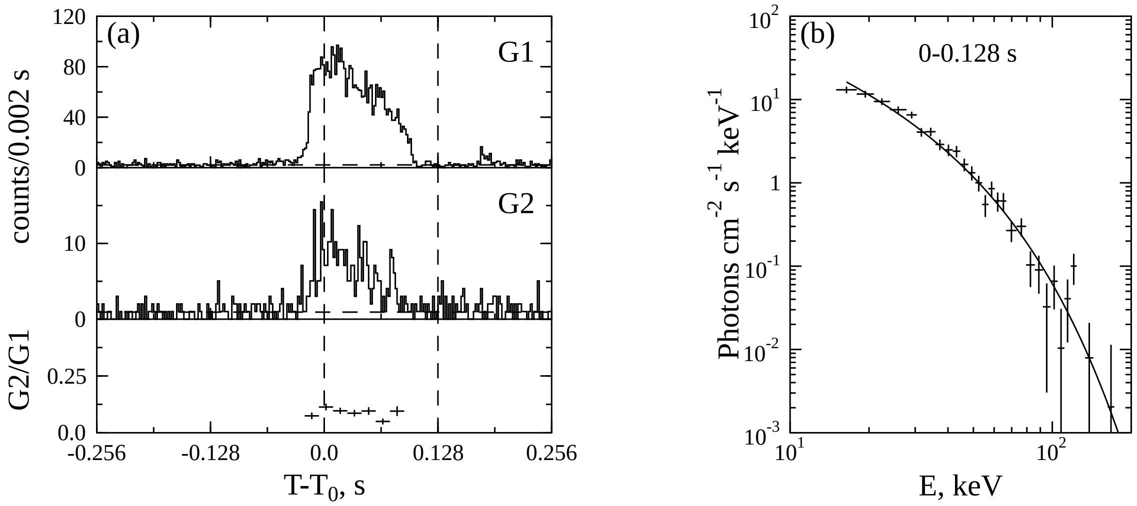

Fig. 3.49.— Burst 980917.

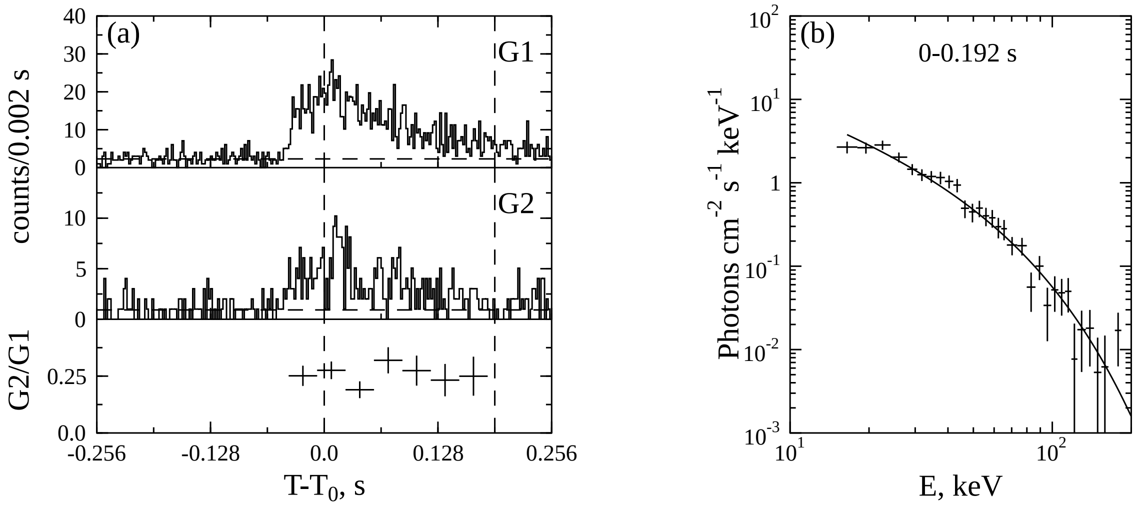

Fig. 3.50.— Burst 980927.

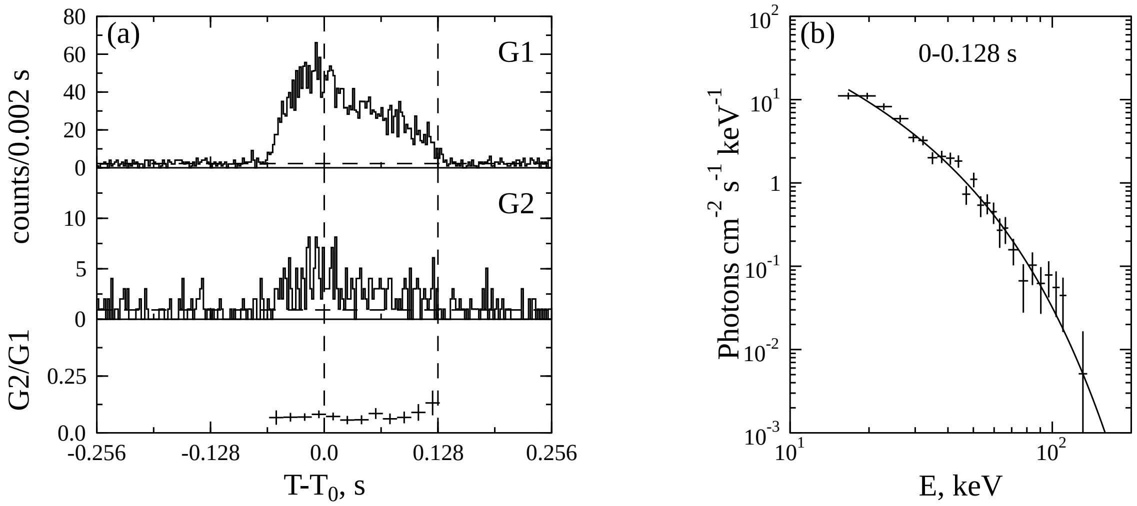

Fig. 3.51.— Burst 981013a.

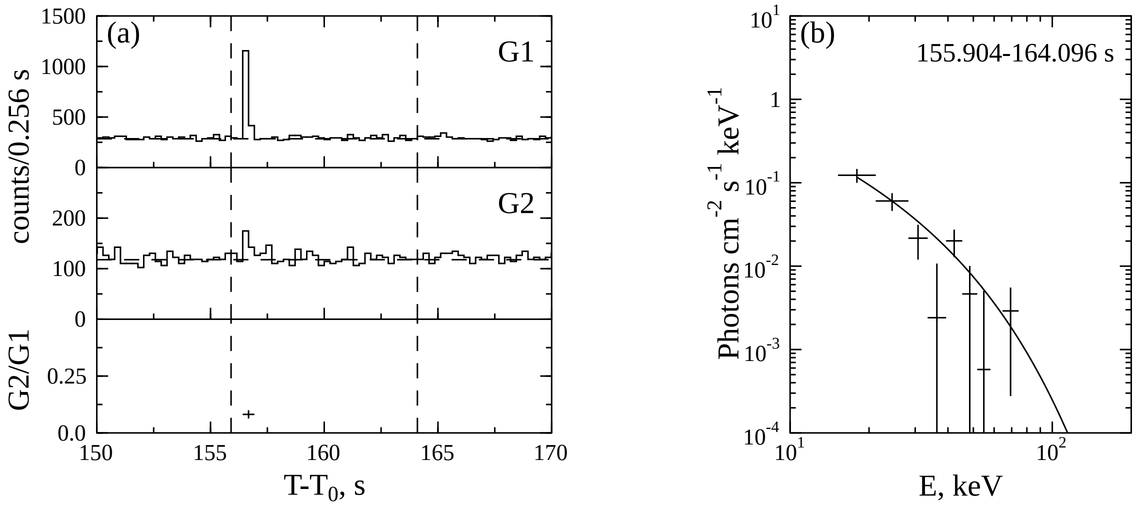

Fig. 3.52.— Burst 981013a (continued).

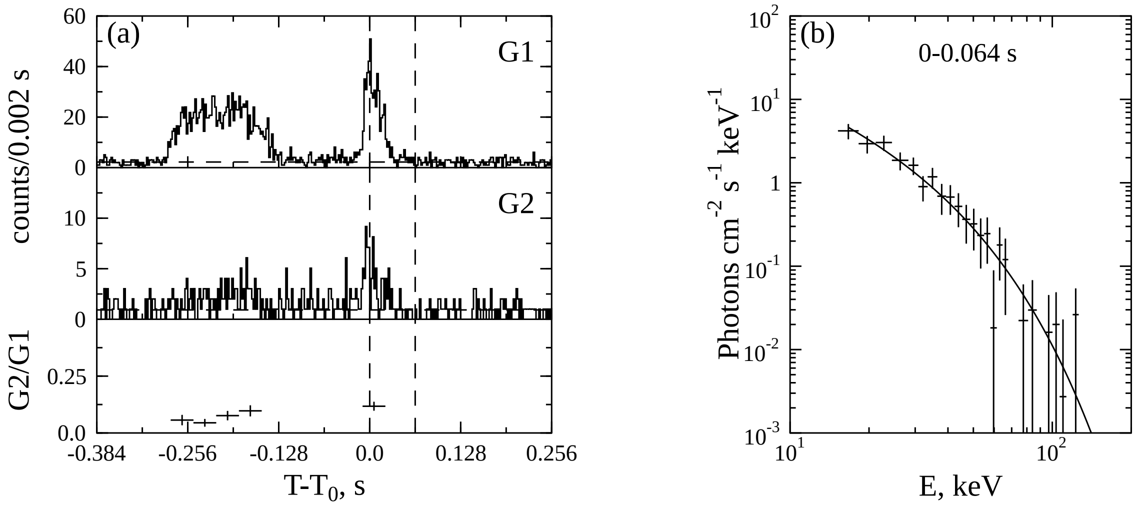

Fig. 3.53.— Burst 981013b.

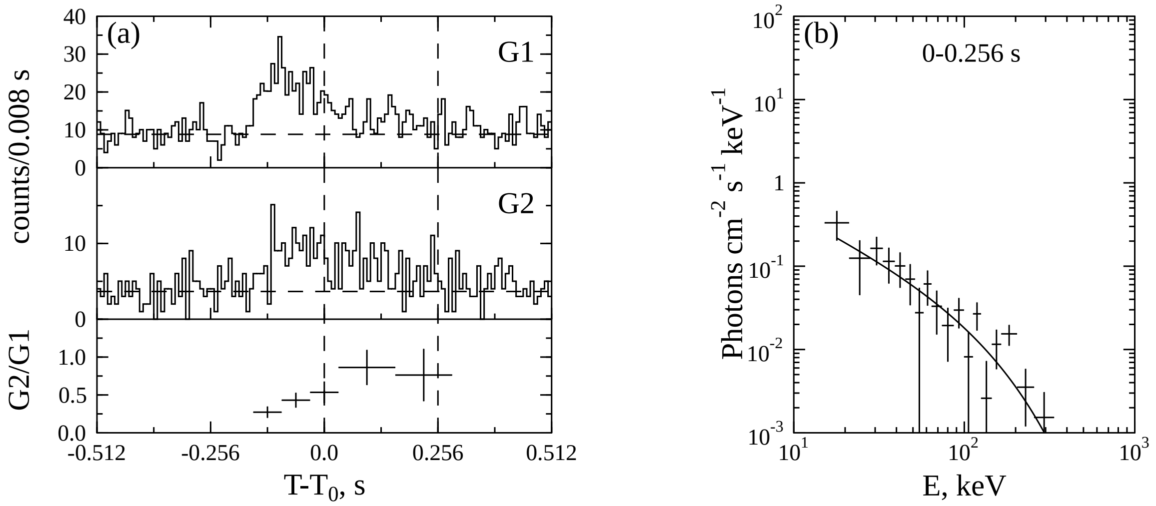

Fig. 3.54.— Burst 981022 exhibits an unusually hard energy spectrum (kT$\sim$ 100 keV) and a hardness-intensity anticorrelation (see Woods et al. 1999b). Another example of such a hard event is burst 990110. A similar hardness-intensity behaviour is also seen in the more common type of soft burst such as 980607a, 980821, 980530d.

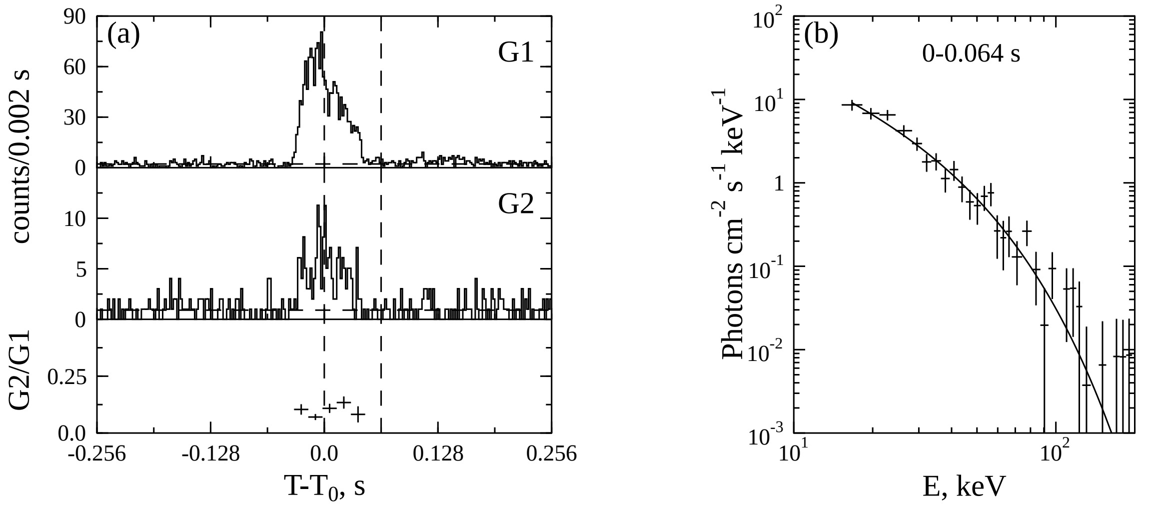

Fig. 3.55.— Event 981024 comprised a series of bursts. First burst caused a trigger.

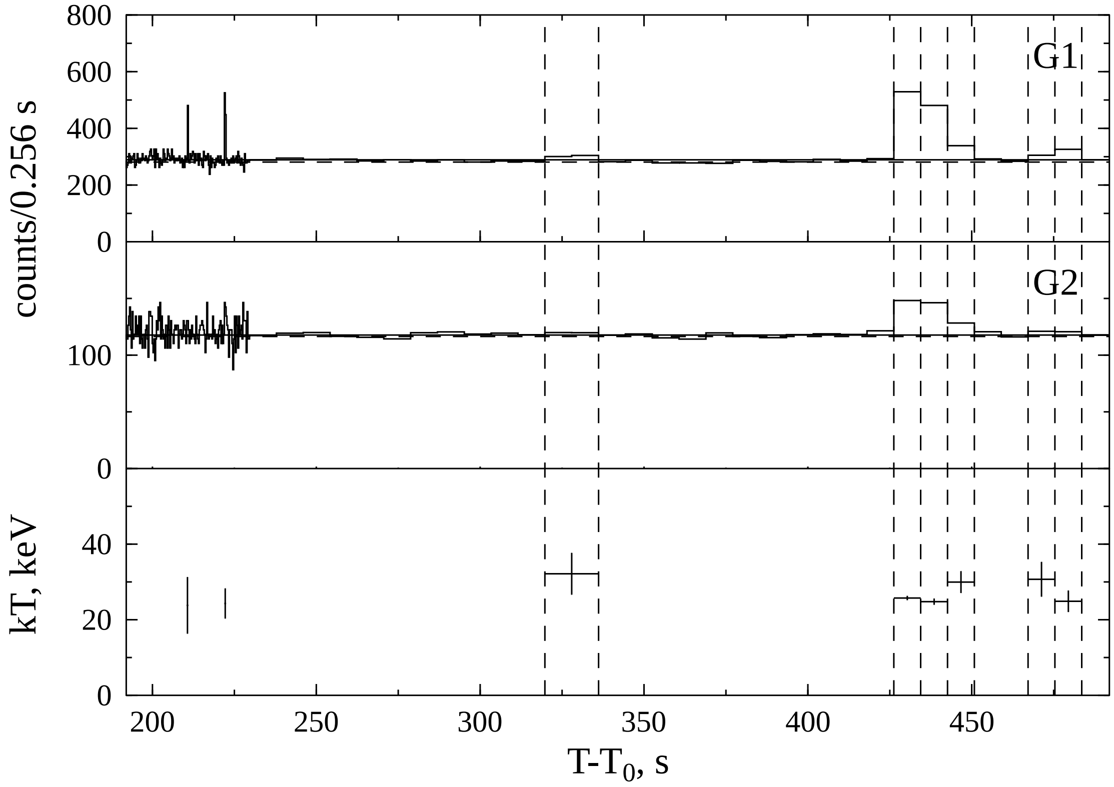

Fig. 3.56.— Event 981024. The final phase of the event. Unresolved cluster of soft bursts.

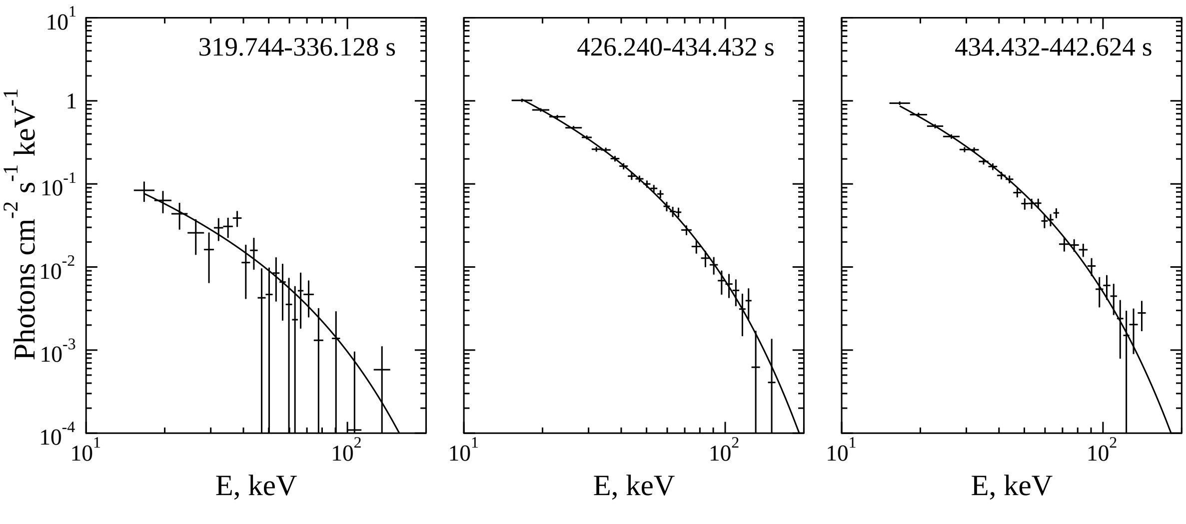

Fig. 3.57.— Event 981024. Energy spectra of the final phase.

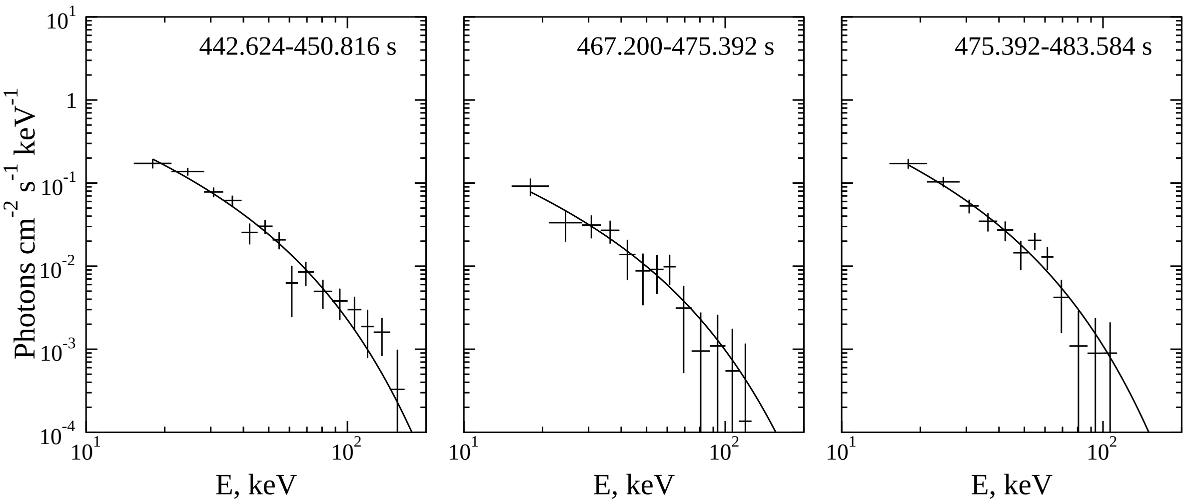

Fig. 3.58.— Event 981024. Energy spectra of the final phase (continued).

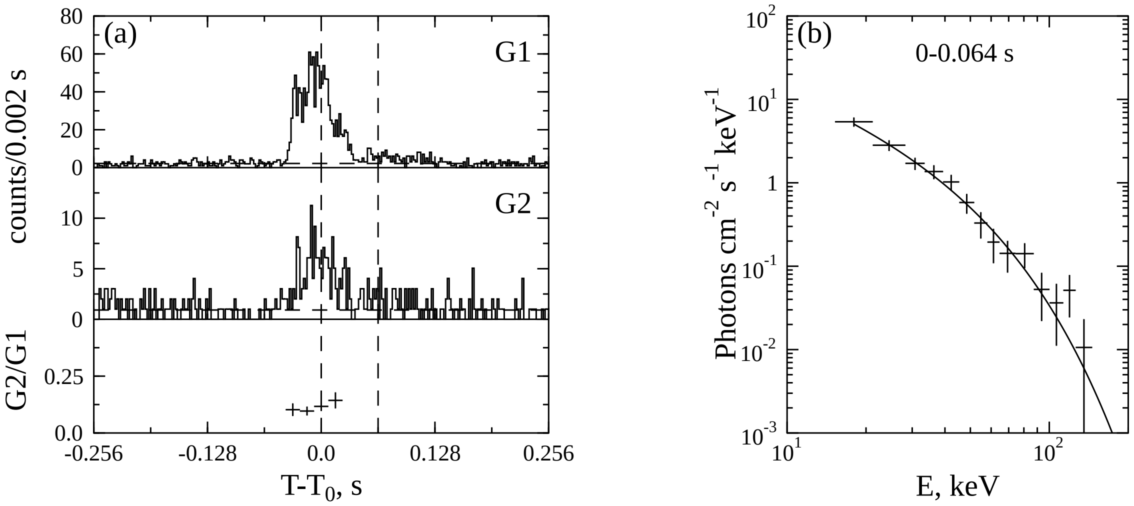

Fig. 3.59.— Burst 981028a.

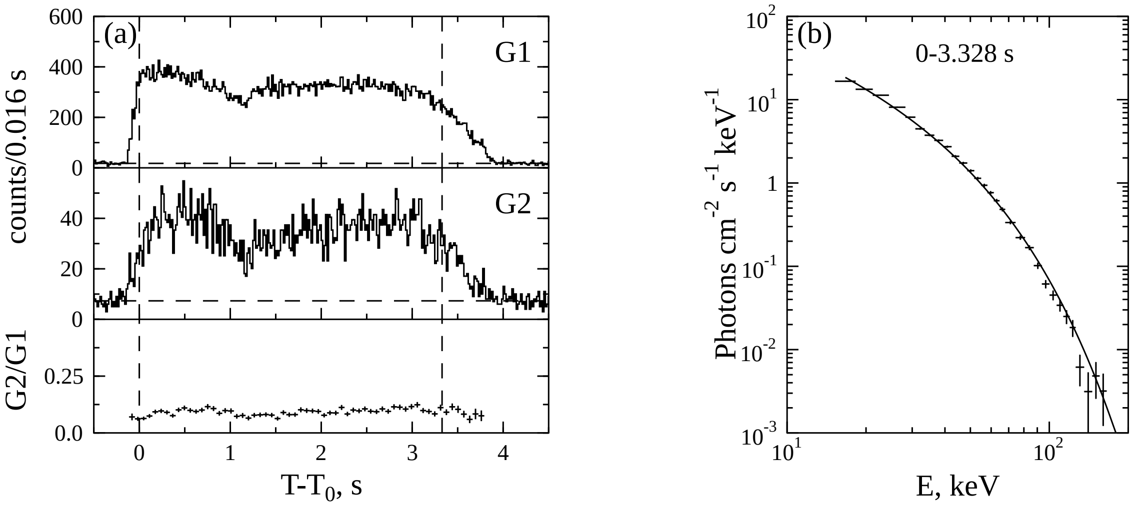

Fig. 3.60.— Long burst 981028b.

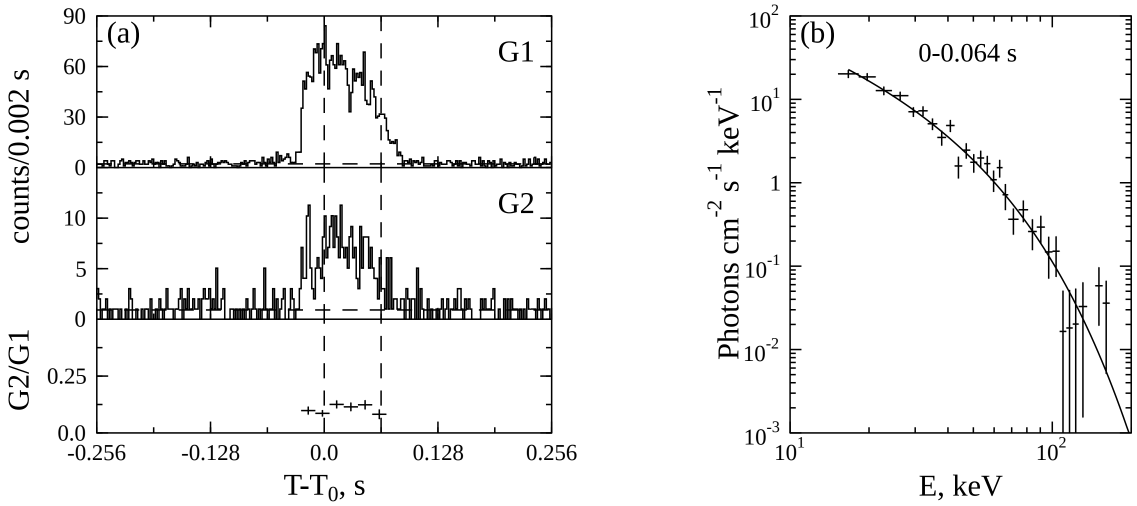

Fig. 3.61.— Burst 981029.

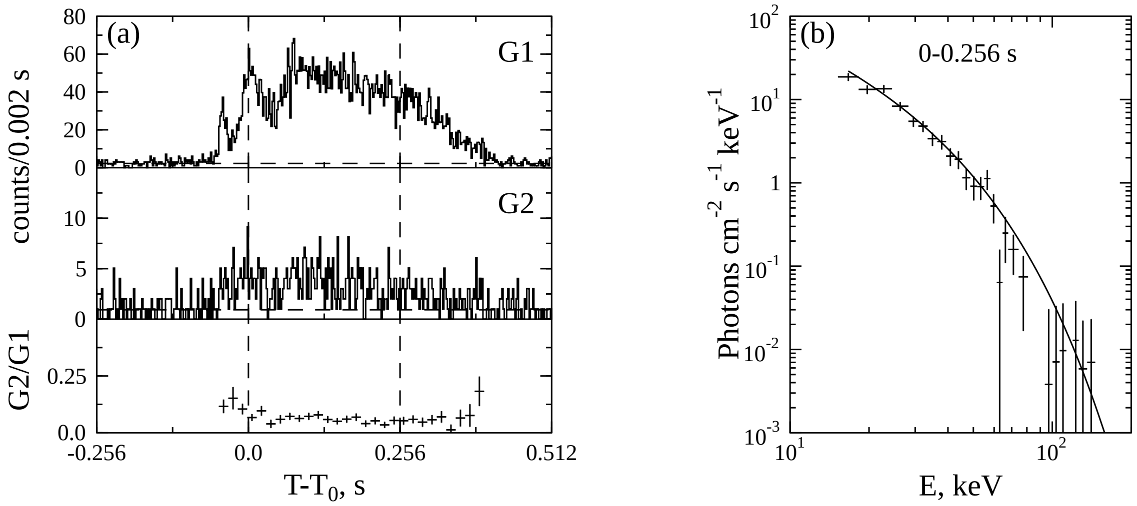

Fig. 3.62.— Burst 981031a.

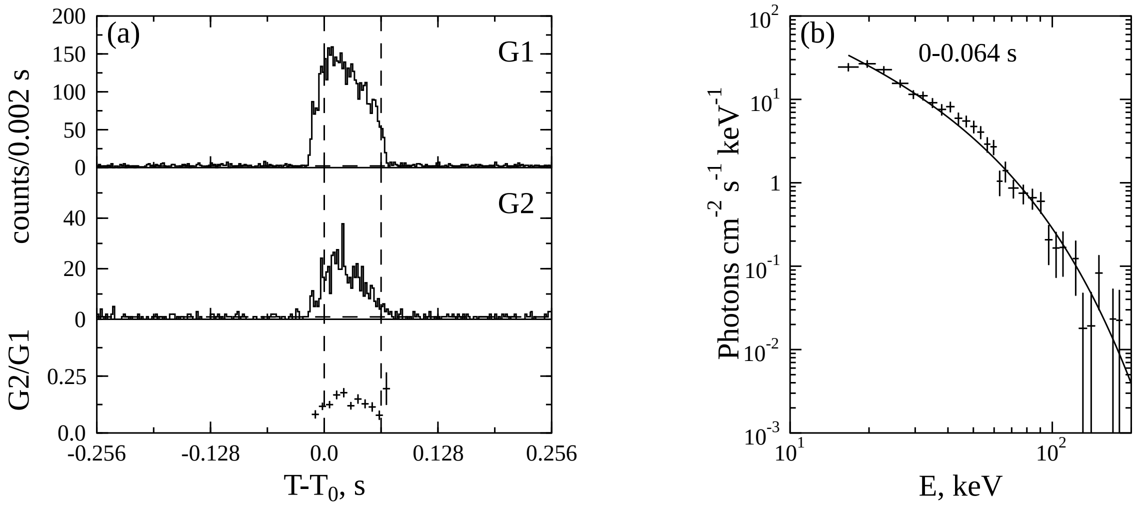

Fig. 3.63.— Burst 981031b.

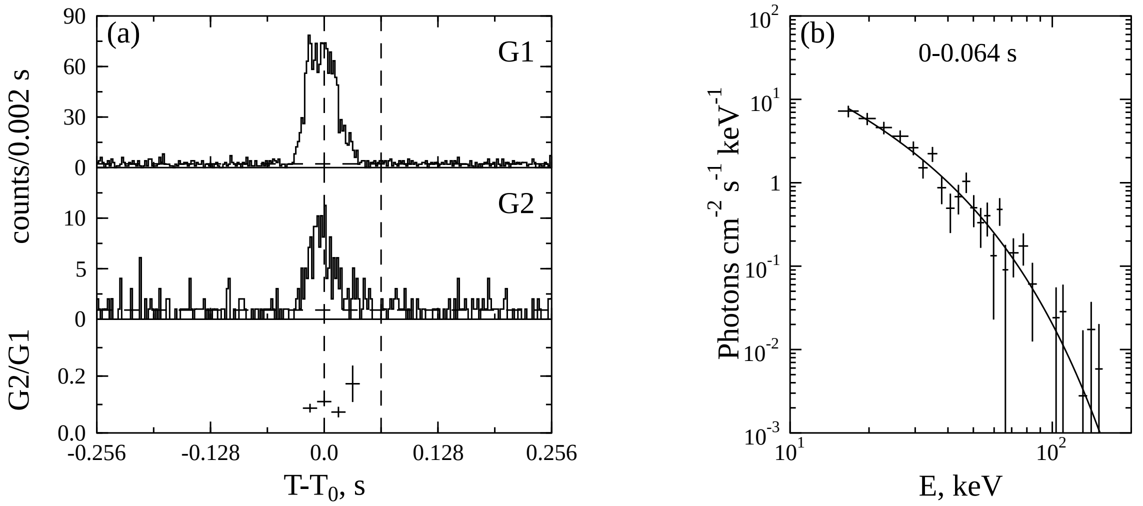

Fig. 3.64.— Burst 981109.

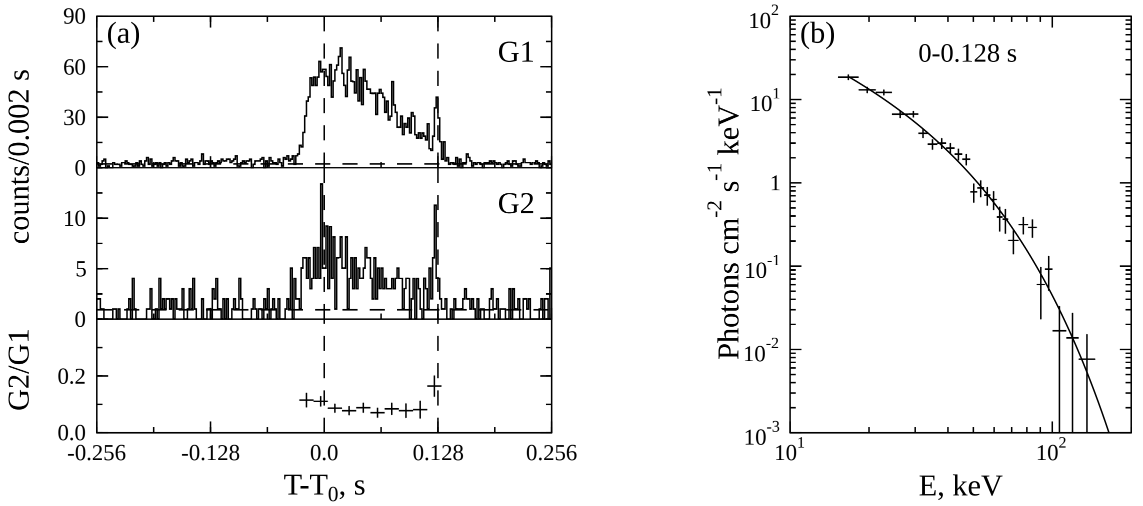

Fig. 3.65.— Burst 981130.

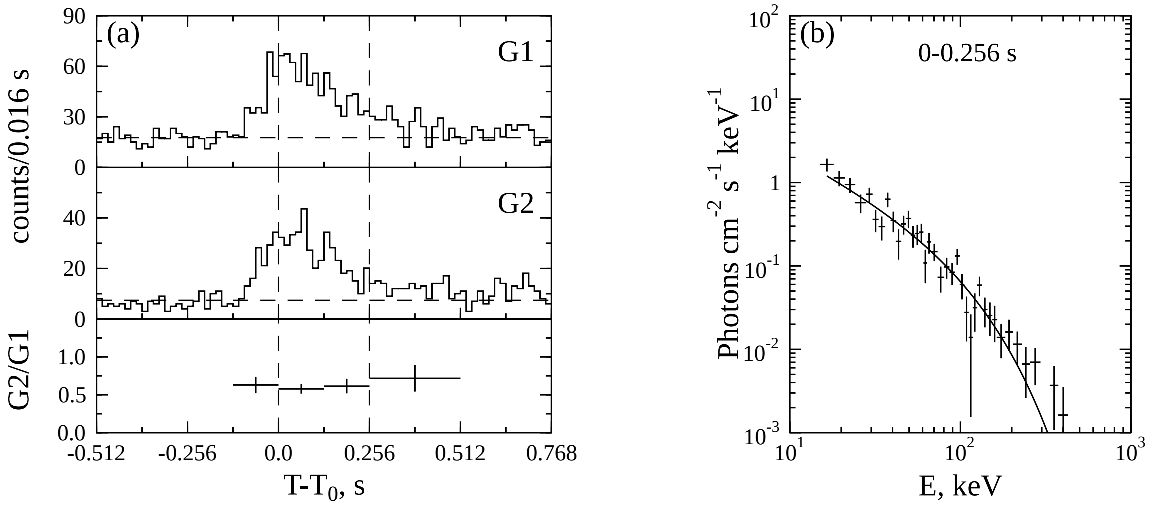

Fig. 3.66.— Burst 990110.

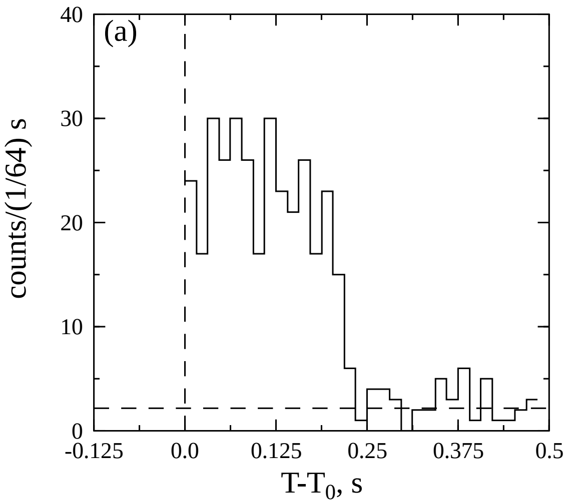

Fig. 4.1.— Burst 790107 (Venera 11).

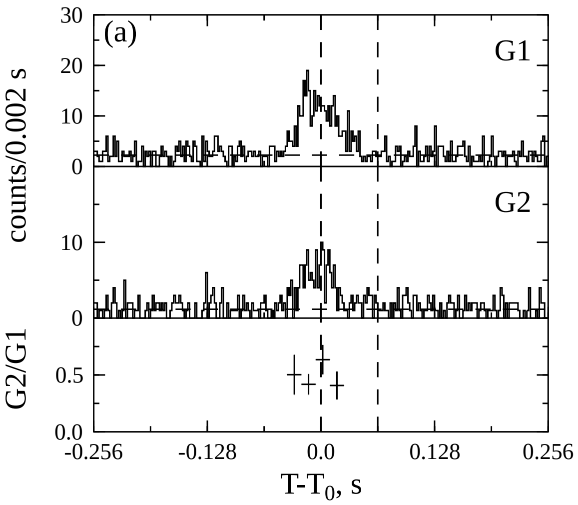

Fig. 4.2.— Burst 961026.

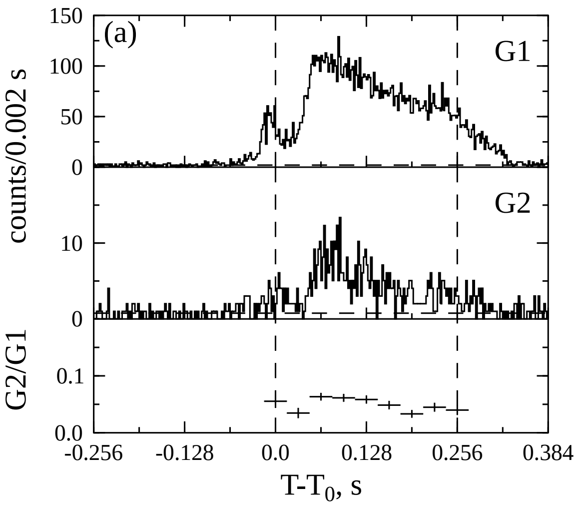

Fig. 4.3.— Burst 961118b (Kosmos 2326).

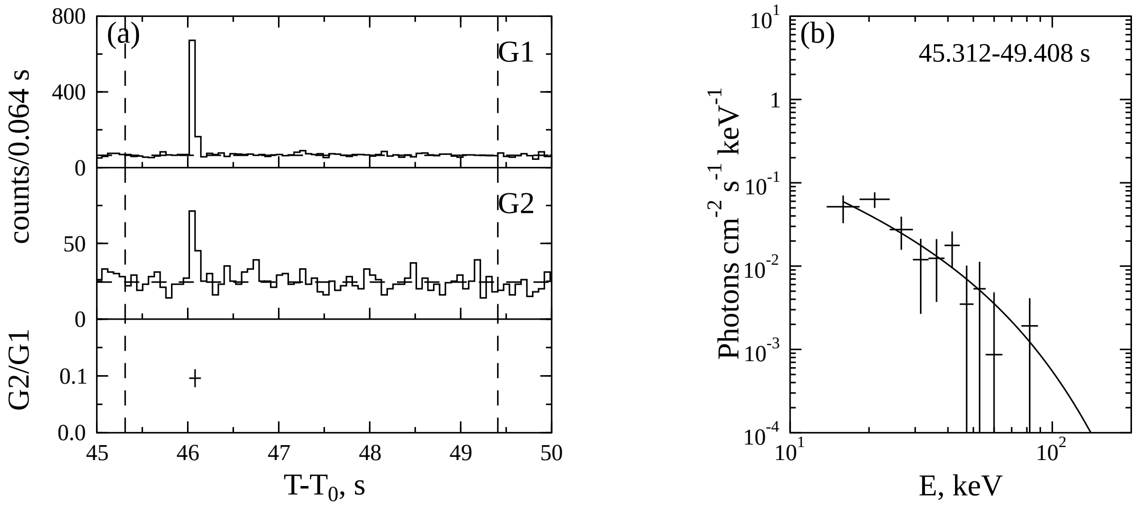

Fig. 4.4.— Burst 961118b (continued).

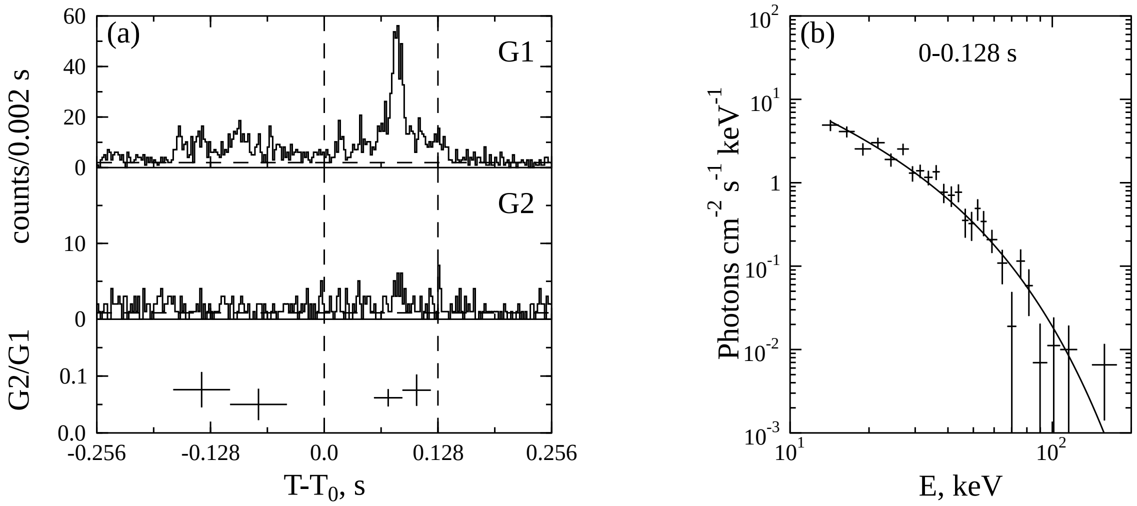

Fig. 4.5.— Burst 961118d (Kosmos 2326).

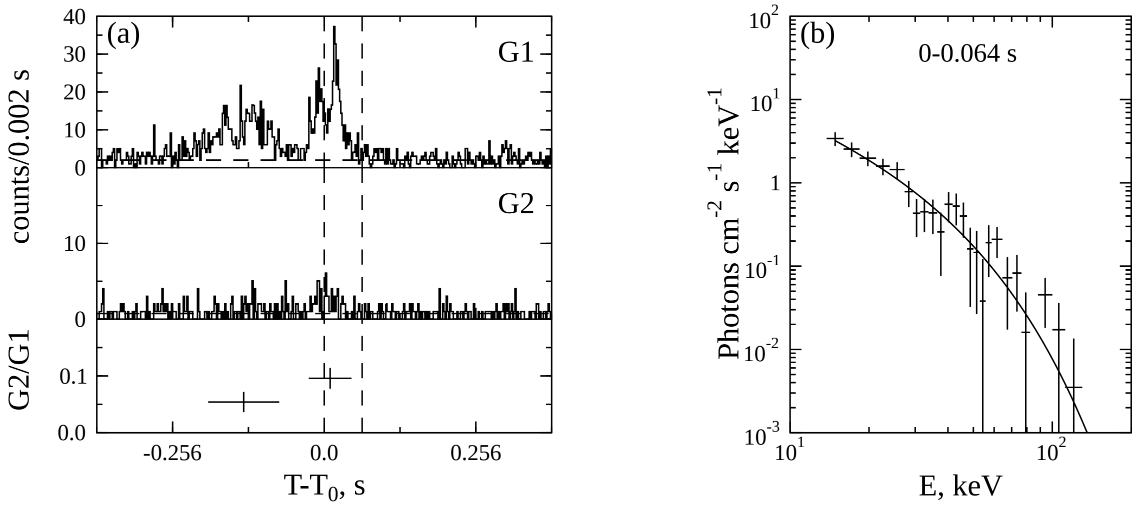

Fig. 4.6.— Burst 961119a (Kosmos 2326).

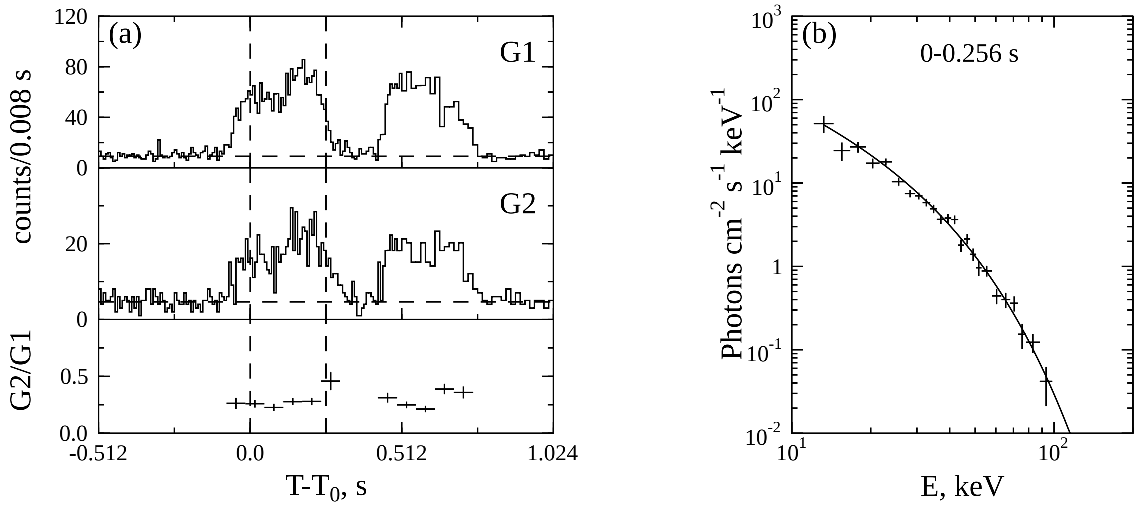

Fig. 4.7.— Burst 961119b.

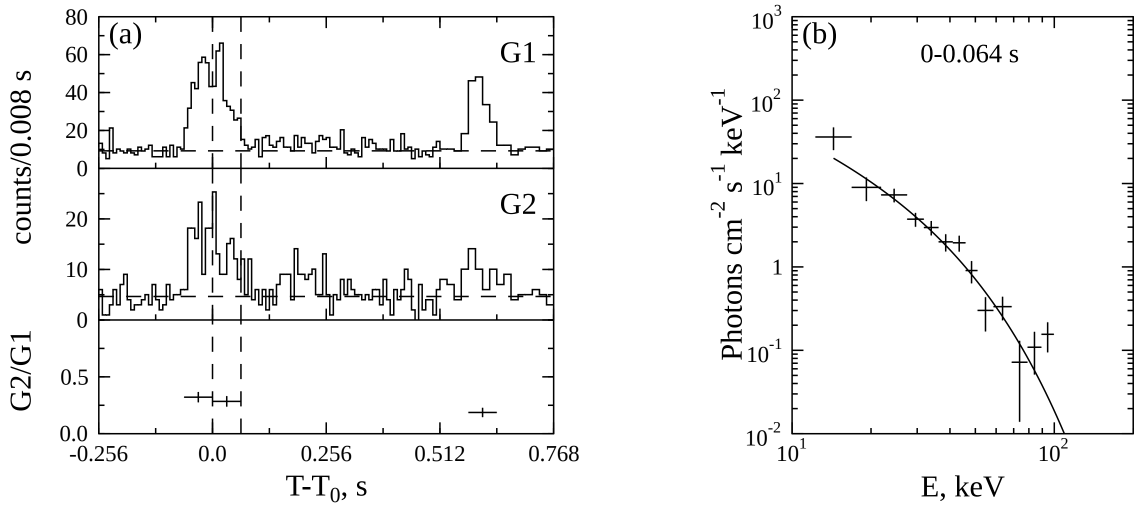

Fig. 4.8.— Burst 961119c.

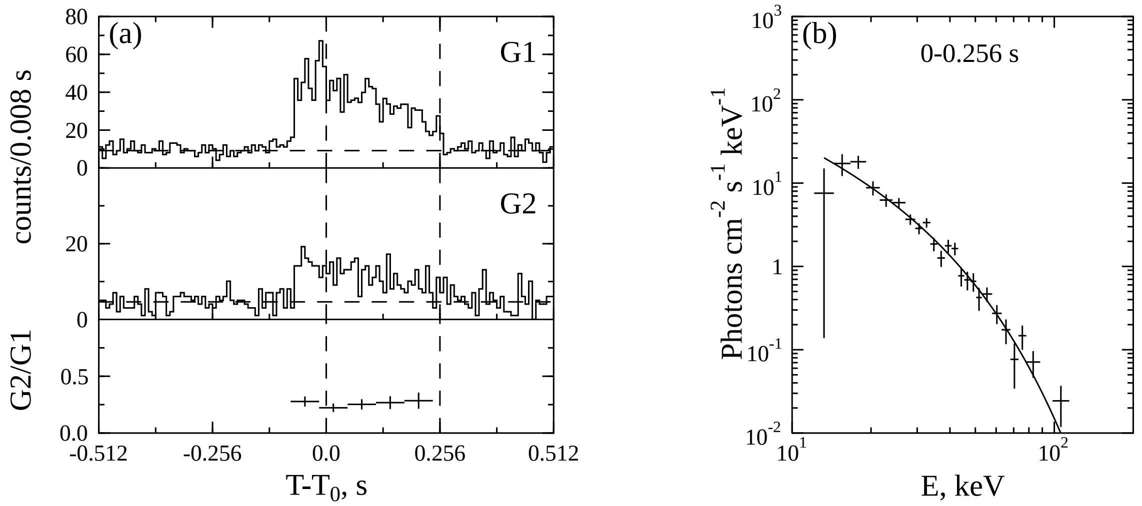

Fig. 4.9.— Burst 961119d.

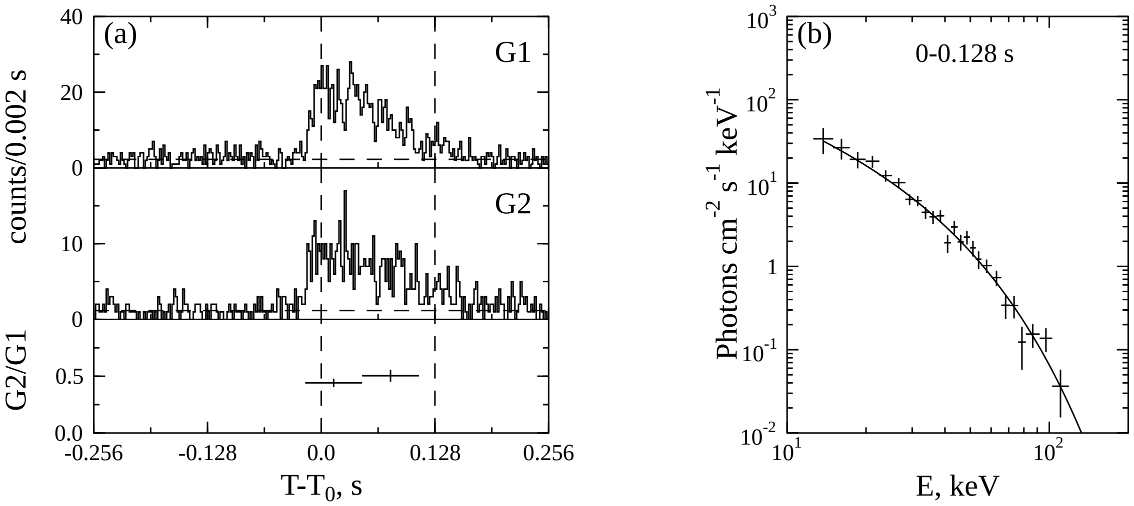

Fig. 4.10.— Burst 961122.

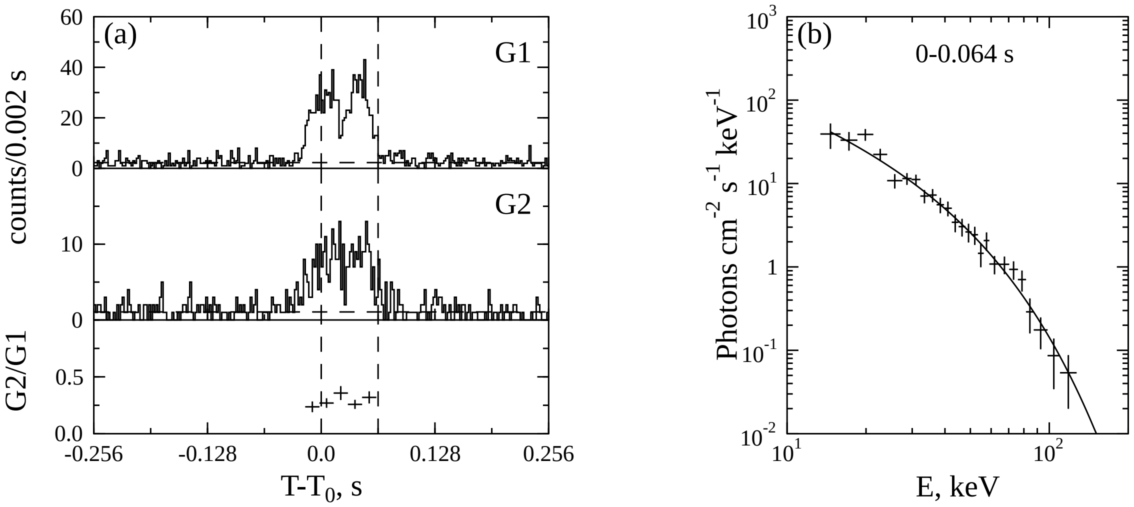

Fig. 4.11.— Burst 970902.

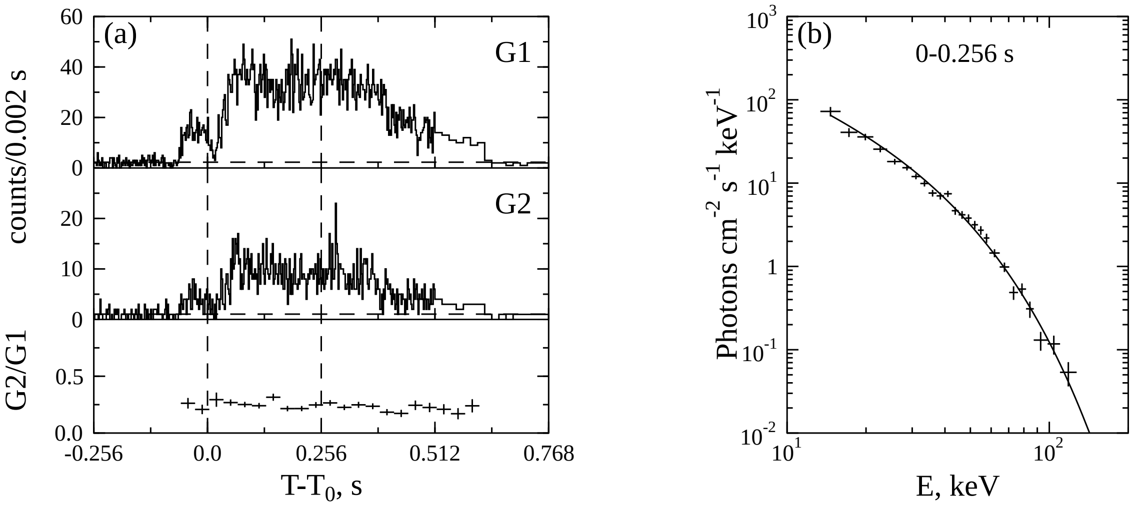

Fig. 4.12.— Burst 970912.

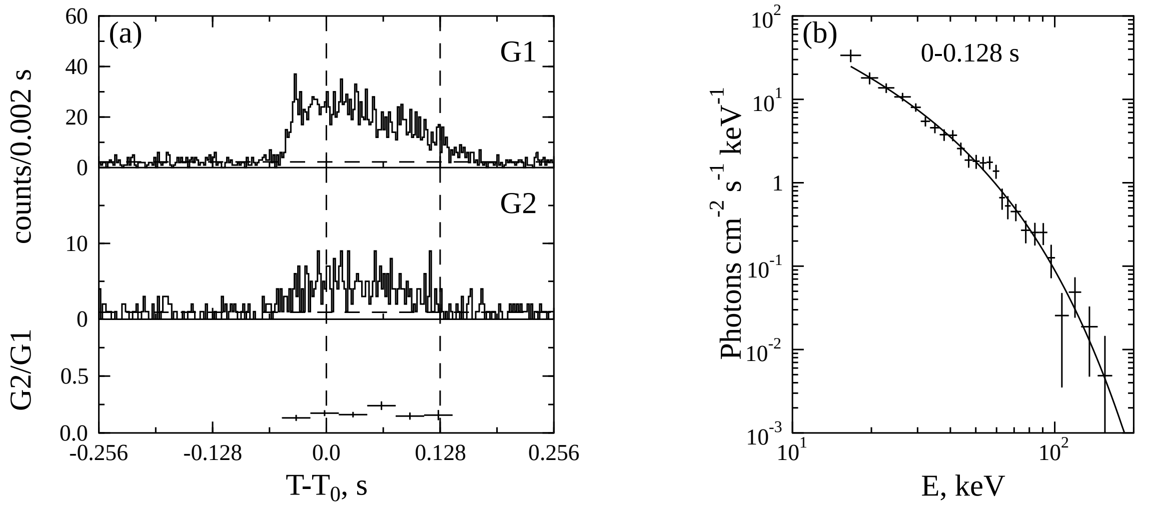

Fig. 4.13.— Burst 981017.

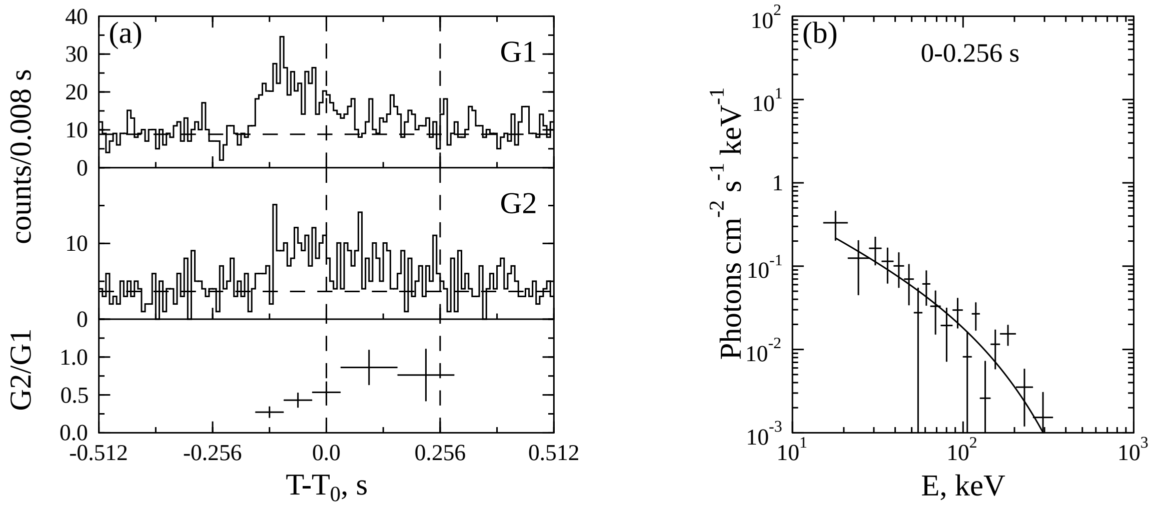

Fig. 4.14.— Burst 981022.

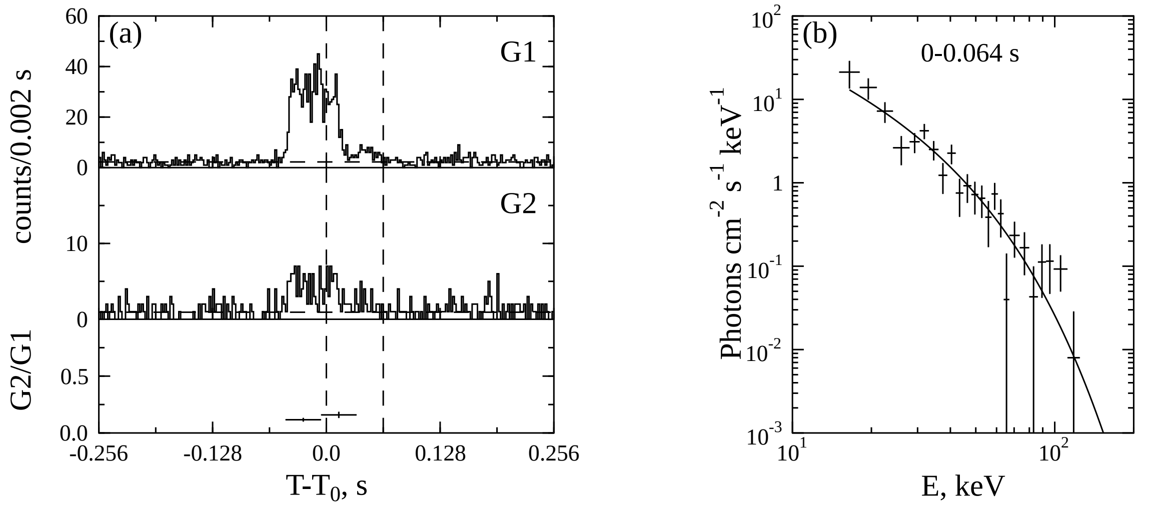

Fig. 4.15.— Burst 981217a.

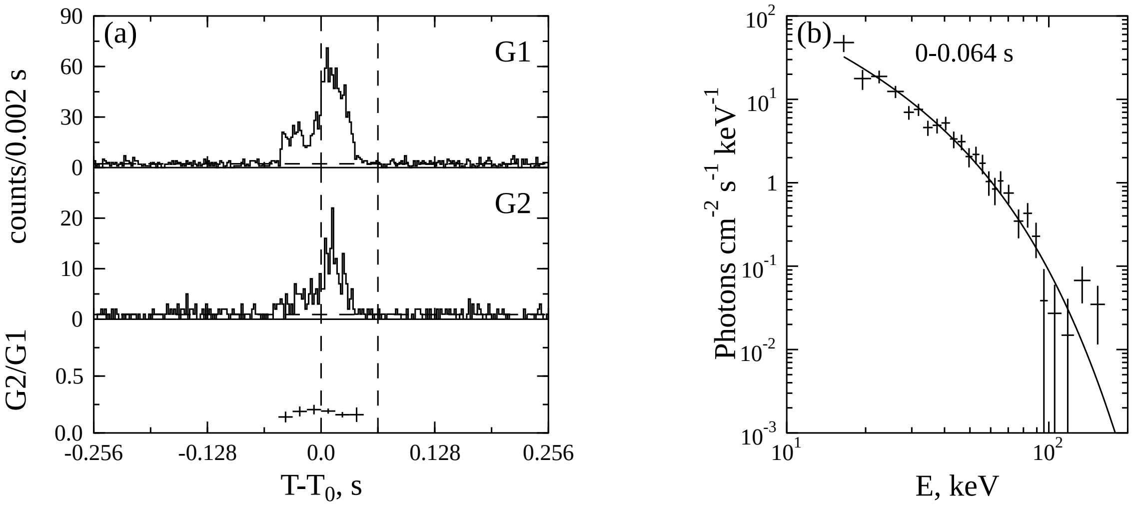

Fig. 4.16.— Burst 981217b.

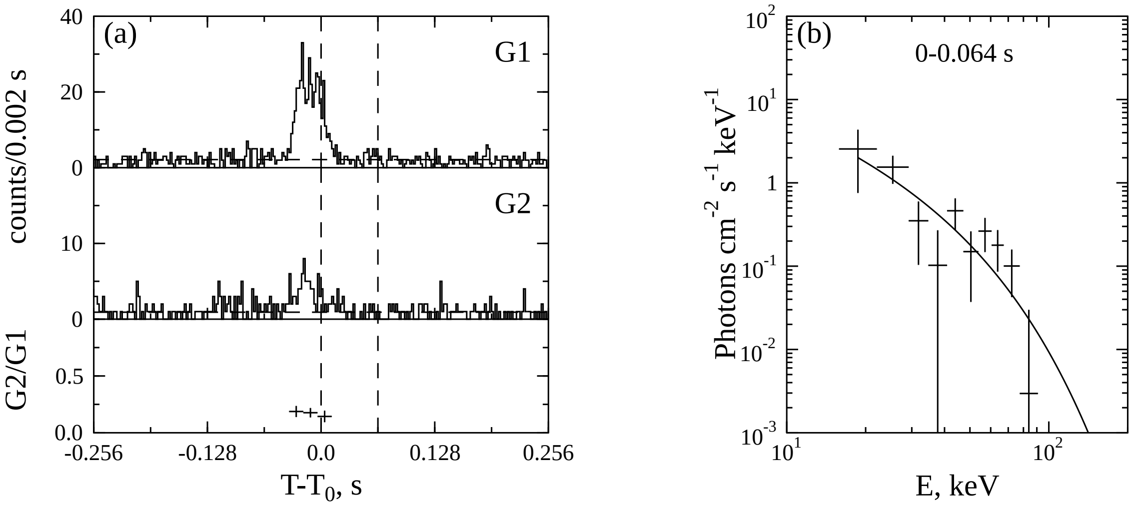

Fig. 4.17.— Burst 990104.

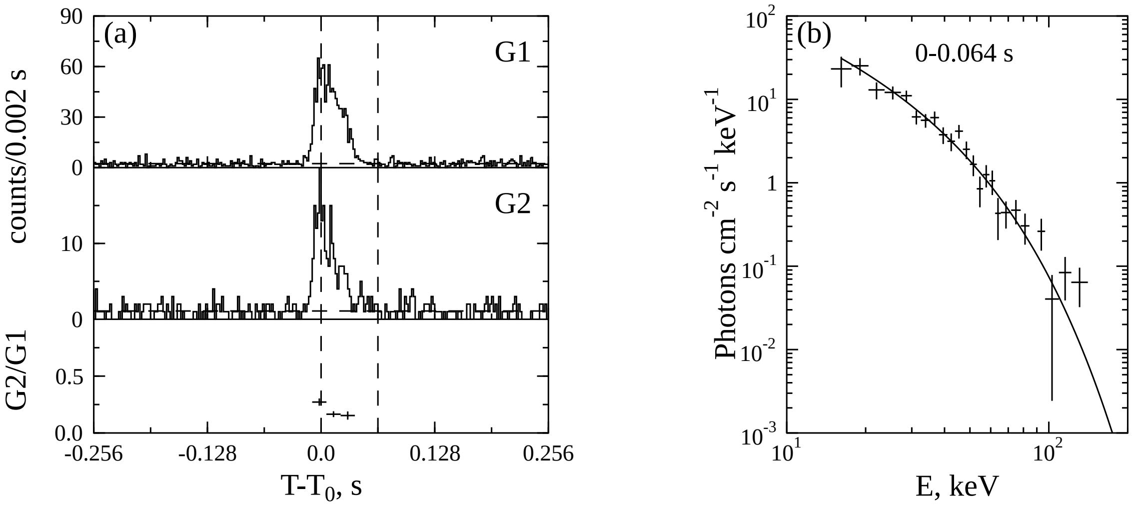

Fig. 4.18.— Burst 990125.

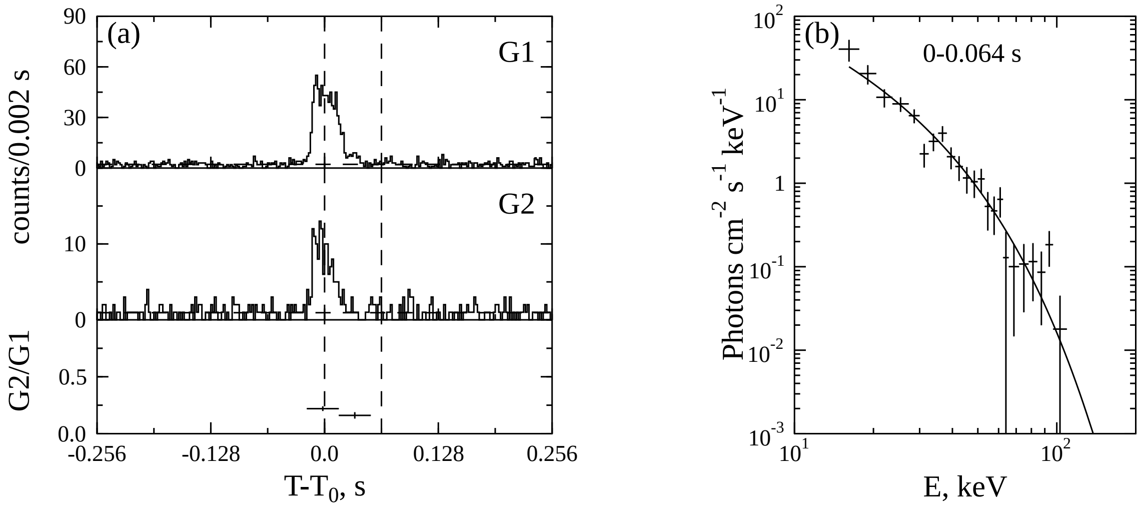

Fig. 4.19.— Burst 990206.

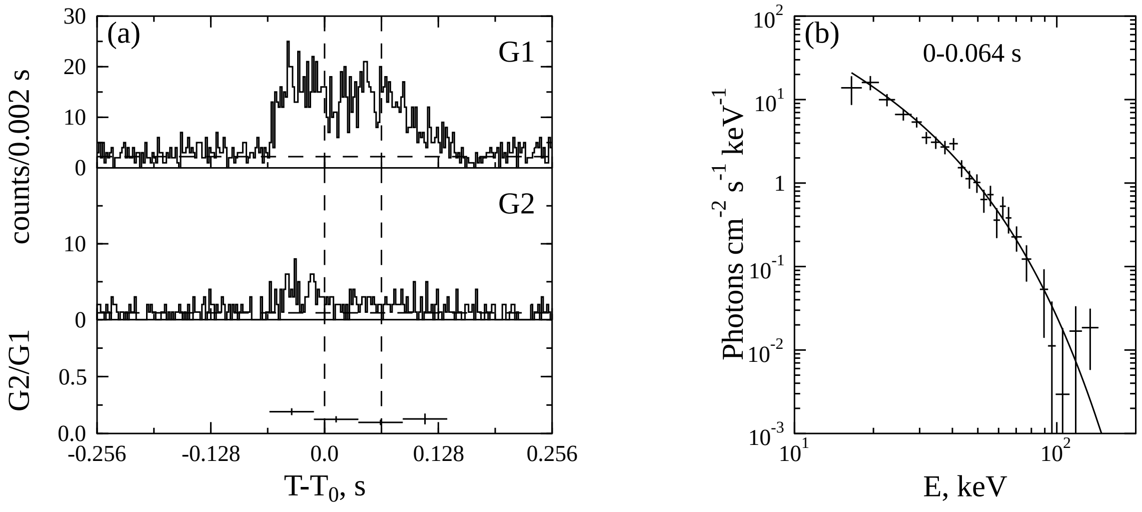

Fig. 4.20.— Burst 990601.

Figures 4.1-4.20 exhibit a variety of time structures of SGR 1806-20 bursts with no noticeable spectral variability. The second pulses in events on November 19 b,c could be considered separate bursts. kT estimates for them are respectively 18$\pm$2 keV and 17$\pm$2 keV, confirming a weak spectral evolution.

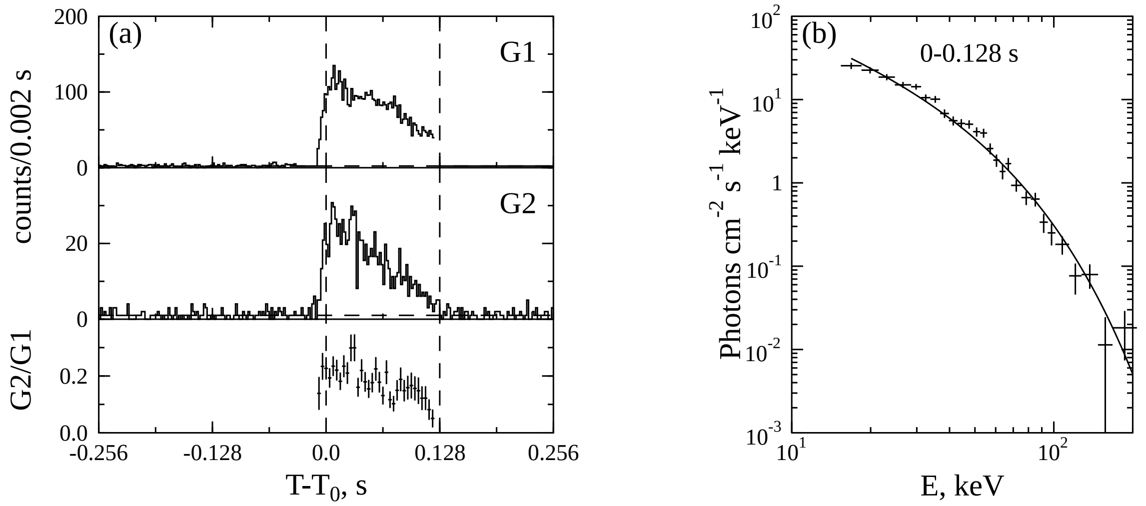

Fig. 5.1.— Burst 980617d.

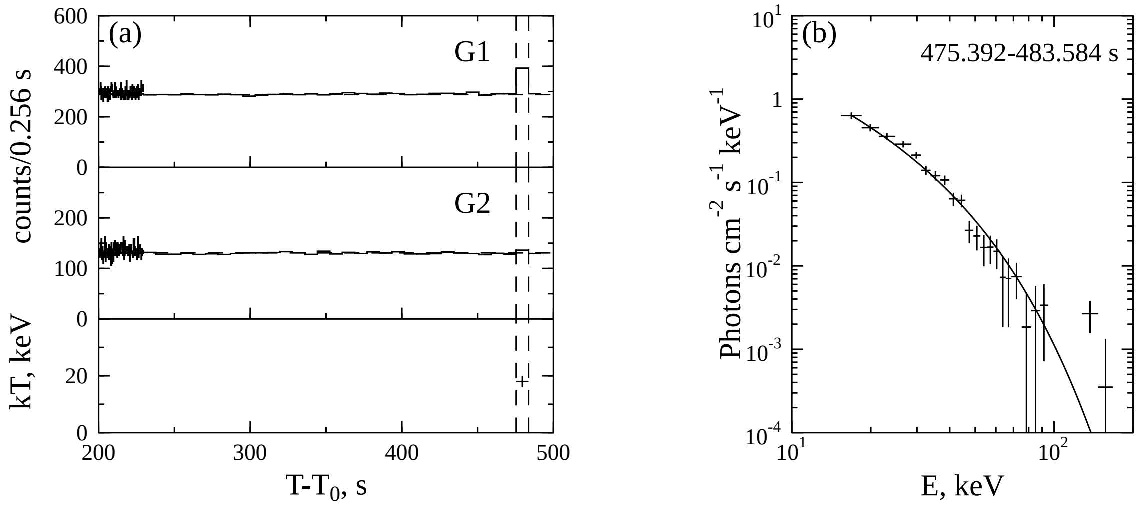

Fig. 5.2.— Burst 980617d (continued). See comments to Fig. 3.42.

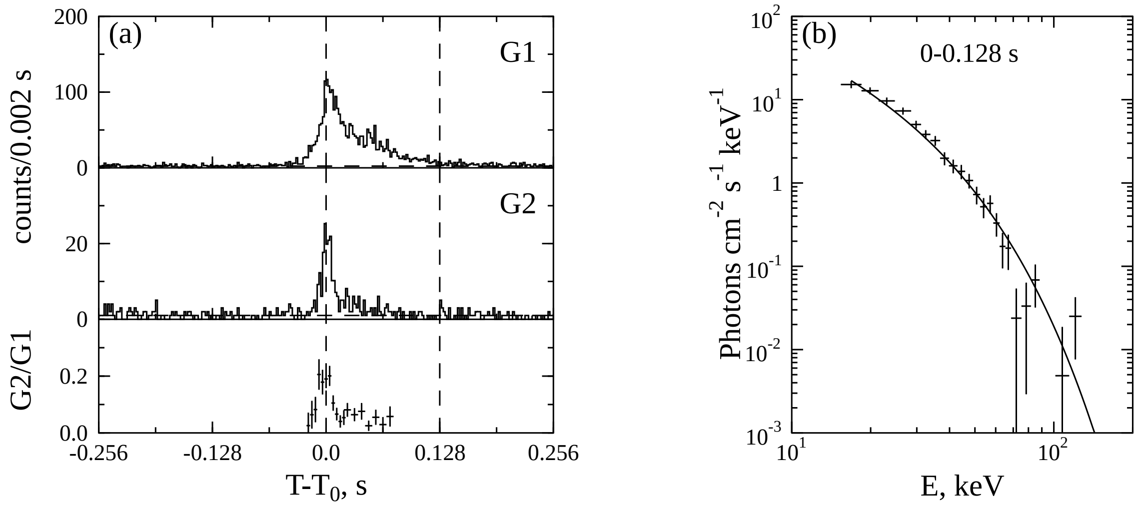

Fig. 5.3.— Burst 980617e.

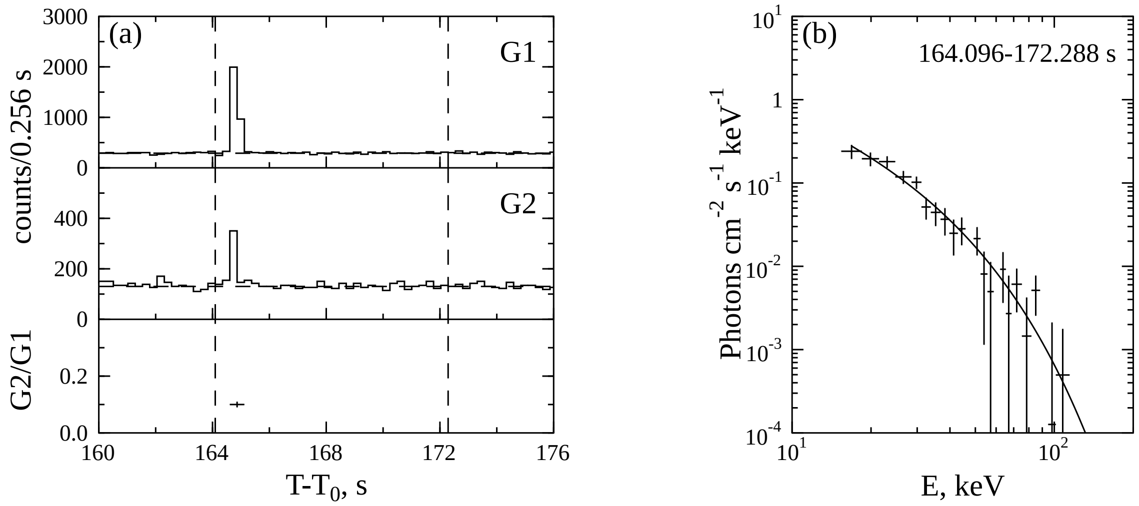

Fig. 5.4.— Burst 980617e (continued).

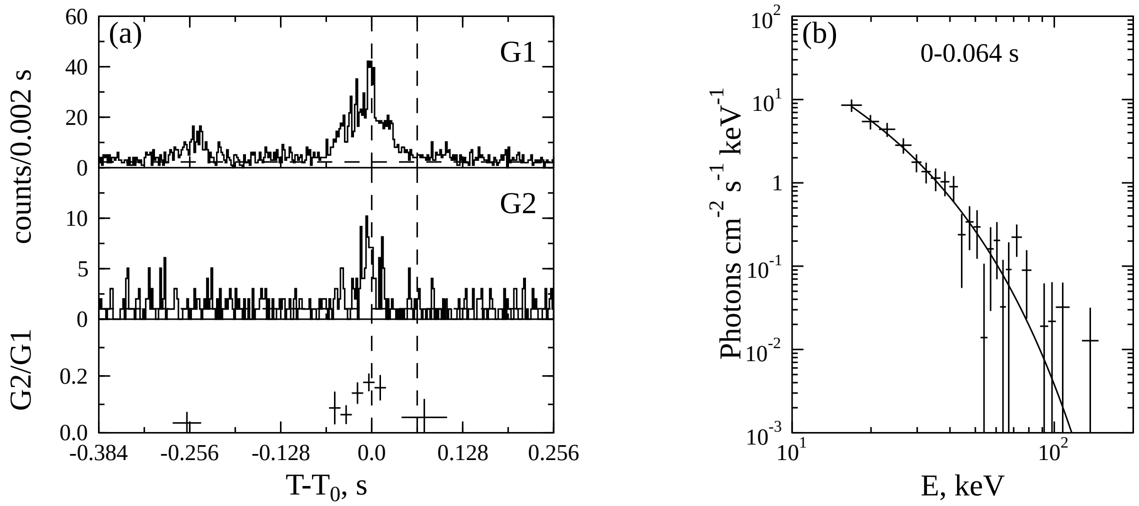

Fig. 5.5.— Burst 980617i.

Figures 5.1-5.5: Bursts observed before a huge outburst on June 18.

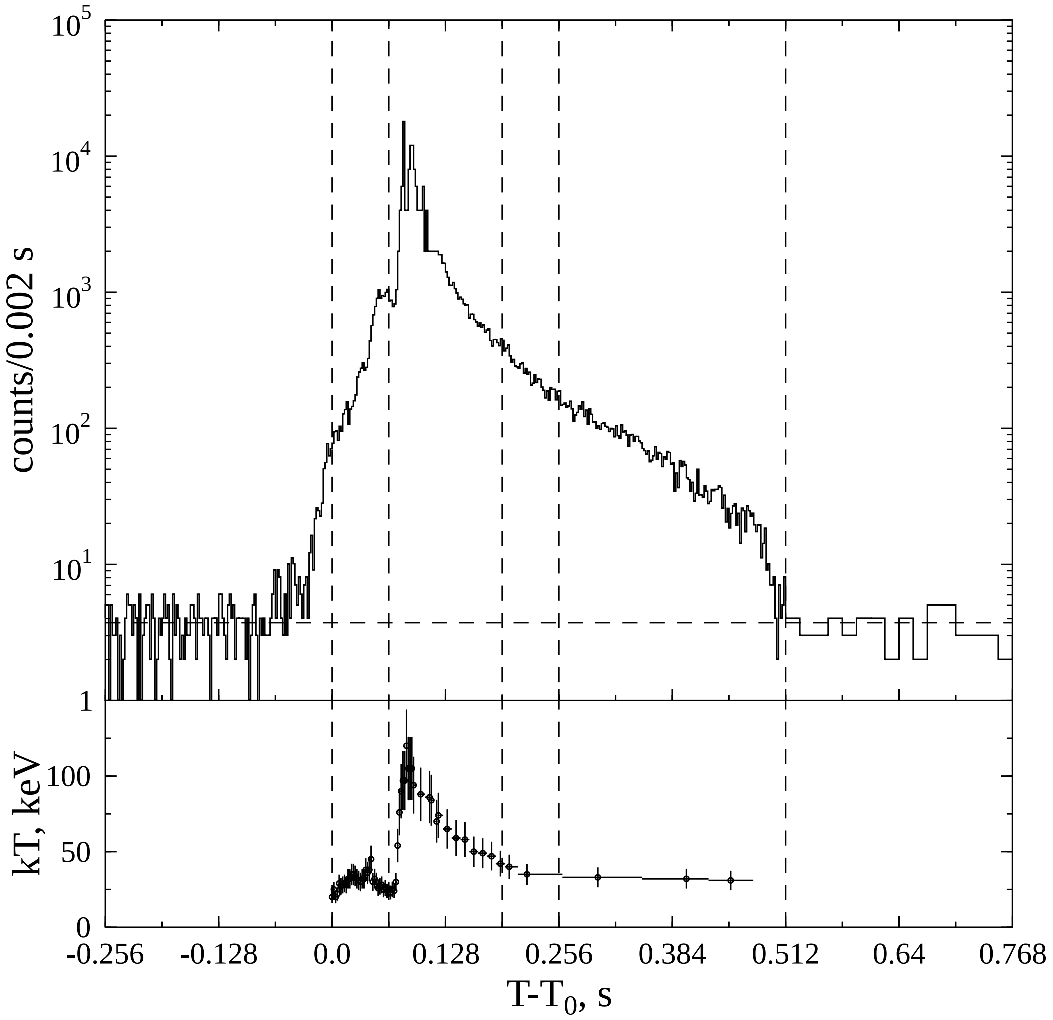

Fig. 5.6.— Extraordinarily intense 980618d outburst on 1998 June 18. Time history correctred for dead time (see Mazets et al. 1999a for details).

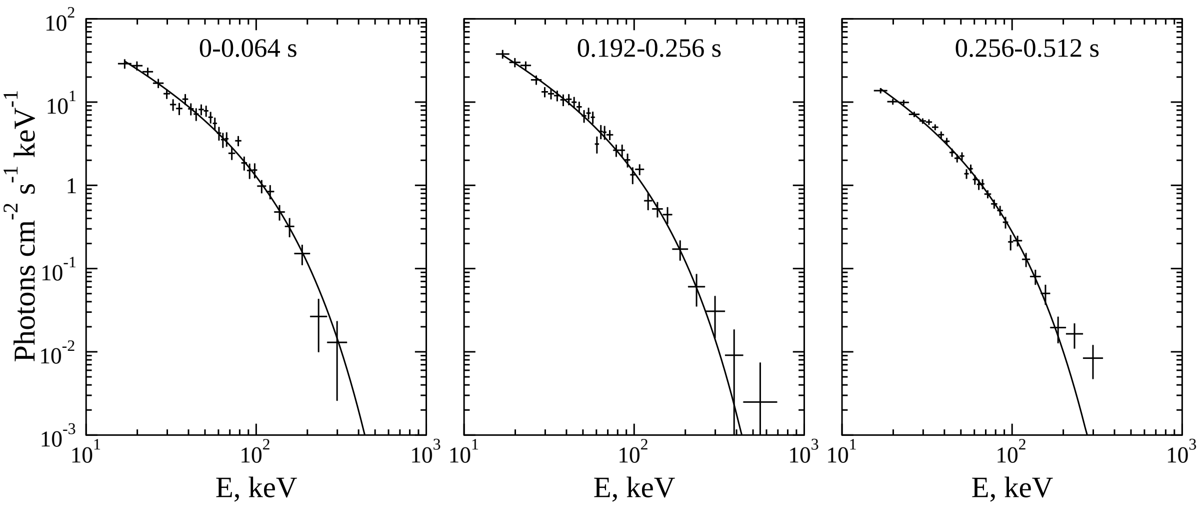

Fig. 5.7.— Energy spectra of the giant 980618d outburst.

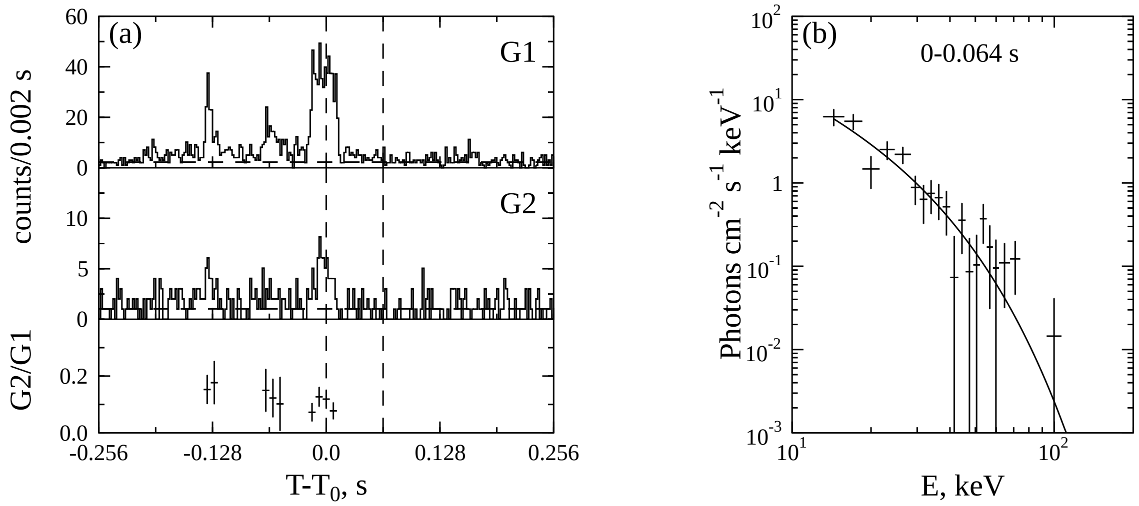

Fig. 5.8.— Burst 980618f.

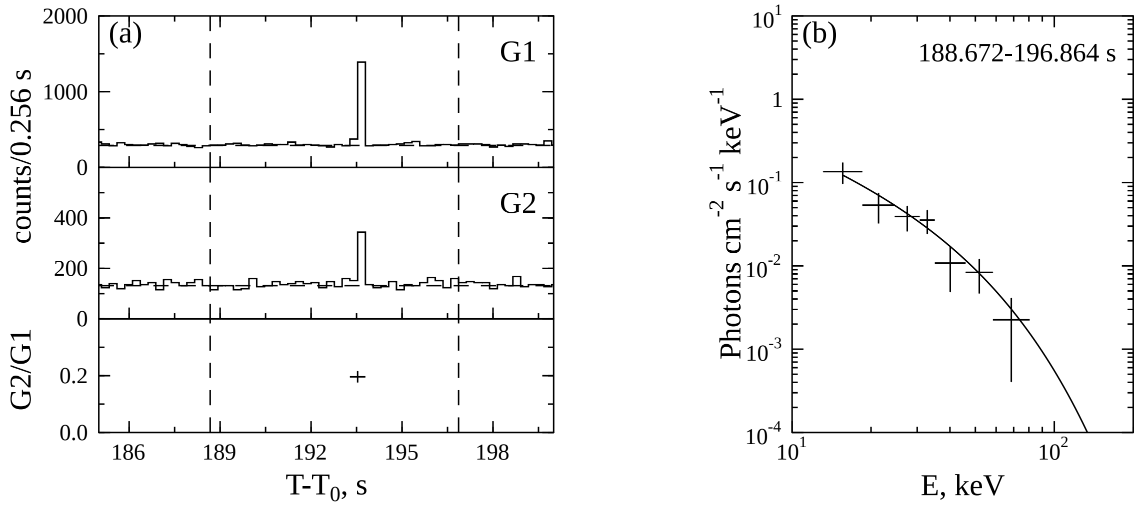

Fig. 5.9.— Burst 980618f (continued).

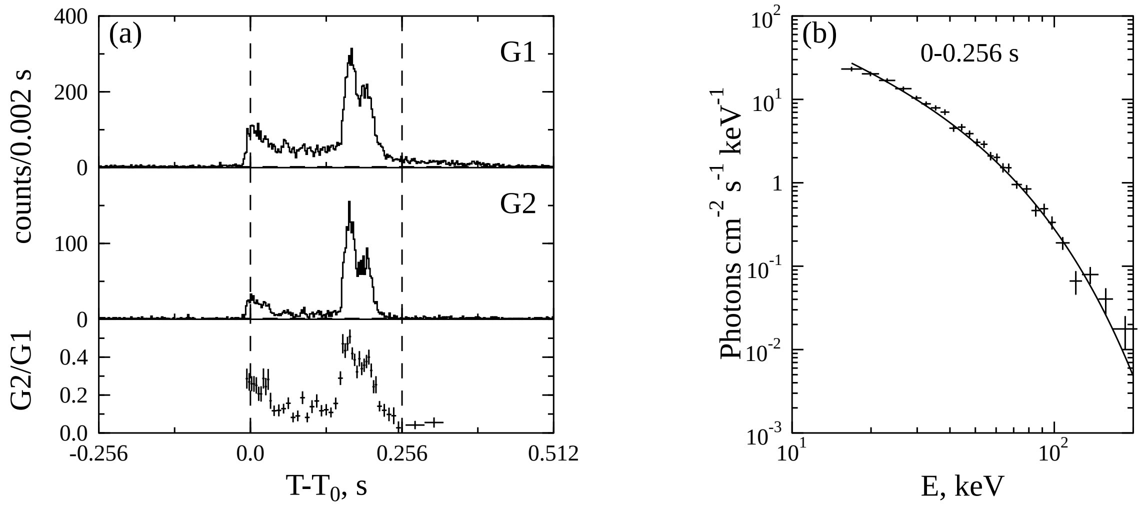

Fig. 5.10.— Burst 980618h.

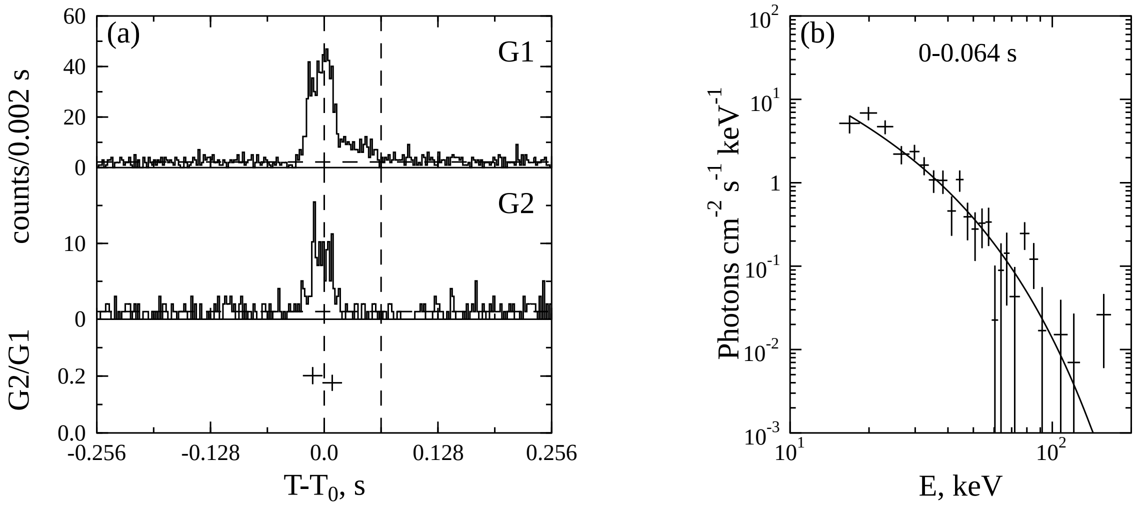

Fig. 5.11.— Burst 980618k.

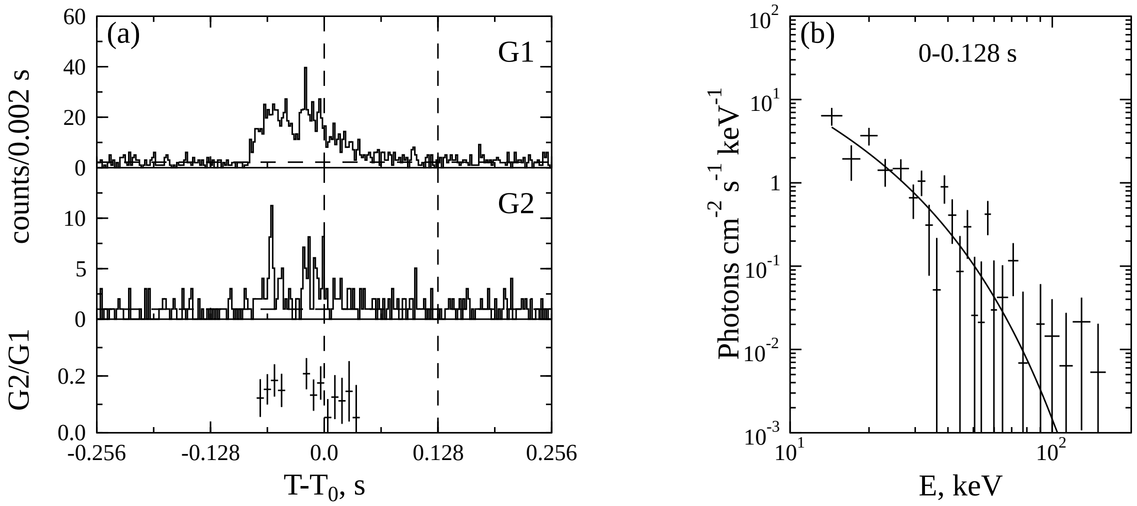

Fig. 5.12.— Burst 980618n.

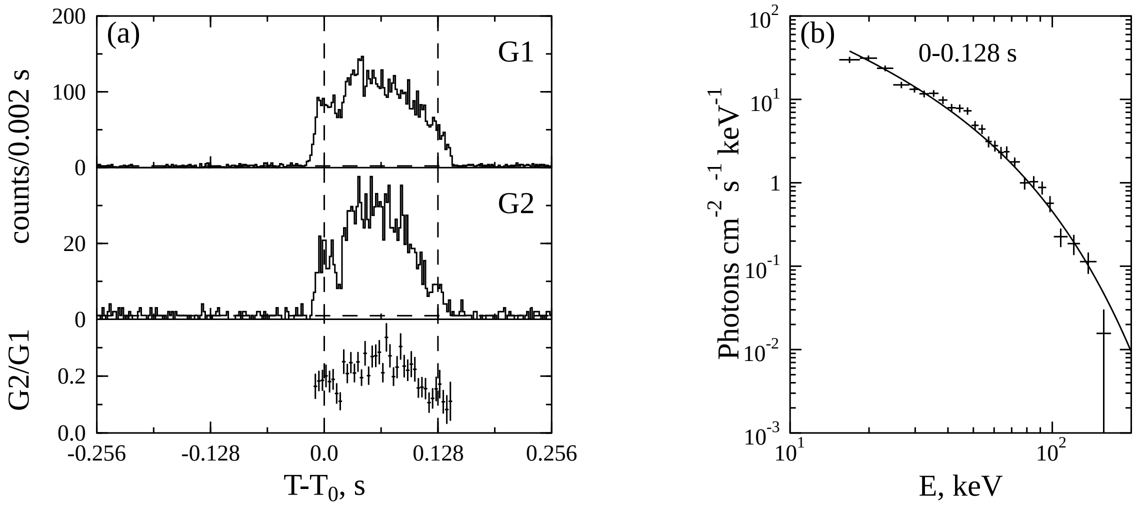

Fig. 5.13.— Burst 980622a.

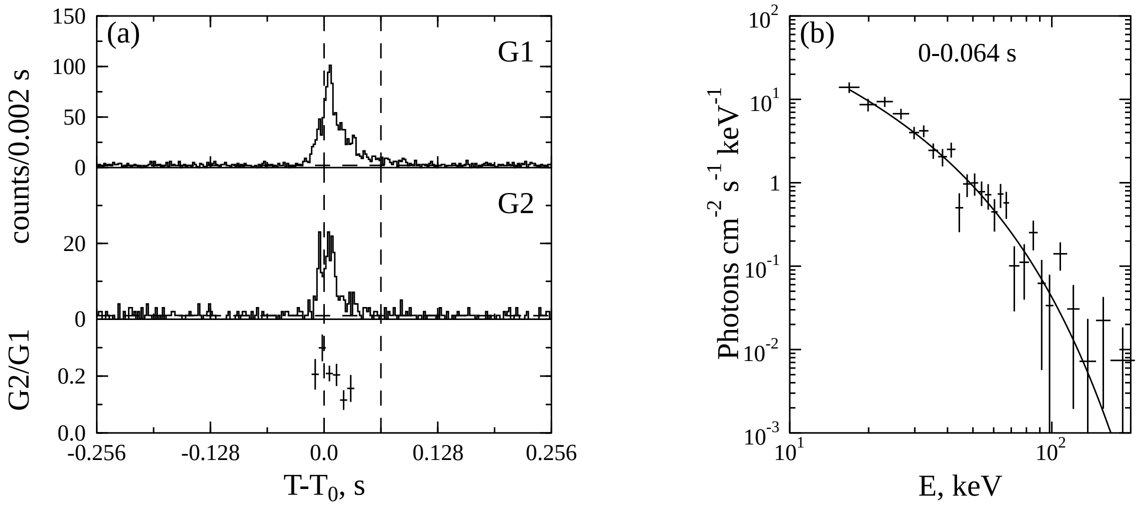

Fig. 5.14.— Burst 980622c.

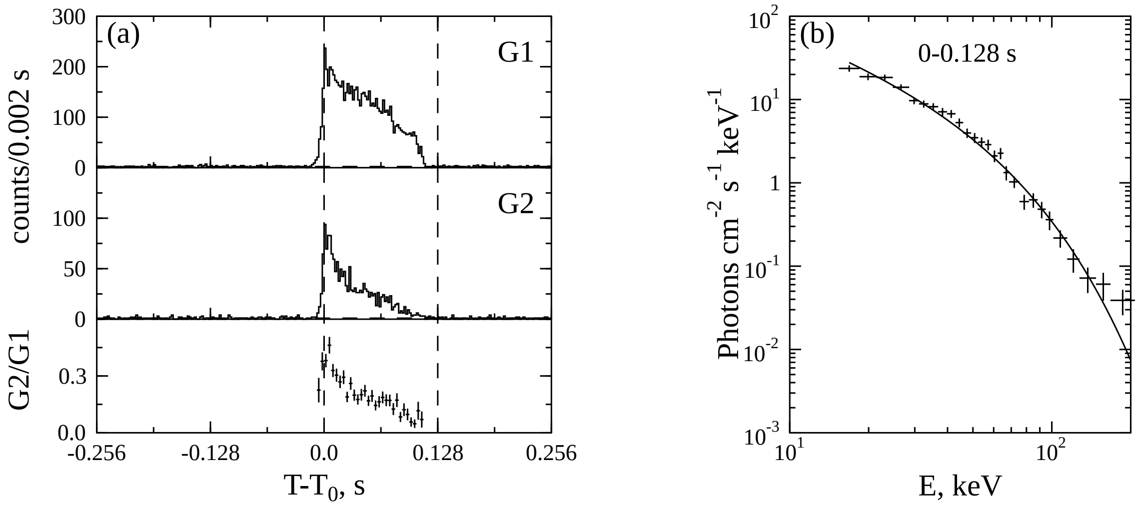

Fig. 5.15.— Burst 980625.

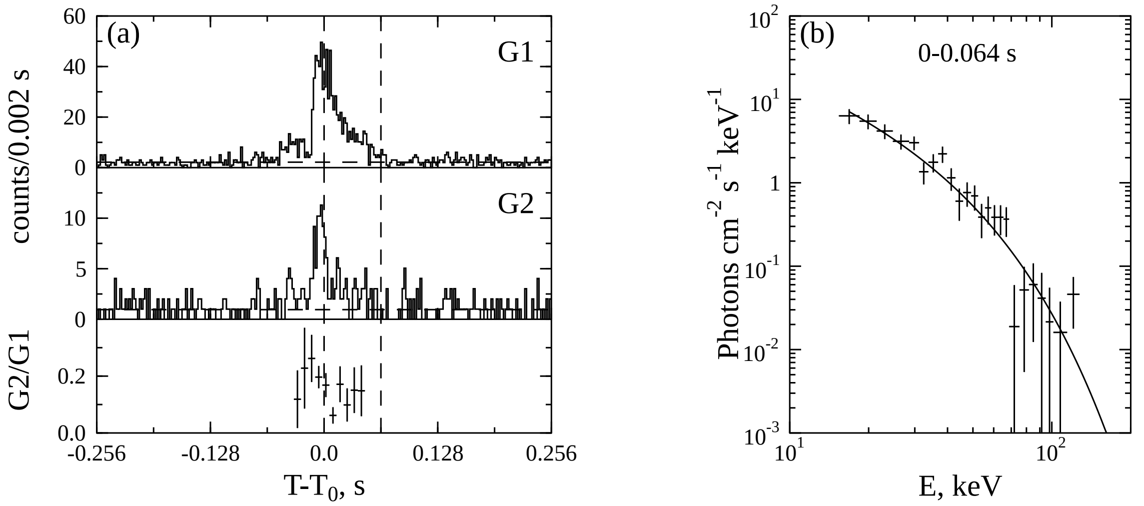

Fig. 5.16.— Burst 980629.

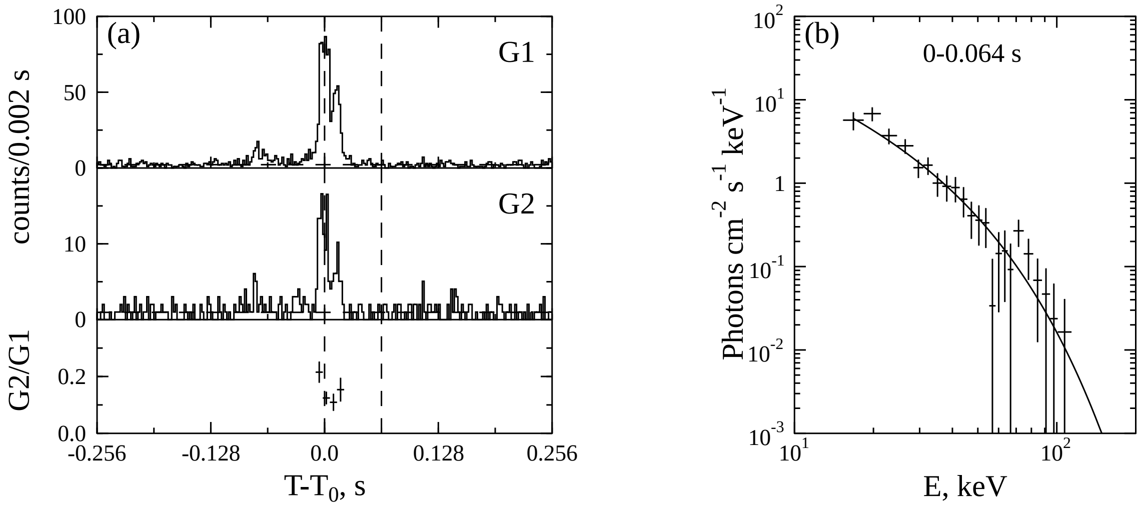

Fig. 5.17.— Burst 980712.

Figures 5.8-5.17: Repeated bursts. These data show that another remarkable feature of this source is a strong spectral evolution during bursts, with a pronounced hardness-intensity correlation.

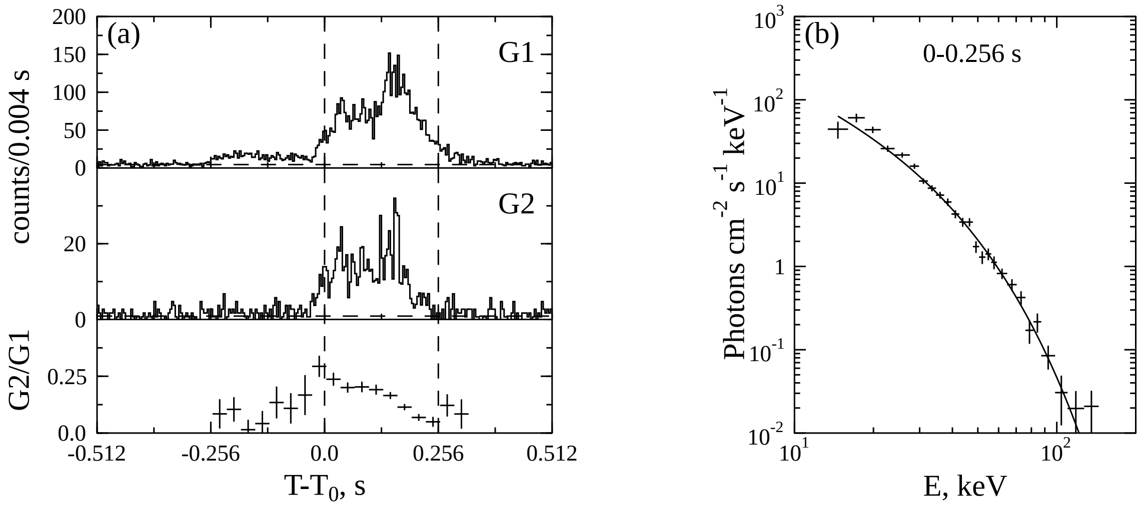

Fig. 6.1.— Burst 970629.